UNIVERSIDAD AUTÓNOMA DE NUEVO LEÓN

FACULTAD DE CIENCIAS QUÍMICAS

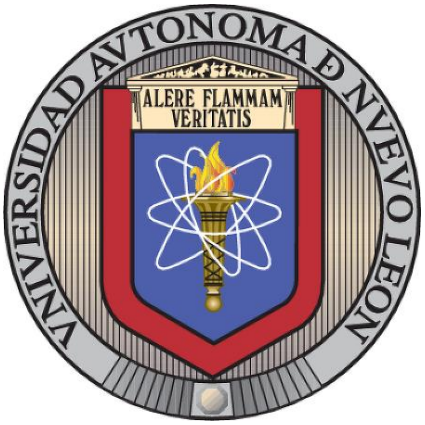

PREPARATION OF NEW TIN MATERIALS DERIVATIVES FROM LIGANDS MULTIDENTATE FOR POTENTIAL FABRICATION OF OPTOELECTRONIC DEVICES

BY

ARELLY MONTSERRAT CANTÓN DÍAZ

AS PARTIAL REQUIREMENT FOR THE DEGREE OF DOCTOR

OF SCIENCE WITH ORIENTATION IN MATERIALS CHEMISTRY

August, 2019

SUMMARY

M. C. Arelly Montserrat Cantón Díaz **Graduation Date: August 2019**

Universidad Autónoma de Nuevo León

Facultad de Ciencias Químicas

Study Title: Preparation of new tin materials derivatives from ligands multidentate for potential fabrication of optoelectronic devices.

Page number: 134

Candidate for the degree of Doctor of Sciences with Orientation in Materials Chemistry

Study area: Materials Chemistry

Purpose and study method: Complexes derived from Schiff bases offer an interesting alternative for the synthesis of tin compounds with luminescent properties. It is important to notice that have been reported organotin compounds mostly derivatives of bidentate ligands with interesting photo, and electroluminescent properties. However, studies of tin compounds derived from multidentate ligands have been scarcely explored. Based on the above, this work research was synthesized four new compounds derived from multidentate ligands with potential application as optoelectronic device, using an organotin compound as emitter material and an electron transport layer in the assembly of electroluminescent devices type OLED.

Conclusions and contributions: In this work research was reported two structures of multidentate ligands and four tin compounds, which were characterized by spectroscopic and spectrometric techniques and x-ray diffraction. The same way the photophysical parameters, thermal and cyclic voltammetry properties of all materials were studied. Electroluminescent devices type OLED were fabricated with **4** obtained as a results current-voltage curves, indicating the presence of the electroluminescence phenomenon.

ADVISOR SIGNATURE

_____

Ph.D. Víctor M. Jiménez Pérez

This thesis was realized at Laboratory of Materials III into the Postgraduate area of Facultad de Ciencias Químicas from Universidad Autónoma de Nuevo León guided bye Ph.D. Víctor M. Jiménez Pérez.

This project was carried out with the financial support from CONACYT (grant: 592501) and it was complemented with one stays with the collaboration of Ph.D.s Ivana Moggio and Eduardo Arias.

DIVULGATION PROYECT AND STAYS PERFORMED

The study realized in this thesis has been divulged in a national meeting and it has been generated 2 publications y 1 under review

Arelly M. Cantón-Díaz, Blanca M. Muñoz-Flores, María C. García López, Ivana Moggio, Eduardo Arias, Arxel de León, María E. Ochoa and Víctor M. Jiménez-Pérez. Síntesis asistida por microondas de compuestos de estaño fluorescentes derivados de bases de Schiff: propiedades fotofísicas, electroquímicas y fotovoltaicas. Mérida, Yucatán, México. realizada los días 22-23 de marzo de 2018.

Arelly M. Cantón-Díaz, Blanca M. Muñoz-Flores, María C. García López, Ivana Moggio, Eduardo Arias, Arxel de León, María E. Ochoa and Víctor M. Jiménez-Pérez. One-pot microwave-assisted synthesis of organotin Schiff bases: an optical and electrochemical study towards their effects in organic solar cell. *New J.Chem*. 2018, 42, 14586.

In this project, a short stay was made at the Materials Chemistry Investigation Center (CIQA) in the materials laboratory III Saltillo, Coahuila from august to november 2017

ACKNOWLEDGEMENTS

I am grateful to Ph.D. Victor M. Jiménez Pérez for the opportunity to take part of his research group as well as shared knowledge but most of all for their trust.

I am also grateful to Ph.D. Rodrigo Chan Navarro for their trust and friendship. Awarded, as well as Ph.D.s Concepción García, Arxel de León, Carlos Gallardo, Ivanna Moggio and Eduardo Arias for their supported and collaboration in this project. I also want to thank all the staff of the research center in Applied Chemistry, both the Ph.D.s of the research group, students, engineers, technicians, etc; that made me happy in the day so that the heavy days did not feel.

I also thank to thesis committee, Ph.D.s Eduardo Sanchez, Salomé de la Parra, and Alberto Gómez, for their corrections, suggestions and interest, in the review of these research work.

I am indebted with my second mom... Sra. Lidiet Garza and her family.

Finally, I greatly appreciate the support of my parents in all moment, mi husband Felix Alberto Valles León by their patience and unconditional support for achieving my goal.

My little baby...

Aidán I thank you for giving me the courage with your beautiful smile behind a screen to survive without you all this time.

Nothing was easy, but all these tears that fell from those eyes... someday they will see glory.
everything is for you... loves you mom

CONTENTS

LIST OF FIGURES

LIST OF SCHEMES

LIST OF TABLES

LIST OF ABBREVIATIONS

–C=N-	azomethine group	IR	infrared
HOMO	highest occupied molecular orbital	MNR	nuclear magnetic resonance
OLED	organic light emitting diode	APCI	atmospheric pressure chemical ionization
mA/cm^2	unit of current density	u.m.a.	unit of molar mass
ppm	parts per million	δ	chemical shift
LUMO	lowest unoccupied molecular orbital	IR	infrared
Å	Armstrong	DMSO	dimethyl sulfoxide
T_{d5}	decomposition temperature at 5%	cd/m^2	unit of luminance
Tm	melting transition process	HSQC	heteronuclear single-quantum coherence
HETCOR	2-D heteroclorrelation	A	agregation-caused quenching
		CQ	
TCSPC	time correlated single photon counting	COSY	correlation spectroscopy
PEDOT:PSS	poly(3,4ethylenedioxythiophene)	MHz	megahertz
$M^{-1}cm^{-1}$	unit of molar extinction coefficient	ITO	indium tin oxide
Å	length measurement unit	Knr	non-ratiative decay
Eg	optical band gap	UV	ultraviolet region
λ	wavelength	Φ	quantum yield
nm	nanometers	Δv	difference frecuently
^1H	proton NMR	ppm	parts per million
^{119}Sn	tin NMR	eV	unit of energy
^{13}C	carbon NMR	AFM	atomic force microscopy
TGA	thermogravimetric analysis	τ	life time
XRD	X-ray powder diffraction	m.p	melt
HTL	hole transport layer	EML	emissive materials layer
ETL	electronic transport layer	STM	scanning tunneling microscope

LIST OF ORGANIC COMPOUNDS SYNTHESIZED

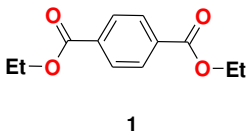

1

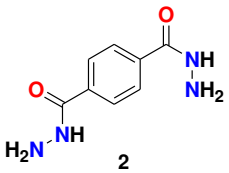

2

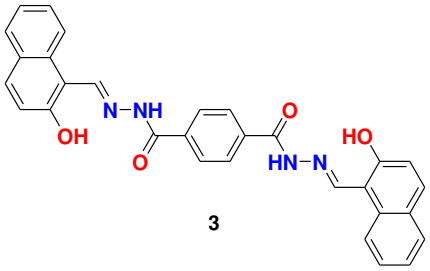

3

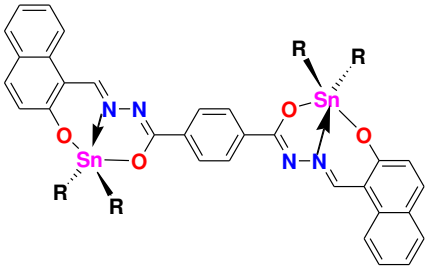

4:R = ^{n}**Bu**
5:R = **Ph**

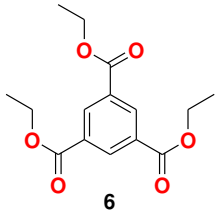

6

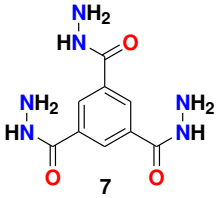

7

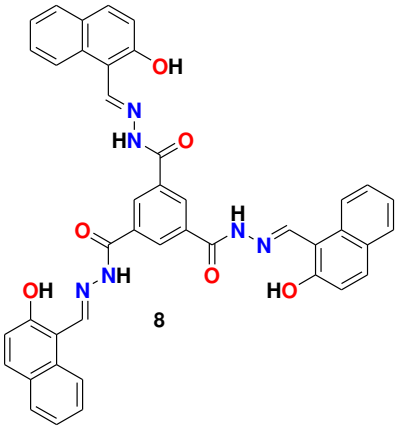

8

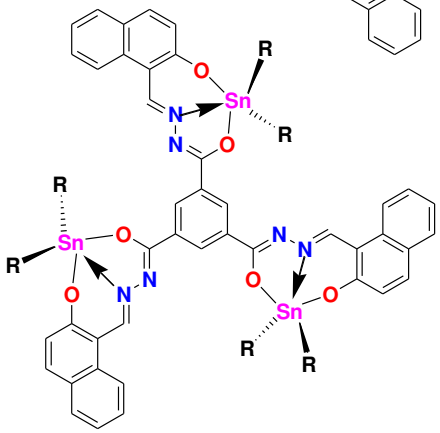

9:R = ^{n}**Bu**
10:R = **Ph**

1. INTRODUCTION

The irrational exploitation of fossil fuels for decades by mankind has compromised the quality of the environment.[1] To solve these problems, promote sustainable development is importance vital. The use of new technology to efficiently exploit the various forms of energy is one of the most attractive alternatives to replace or optimize conventional forms of energy. Among the various forms of energy, lighting is one of the most basic applications in humanity. According to CoNUEE (National Commission for the efficient use of energy) globally, lighting accounts for approximately 15 % of total electricity consumption. In Mexico, the energy consumption for lighting concept represents approximately 18% of total electricity consumption. High consumption of electricity for lighting concept is attributed to lighting devices using low efficiency.[2] Against this background, the lighting in solid state devices is emerging as an efficient and versatile technology, which presupposes a greater level of illumination for a given activity, satisfying the needs with minimal energy consumption. Among emission devices in solid state, organic light emitting diodes (OLEDs, for its acronym in English) are considerate an alternative due to the offer significant energy savings, flexibility, higher resolution, wider viewing angle, and reduced volume of the devices. The success of these devices is based on the phenomenon of electroluminescence, generated from a semiconductor organic material.

Currently, there is a strong demand for new materials that can be used as electroluminescent layer in OLEDs for use in lighting devices in solid state. In particular, interest has focused on the search for materials simple architecture that can generate light from the combination of the emission of primary colors. In addition, organotin compounds are considered of particular interest because of their diversity in structural design and easy of synthesis with applications such as tumor agents, nonlinear optical materials, contrast agents in bioimaging as well as in emitting organic diodes. Furthermore, the Schiff bases play an important role in the synthesis and organic catalysis, as well as ligands in the coordination chemistry of metals, since they and their metal complexes have a variety of applications in medical, catalytic chemistry, coordination and materials.[3] In particular, the attention has increased to those organotin complexes derived from Schiff bases, because they provide an interesting wide variety of molecular structural conformation,[4] and addition the electron withdrawing –C=N– group interacts with metal ions giving complexes with different optoelectronic properties and potential applications.[5]

Recently, it has reported the fabrication of OLEDs with tin derivatives, which offer several advantages over other elements of main group and transition metals as these are characterized by attractive luminescent properties, easy handling, stable air and structural versatility. However, there are few reports about making OLEDs with tin complexes as an electroluminescent layer.[18, 19, 20, 21, 23, 24]

Our research group is interested in the synthesis, characterization and potential application of tin complexes as drugs, decomposers of polyethylene acetate (PET, for its acronym in English polyethylenterephtalate)[6] and in the fabrication of OLEDS.[7] In recent reports of synthesis of tin complexes have been observed acceptable photophysical properties. Once fabricated the OLED, the graph of voltage *versus* current showed conduction effectively, however did not adecuate electroluminiscence. The explanation for the low luminescence is due to the presence of the nitro group. Based on the above, the synthesis of complexes of tin (IV) with more conjugated aromatic systems without electron withdrawing and good solubility in organic solvents are proposed.

Therefore, in this work, it was proposed to synthesize pentacoordinated tin compounds derived from Schiff bases with fused rings for increase the coplanarity and structural rigidity of the molecules, π-π* systems to obtain conjugated molecules and increase the delocalisation of the molecules. Finally, the electroaccepting were eliminated to obtain an increase of the luminescence are proposed. The molecules were characterized by UV-vis, spectroscopic methods (IR, 1 and 2D-NMR,) and mass spectrometry, the compounds were analyzer by X ray monocrystal, TGA, photophysical properties, AFM and voltammetry ciclyc

2. BACKGROUND

2.1. Luminescence and electroluminescence

The luminescence phenomenon is defined as the emission of ultraviolet, visible or infrared an electronically excited, as opposed to filament species; which it is generated at room temperature.[8] Depending on the way the energy is applied, you can be observed different types of luminescent processes such as phosphorescence, thermoluminescence, chemiluminescence, radioluminescence, and electroluminescence; this luminescence can be observed in optoelectronic devices. Electroluminescence is the result of radiative recombination of electrons and holes in a material, often a semiconductor by electric current. This phenomenon occurs in electroluminescent devices such as organic light emitting diodes.

2.2. OLED structure

OLEDs are formed by a cathode, emitting film, conductive film and the anode. (Figure **1**) The emitter layer is an electroluminescent compound should be capable of: a) form a uniform thin film, b) have drivability and emission of electrons, c) possess a high fluorescence yield, d) be heat stable, e) possess adequate

energy difference between HOMO molecular orbital / LUMO facilitating transport and charge injection.

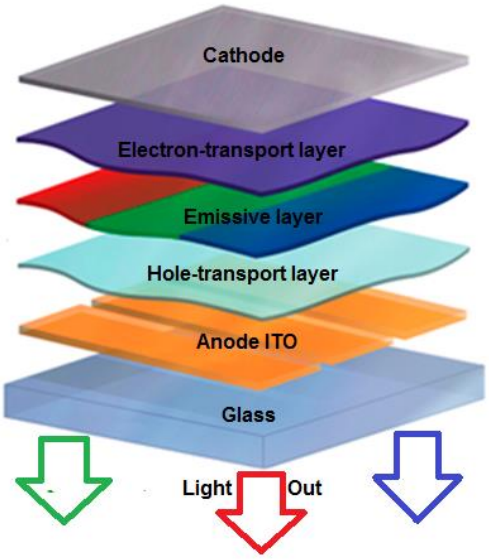

Figure 1. OLED structure.

Furthermore, there has observed progress in the design and synthesis of new tin compounds, which have improved chemical and optical properties compared with aluminium derivatives, such as good solubility in organic solvents, fluorescent quantum yields high (Φ), air stable, inexpensive and easy deposition on substrate surfaces by direct thermal evaporation.[9] In this sense, it has paid much attention to the transition metal complexes due to their interesting electroluminescent emission properties such as high thermal stability and good.[10] However, heavy metals such as Ir,[11] Pt,[12] and Cu[13] are extremely sensitive to moisture and / or oxygen.

The semiconductive organic molecules can be designed in many ways to optimize its reasons, it is expected that semiconductor organic compounds found widespread use in many technological devices,[1-5] as optoelectronic photoreceptors for xerography,[14] transistors and field effect sensors,[15] photovoltaic cells[16] organic light emitting diodes[17]. There are reports of luminescent organic compounds some made for the manufacture of organic diodes, however the field is still scarcely explored, In 2008 *Park et al*. two new organotin complexes were synthesized ($SnDPQ_2$ y $SnDP(HPB)_2$), with blue and green luminescence with an emission band around 440-490 nm y 535 nm, for assembly of the device was used a structure type ITO/NPB/Alq_3/ $SnDP(HPB)_2$LiF/Al, the layers were deposited by the spin coating method, this device showed a luminance of 17600 cd/m^2 to 9.5 V.[18]

In 2000 Tao *et al.* reported the synthesis and properties of organometallic complexes electroluminescent diphenyltin hydroxyquinoline derivate ($SnPh_2q_2$). These compounds showed absorption at wavelength of 460 nm and a bright photoluminescence at 508 nm. Electroluminescent properties and load ejection properties Sph_2q_2 characteristics of compounds are those which are easily soluble in organic solvents. For assembly of the device structure used ITO/PVK:TPD/Sph_2q_2/Mg:Ag, the layers were deposited by spin coating and the cathode by thermal evaporation, the device showed a luminance of 1cd/m^2 to 5 V, the results indicated that the compound of tetravalent tin is a potential emission and charge injection materials for application electroluminescent.[19]

In 2012 Fazaeli *et al.* reported a series of six tin compounds (IV) derivatives hydroxyquinolines with yellow and red emission, which have a variation in photoluminescence property.this can only be affected by more than slight changes in bond distances or angles in the binder by modifying the substituent groups. For the fabrication of diode an assembly was performed with /PEDOT:PSS/PVK:PBD:Sn/HQ-Cl/Al, the layers were deposited by thermal evaporation, the graph J-V showed a current of approximately 460 mA/cm^2 to 18 V. One advantage, is that the device OLED has good stability compared to an OLED Alq_3.[20] Furthermore, the emission of compound with Cl is narrow and centered at 560 nm with a lifetime relatively longer life compared with 526 nm emission and 15 ns lifetime of Alq_3.[21]

In 2014 García-Lopez M.C. *et al*., reported the synthesis of four organic tin complexes using multidentate ligands aminophenol derivatives and diphenyltin oxide solvent by acetonitrile, the quantum yield of the complex **III** found about 5%, for the assembly of the device, the deposition of the films were made by spin coating and the cathode was performed by thermal evaporation, the device structure was ITO/PEDOT:PSS/tin complex/Al, the graph showed driving voltage versus current, however the phenomenon of electroluminescence is observed very low. In this case the authors thought the nitro group was affecting the quantum yield of the molecule that is an electron withdrawing group prevents relocation of the molecule.[22] (Figure 2)

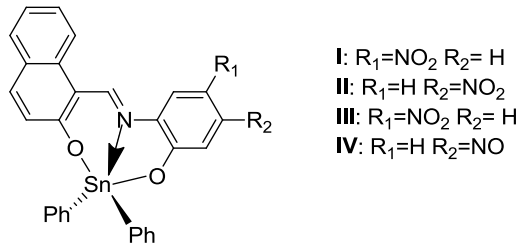

Figure 2. Pentacoordinated tin complexes.

In 2015 Berrones-Reyes J.C. *et al*., reported the synthesis of a series of eight new multidentated organic complexes derived from Schiff bases using benzohydrazide and corresponding diorganotin (R_2SnO R= ^{n}Bu or Ph), where its quantum yield is near 0.02 to 56.0%, in this report is relevantquantum yield of compound **VII** y **VIII**, with a percent of 56 and 36.2 % respectively.[23] In this case, it can be seen that molecules in their structure the nitro substituent show low luminescence, as molecules obtained by García Lopez M.C. *et al*.

In 2016 Cantón-Díaz in the master's thesis, a series of luminescent compounds of tin, which compared the work reported by García-Lopez M.C., *et al.,* the nitro substituent is removed and added a substituent donor, one electron- donor and with good solubility. In this case, it was observed that molecules with carboxylic acid group showed a quantum yield of 1.44 and 1.87 % relatively larger than the molecules of proton with yield 1.25 % , so even making changes in the substituents on the part of aminophenol, good delocalization failed.[24] Making a comparison of the structure of molecules

Jimenez-Perez with this report, a possible chemical explanation is that the molecule delocalization needs and would have to be a conjugated molecule. (Figure 3)

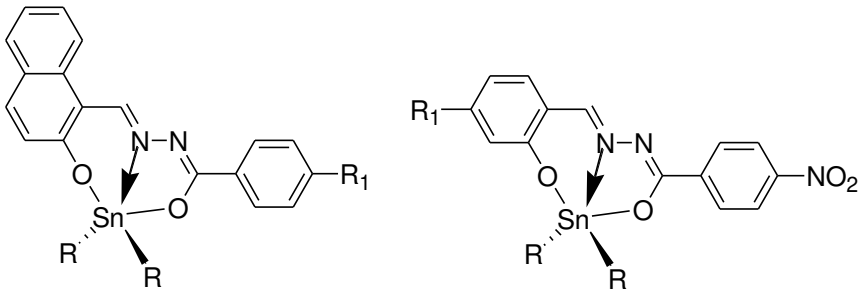

V: R=^{n}Bu R_1=NO_2
VI: R=Ph R_1=NO_2
VII: R=^{n}Bu R_1=H
VIII: R=Ph R_1=H

IX: R=^{n}Bu R_1=Et_2N
X: R=Ph R_1=Et_2N
XI: R=^{n}Bu R_1=MeO
XII: R=Ph R_1=MeO

Figure 3. Pentacoordinated tin complexes studied previously.

In 2016 Pérez-Pérez E.G. in his master's thesis reported the synthesis of two new multidentated organic complexes derived from Schiff bases using benzohydrazide and its corresponding diorganotin (R_2SnO R=^{n}Bu or Ph), where the quantum yield obtained is of 33.7 and 33%, making a comparison with this work and reported by J. C. Berrones-Reyes, the corresponding diorganotin is not affected in molecules, the group –OH although is a donor is not helping in increasing the luminescence.

Based on the above it will be done the synthesis of hydrazine derivative molecules with chains of molecules with double bond, make a dinuclear and trinuclear molecule and further conjugation and therefore greater delocalization of the molecules. (Figures **4** and **5**)

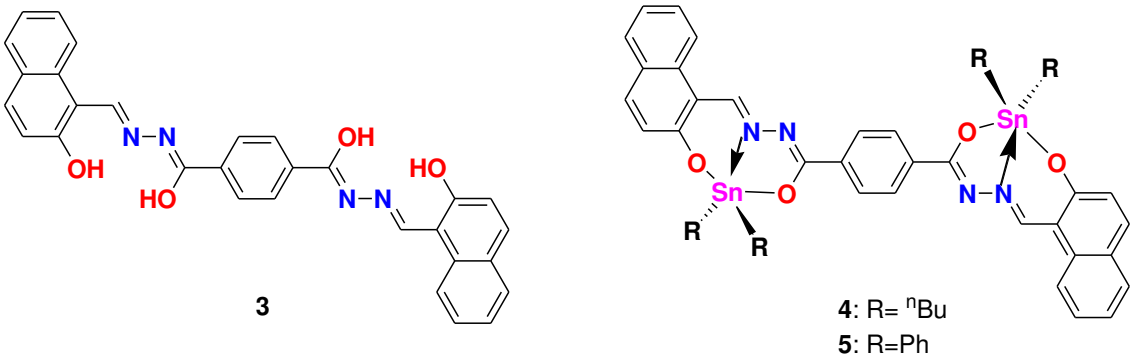

Figure 4. Compounds **4** and **5** and ligand.

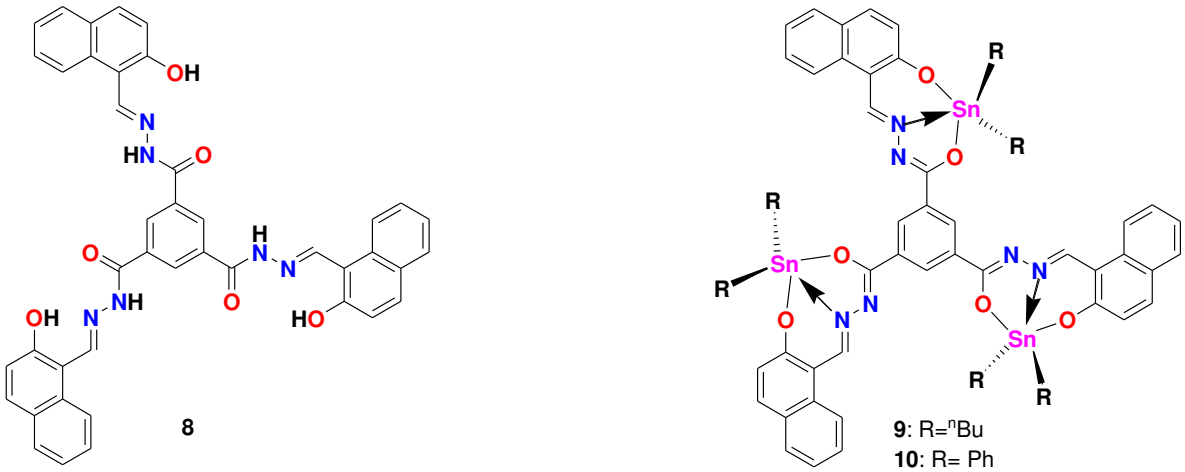

Figure 5. Compounds **8**-**10.**

Currently there are different synthetic methods as conventional, mecanosynthesis, electrosynthesis, sonosynthesis, and microwave. We are interested in the latter method in which heating is almost instantaneous "at the core" of materials homogeneous and selectively, the reactions can be completed in just a few minutes with an energy savings performance between synthesis microwave is higher than the conventional method is less solvent with the synthesis method used, developed an easy and convenient for organotin synthetic procedure and also deals with environmental protection.[25]

3. HYPOTESIS.

The new organic compounds derived from multidentate ligands show optoelectronic properties for the fabrication of an optoelectronic device.

3.1. General Objetive.

Synthesize, characterize, new fluorescent organotin compounds derivatives multidentate ligands and potential fabrication an optoelectronic device with the material having the suitable characteristics.

3.2. Specific Objetive.

- Preparation of eight new organotin compounds derived from tridentated ligands through condensation reaction.
- Full characterization of tin (IV) compounds by spectroscopic techniques such as nuclear magnetic resonance (^{1}H, ^{119}Sn, ^{13}C, HETCOR, HMBC, COSY), infrared spectroscopy and UV-Vis, the characterization is also complemented by mass spectrometry, X-ray diffraction, determination of the photoluminescent and eletroluminescent properties.
- Finally, the assembly of an optoelectronic device made from tin compound present the adequate features for its manufacturing.

4. MATERIALS AND METHODS.

4.1 Materials and equipment.

All starting materials were purchased from Sigma-Aldrich Chemical Company. Solvents were used without further purification. Melting points were determined on an Electrothermal Mel-Temp apparatus and are not corrected. Infrared spectra were recorded using a Burker Tensor 27-FT-IR spectrophotometer equipped with a Pike Miracle ^{TM} ATR accessory with a single reflection ZnSe ATR crystal.

Multinuclear magnetic resonance experiments as ^{1}H, ^{13}C and ^{119}Sn- NMR spectra were recorded on a Bruker advance DPX 400. Chemical shifts (ppm) are relative to $(CH_3)_4Si$ for ^{1}H and ^{13}C. High-resolution mass spectra were acquired by LC/MSD TOF on an Agilent Technologies instrument with APCI as ionization source.

UV-Vis absorption spectra were measured on a Shimadzu 2401 PC spectrophotometer. The emission spectra have been recorded with a Fluorolog 3 spectrofluorometer, by exciting 10 nm below the longer wavelength absorption band. Raman spectra were obtained with a Horiba Xplora equipment, focusing the sample as powders on a microscopic slide with a 10X objective. The excitation

wavelength was 785 nm and the Nanoled power was 10% of total laser power (25 mW). Spectra were acquired with 10s acquisition time and 10 accumulations, spectral resolution of 2 cm^{-1}. The thermal stability of compounds (vacuum dried samples) was determined in a thermogravimetric analyzer (TGA 951 from DuPont Instruments) connected to a N_2 vector gas, heating from 25 to 600 °C at 10 °C $min^{-1.}$

APCI as ionization source. Simultaneous thermal analysis (TGA-DTA) were carried out in the temperature range 25 to 600 °C under nitrogen atmosphere at a heating rate of 10 °C min^{-1} using a TA instruments-SDT 2960 thermal analyzerThe photophysical measurements were carried out in spectrophometric grade solvents (tetrahydrofuran and chloroform) freshly distilled and the solutions were studied just as prepared.

4.2. X-ray crystallography.

The crystal data of **1** and **2** were recorded on an Enraf Nonius Kappa-CCD (λ Mo Ka=0.71073 Å, graphite monochromator, T = 293 K-CCD rotating images scan mode). The crystal was mounted on a Lindeman tube. Absorption correction was performed using the *SHELX-A* [26] program. All reflection data set were corrected for Lorentz and polarization effects. The first structure solution was obtained using the *SHELXS-97* program and then *SHELXL-97* program was applied for refinement and output data. All software manipulations were done under the WIN-GX

environment program set.[27] All heavier atoms were found by Fourier map difference and refined anisotropically. Some hydrogen atoms were found by Fourier map differences and refined isotropically. The remaining hydrogen atoms were geometrically modelled and are not refined.

4.3. Photophysical characterization.

For the photophysical characterization, spectroscopic grade chloroform from Aldrich was freshly distilled and the solutions were studied as prepared in order to avoid any solvolysis or photodegradation effect.[28] UV-Vis absorption spectra were measured on a Shimadzu 2401PC spectrophotometer. The emission and excitation spectra have been recorded with a Perkin-Elmer LS 50B spectrofluorimeter. Excitation spectra were obtained by fixing the fluorescence maxima as the emission wavelength. Fluorescence quantum yields in solution (ϕ) were determined according to the procedure reported in literature[29] and using quinine sulphate in H_2SO_4 0.1 M (ϕ = 0.54 at 310 nm) as the standard. Measurements were carried out by controlling the temperature at 25.0±0.5 °C with a water circulating bath. Three solutions with absorbance at the excitation wavelength lower than 0.1 were analyzed for each sample and the quantum yield was averaged. Lifetimes were obtained by Time-correlated single photon counting (TCSPC) with a Tempro Horiba equipment with 370 nm and 455 nm nanoLEDs. A 0.01% suspension of Ludox AS40 (Aldrich) in ultrapure water was used for the

prompt signal. Calibration of the equipment was realized with a POPOP [1,4-Bis(4-methyl-5-fenil-2-oxazolyl)benzene] methanol solution (optical density <0.1 and lifetime of 0.93 ns.[30] Data were fit in the software DAS6 available in the equipment.

4.4. Theoretical Calculations.

All calculations were performed with Spartan 14 v.1.1.2 (Wavefunction. Inc). The geometry of the equilibrium conformer at ground state found at AM1 level was further optimized through Density Functional Theory (DFT) calculations at the restricted B3LYP level with 6-31G(d) basis set. The coordinates generated during the DFT optimization processes were used as input for the electronic excited state calculations and the first 6 singlet electronic excited states were calculated by TDDFT with the same basis set and in vacuum. By default, the software considers only pairs of filled/unfilled orbitals which have amplitudes larger than 0.15. The UV/Vis spectra were constructed as Gaussian convolution from the calculated excitations fixing a Half Height Band Width of 30 nm.

4.5. Cyclic voltammetry.

Cyclic voltammetry was performed in a C3 Stand cell from Basi, coupled to an ACM Gill AC potentiostat/galvanostat. The system consisted in a conventional three-electrode cell: Glassy carbon as a working electrode (polished with alumina after each run), Pt wire as the counter electrode, Ag/AgCl as reference electrode (-

45 mV of viability against the Calomel electrode) and ferrocene/ferrocenium as reference (formal potential E°= 0.436 V); a value of -4.8 eV below the vacuum level was considered. Voltammetric measurements were performed at room temperature in CH_2Cl_2 containing Bu_4NPF_6 (0.1M) as the supporting electrolyte. Prior to recording the voltammograms, all of the solutions (~0.1 mmol) were deoxygenated by bubbling nitrogen at least for 15 min. The experiments were carried out under nitrogen atmosphere at a scanning rate of 50 mV/s.

4.6. STM characterization.

It was performed between ~23 and 25° C using an AA5000 Scanning Probe Microscope (Angstrom Advanced Inc., Braintree, MA USA). The scanner tube calibration was performed by means of atomic resolution images obtained using commercial HOPG substrates from Ted Pella (Redding, CA USA) and SPI Supplies (grade SPI-3). Samples were exfoliated before each measurement by the adhesive tape method. Pt/Ir tips were prepared by mechanically cutting a 0.25 mm diameter 80/20 wire from Nanoscience, Switzerland. 1,2,4-Tricholorobenzene (TCB) (Sigma Aldrich, ≥ 99 %) was used as received. The Sn-complexes **5**, **6** were dissolved in TCB (2.8 mM), sonicated and heated to 60 °C for one hour. A droplet of the solution, ~3 µL, was placed by using a micro-syringe between the substrate and tip, then a pulse of 2 - 6 V was applied up to obtain a monolayer. STM images were taken in the constant-current mode at the solid-liquid interface. The bias and

current values were constantly adjusted during each scan. Details on the experiment bias and current set-point are given below each image. The raw and FFT images were processed from WSxM 5.0 software with the aim to reduce noise and normally observed drift. [31]

4.7. Fabrication of electroluminescent devices.

Diodes were prepared in typical configuration of ITO/PEDOT:PSS/5/Al (Figure 6). ITO substrates (Spi. Inc, 8-10 Ω/cm2) were first cleaned in ultrasonic bath (Branson 200) in dichloromethane for 10', hexane for 10' and methanol for 60', and then dried in an oven. Lithography was carried out in order to obtain active areas of x 0.6 mm^2. PEDOT:PSS (Clevios P by Clevios) was filtered and then deposited on the ITO slides by spin coating at 5000 rpm to give a 20 nm layer. The active layer of 10 was deposited by spin coating technique on the ITO-glass substrate. The aluminium was vacuum evaporated at a rate of 1.5 to 3 Å/s at a typical pressure of 10-6 torr in an Intercovamex TE18P vacuum chamber; the thickness was controlled by the quartz balance monitor ~100 nm. The electrical and luminescent characteristics of the devices were measured by using a source measurement unit (Keithley 2420) and an optical powermeter (Newport 1930-C).

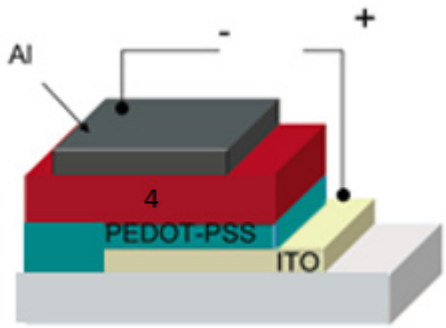

Figure 6. Schematic configuration of the device.

4.8. Synthesis and characterization.

*4.8.1. Synthesis procedure the compounds **4-5** and **9**-**10**.*

To obtain the new organotin compounds, the Fischer esterification synthesis was first carried out to obtain the raw materials by traditional method. Once the raw materials were obtained, then the ligands were carried out for the comparison method by traditional condensation synthesis. As a last step we proceeded to the synthesis by microwave irradiation by the multicomponent method to obtain **4-5** and **9-10.**

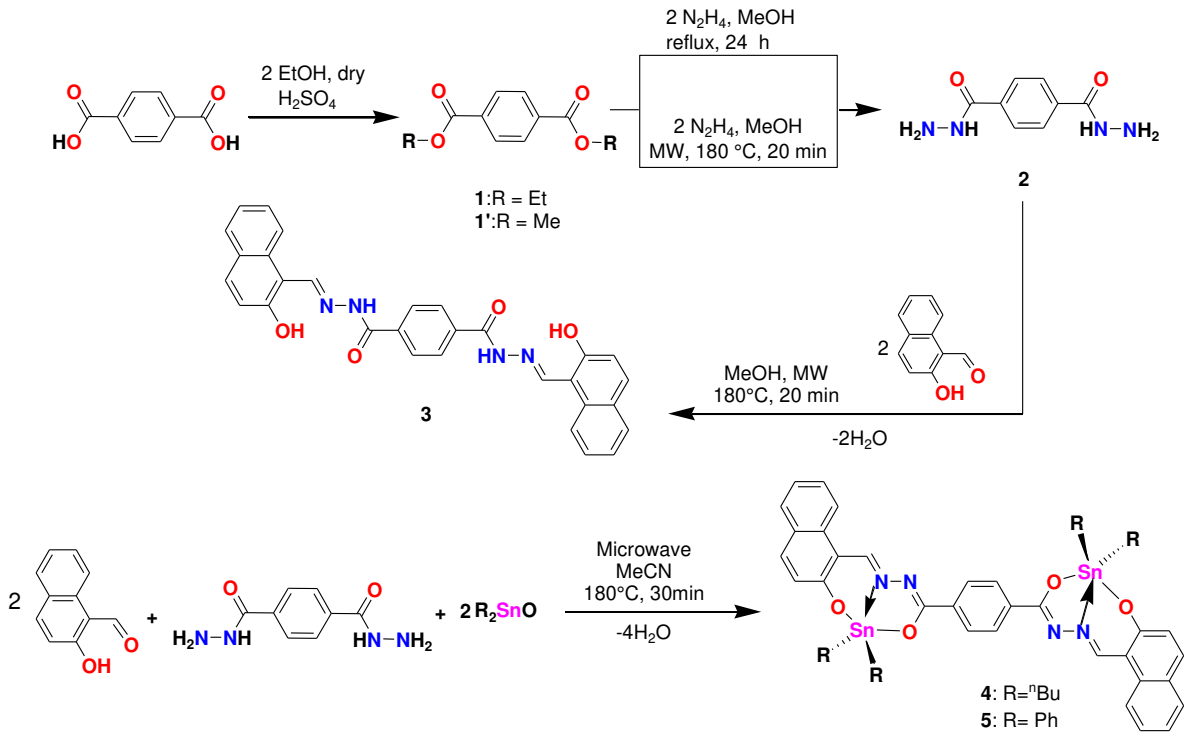

Scheme 1. Rote of synthesis of the new organotin binuclear compounds derivatives from Schiff base

.

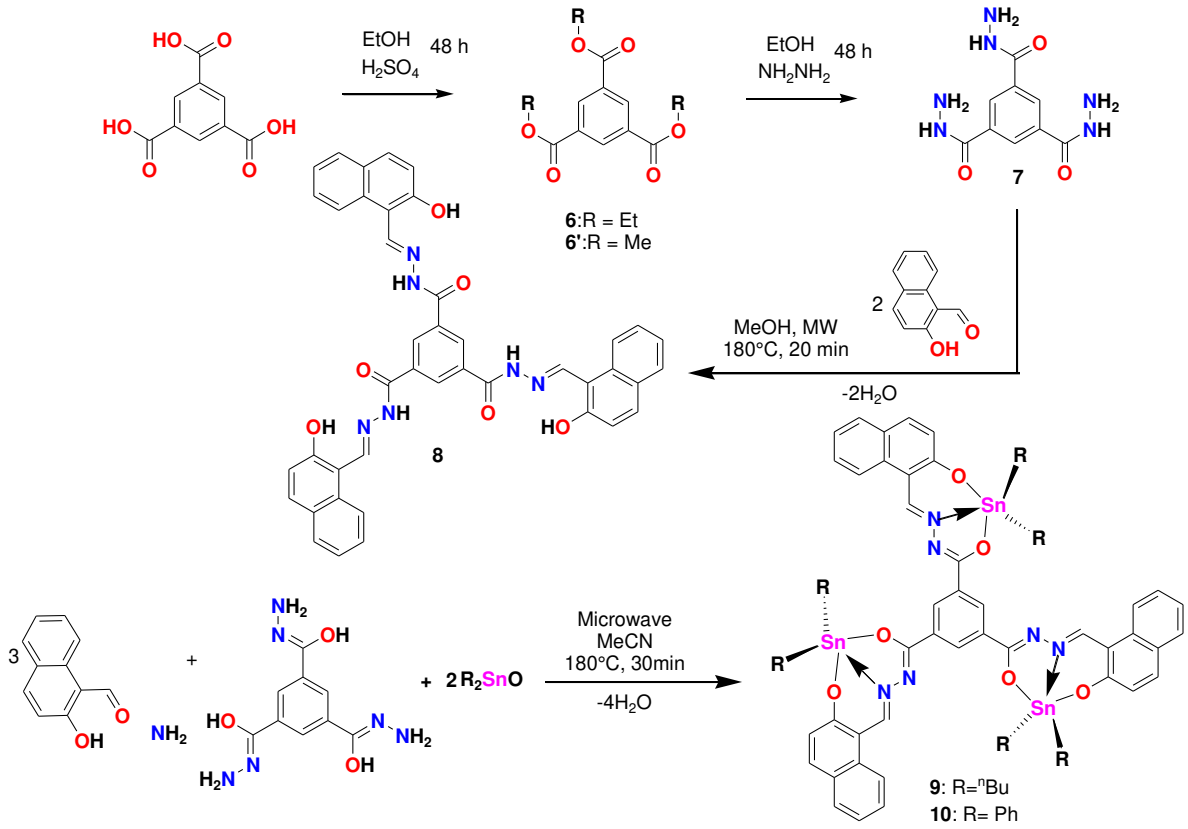

Scheme 2. Rote of synthesis of the new organotin trinuclear compounds derivatives from Schiff base.

4.9. The general procedure of synthesis of precursor.

4.9.1. Synthesis of Diethyl Terephthalate. (1)

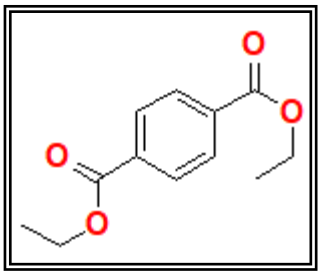

Terephthalic acid (1.6 g) in super dry ethanol (60 mL) containing 2-3 drops of conc. H_2SO_4 (AR) was refluxed till it dissolves. Then, the reaction mixture was poured on to ice cold water, immediately a solid started separating from the clear solution. Then sodium bicarbonate was used for the neutralization of excess acid. Addition of sodium bicarbonate was continued till the effervescence seized. The ester was filtered, washed several times with water, and dried in air. Yield: 84% (0.57 g). M.P. 44 °C. ^{1}H NMR (400.13 MHz, $CDCl_3$, 25°C): δ= 1.42 (t, *J* =7.0, 6H; CH3), 4.40 (q, *J*=7.7, 4H; CH2), 8.10 ppm (s, 4H, aryl). (Lit.[32] M.P. 44.5 °C)

*4.9.2. Synthesis of terephthalic dihydrazide (**2**) rute 1.*

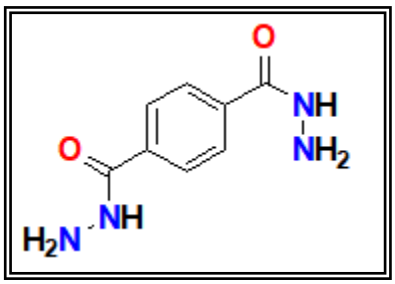

A mixture of diethyl terephthalate 0.5 g (2.25 mmol) was dissolved in 50 mL ethanol and hydrazine monohydrate (1 mL) was added. The reaction

mixture was refluxed for 24 h. The product precipitated from the mixture. After cooling to room temperature, the precipitate was filtered, washed with water thoroughly and dried completely to give solid white powder. Yield 4.27 g (81 %) M.P. >300 °C ^{1}H NMR (400 Mhz, DMSO-d6, 25°C) 9.89 (s, 2H), 7.87 (s, 4H), 4.59 (s, 4H *J*=5.0 Hz). (Lit.[33] M.P. >300 °C)

*4.9.3. Synthesis of terephthalic dihydrazide (**2**) rute 2*

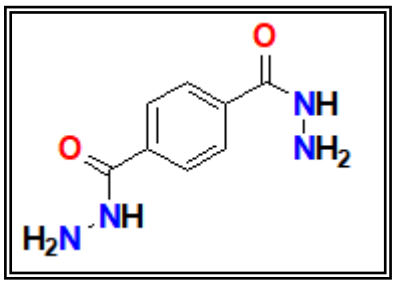

A mixture of dimethyl terephthalate 0.2 g (1.03 mmol) was dissolved in 50 mL methanol and hydrazine monohydrate (0.45 mL) was added. The reaction mixture was refluxed for 24 h. The product precipitated from the mixture. After cooling to room temperature, the precipitate was filtered, washed with water and methanol thoroughly and dried completely to give solid white powder. Yield 0.3g (84 %) M.P. >300 °C ^{1}H NMR (400 Mhz, DMSO-d6, 25°C) 9.87 (s, 2H), 7.86 (s, 4H), 4.54 (s, 4H).

*4.9.4. Synthesis of terephthalic dihydrazide (**2**) rute 3.*

A mixture of dimethyl terephthalate 0.2g (1.03mmol) was dissolved in 5 ml methanol and hydrazine monohydrate (0.45 ml) was added. The reaction mixture

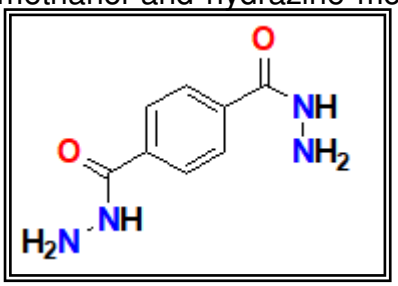

was synthesized by irradiation of microwave for 20 min. The product precipitated from the mixture. After cooling to room temperature, the precipitate was filtered, washed with water and methanol thoroughly and dried completely to give solid white powder. Yield 0.19 g (95%) M.P. 132-136 °C ^{1}H NMR (400 Mhz, DMSO-d6, 25°C) 9.87 (s, 2H), 7.86 (s, 4H), 4.54 (s, 4H).

*4.9.5. Synthesis of 1,3,5-Benzenetricarboxylic Acid Triethyl ester (**6**).*

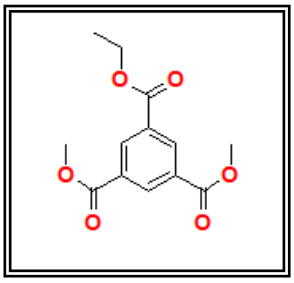

A mixture of trimesic acid (1,3,5-benzenetricarboxylic acid) 0.1g (0.37 mmol) more 1 mL of H_2SO_4 in EtOH in reflux at 80°C by 24 h. the solution was allowed to cool, and the solvent removed in vacuo. The residue was dissolved in dichloromethane (10 ml) and washed with saturated aqueous $NaHCO_3$ (3 10 ml). The organic layer was then dried (Na_2SO_4), giving a sold white. Yield 0.11 g (86 %) M.P. 132- 134°C ^{1}H NMR (400.13 MHz, $CDCl_3$, 25°C) δ= 8.85 (s, 3H), 4.45 (q, 6H, *J*=7.1 Hz), 1.44 (t, 9H, *J*=7.1 Hz). (Lit.[34] M.P. 132-136 °C)

*4.9.6. Synthesis of 1,3,5-Tri[5-phenyl-(1,3,4)-oxadiazol-2-yl] benzene (**7**) (1,3,5-Benzenetricarboxylic Acid Trihydrazide) rute (1).*

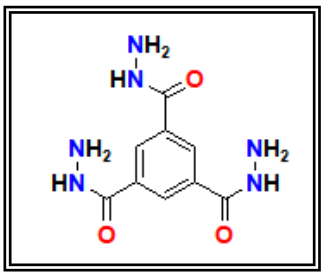

A mixture of 1,3,5-Benzenetricarboxylic acid trimethyl ester 0.5 g (1.98 mmol) was dissolved in 30 ml ethanol and 30 ml toluene under nitrogen atmosphere was added hydrazine hydrate (1.45 mL, 29.70 mmol). The solution was heated at 110 °C for 48 h, and the crude product was precipitated during reaction. The product was collected by filtration and washed with EtOH and toluene to give a white solid (0.46 g, 92%). mp >400 °C. ^{1}H NMR (400 MHz, $DMSOd_6$, δ): 9.83 (s, 3H), 8.30 (s, 3H), 4.57 (br, 6H). (Lit.M.P.[35] >400 °C)

*4.9.7. Synthesis of 1,3,5-Tri[5-phenyl-(1,3,4)-oxadiazol-2-yl]benzene (**7'**) (1,3,5-Benzenetricarboxylic Acid Trihydrazide) rute (2).*

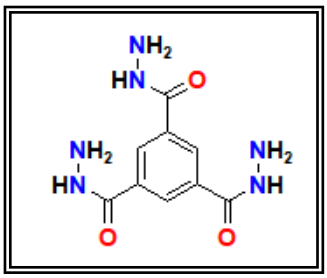

5.8.7. Preparation of **7'** was accomplished following the same procedure of **7** from mixture of 1,3,5-Benzenetricarboxylic acid triethyl ester 0.5 g (1.98 mmol) hydrazine hydrate (1.45 mL, 29.70 mmol) in EtOH. Yield 12.32 g (98%). (4), yield 12.32 g, 98%. Mp 300°C (dec.; lit. >265°C,[13] 300°C[4.6]). δH (DMSO): 9.85 (s, 3H), 8.31 (s, 3H), 5.75 (s, 6H); δC

4.10. The general procedure of synthesis of ligand and organotin compounds 3-5 and 8-10 Schiff base.

*4.10.1. Synthesis of Bis(2-hydroxy-1-naphthaldehyde)terephthalohydrazone(**3**).*

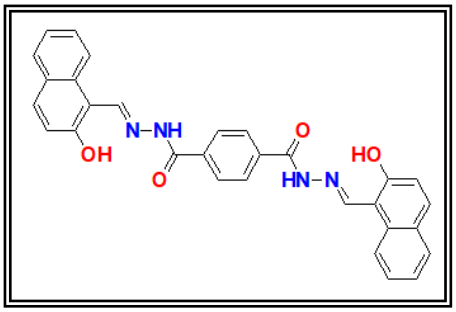

A mixture of terephthalohydrazide 0.100 g (0.51 mmol) and 2- hydroxy-1-naphthaldehyde 0.2047 g (0.10 mmol) was refluxed in methanol for 24 hr. The yellow solid formed was filtered, washed with methanol and vacuum dry. Yield 0.17 g (68 %) M.P. 345 °C $IR_{\upsilon max}$ (ATR): 3189 (s, N-H), 3003 (s, O-H), 1640 (s,

C=O), 1622 (m, C=N) ^{1}H NMR (400 Mhz, DMSO-d6, 25°C) 12.84 (s, 2H, OH), 12.29 (s, 2H, NH), 9.57 (s, 2H, CH), 8.20 (d, *J*=8.0 Hz, 2H, Np), 7.59(t, *J*=7.6 Hz, 2H, Np), 7.40 (t, *J*=7.6 Hz, 2H, Np) 7.21 (d, *J*=8.8 Hz, 2H, Np) EM (TOF) 484.1503 [M+] Found: 502.1641 PPM error: -0.1445

*4.10.2. Synthesis of Bis(2-hydroxy-1-naphthaldehyde)terephthalohydrazone di-n-butyltin(IV) (**4**)*

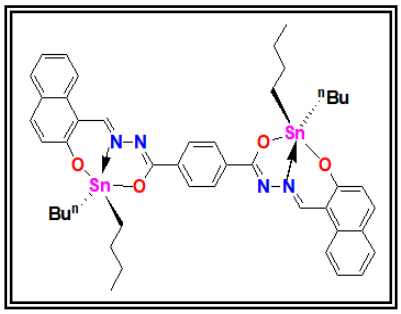

A microwave tube was placed with a magnetic shuffler, it was added terephthalohydrazide 0.05 g (0.25 mmol) and 2-Hydroxy-1-naphthaldehyde 0.08 g (0.51mmol) more dibutylltin oxide 0.12 g (5.51 mmol) in acetonitrile 5ml were heated to 180°C for 20 min. At the end of the heating proceeded to refine the compound to remove the impurities sample. The solvent was then evaporated under reduced pressure and washed with hexane and acetronitrile. The precipitate was collected by filtration and crystalized with dichlorometane/methanol (5:5) for purified, to give 0.23g (0.24 mmol, 96% yield) of 1 as orange-yellow solid. M.P. 172°C $IR_{\upsilon max}$ (ATR) 3057 (C-H ArH), 2326 (O-C=N) 1602 (C=N), 1581 (C=N-N=C), 715 (C-H ArH) UV/vis ($CHCl_3$) λabs/max (nm) [$^{\varepsilon}$max $*10^4$ (M^{-1} cm^{-1})]: 456 [0.08] Fluorescence ($CHCl_3$): λ_{fluor} (nm): 495 ^{1}H RMN (400.13 MHz, $CDCl_3$, 25°C) δ= 9.73 [s, 2H, $^3J(^1H–^{119}Sn)$ = 45.08 Hz H-11], 8.14 (s, 4H, ArH, H-14), 8.09 - 8.11 (d, *J*=12 Hz, 2H, H-9), 7.76-7.78 (d, *J*=8 Hz, 2H, H-4), 7.69-7.71 (d, *J*= 8.0Hz, 2H, H-6), 7.53 (t, *J*= 16 Hz, 2H, H-8), 7.33 (t, *J*= 8Hz 2H, H-7), 6.95-6.97 (d, *J*= 8.0 Hz, 2H, H-3),1.35.1.40 (t, 6H, 3J = 7.2 Hz, CH_3- γ), 0.85-0.89 (m, 4H, CH_2- δ), 1.55-1.59 (t, 4H, 3J = 7.2 Hz, CH_2- α), 1.65-1.71 (m, 4H, 3J = 7.2 Hz, CH_2- β) ^{13}C RMN (100.61 MHz, CDCl3) δ= 13.41 (δ, CH_3,), 26.27 [Cγ, $^3J(^{13}C-^{119}Sn)$ = 83.86Hz] , 26.66, [Cβ, $^2J(^{13}C-^{119}Sn)$ = 33.75Hz],

21.87 [Cα, $^{1}J(^{13}C\text{-}^{119}Sn)$ = 595/568 Hz], 107.24 (C1, 1C), 169.24 (C2, 1C), 119.31 (C3, 1C), 136.81 (C4, 1C), 127.31 (C5, 1C), 128.18 (C6, 1C), 123.15 (C7, 1C), 124.52 (C8, 1C), 129.30 (C9, 1C), 135.97 (C10, 1C), 157.26 (C11, 1C), 168.17 (C12, 1C), 135.83 (C13, 1C), 127.51 (C14, 1C) ^{119}Sn RMN (128.0 MHz, C6D6) δ: -189.28) EM (TOF) 966.2261 [M+] Found: 967 .226181 PPM error: 0.1445

4.10.3. Synthesis of Bis(2-hydroxy-1-naphthaldehyde)terephthalohydrazone di-n- diphenyltin(IV) (5)

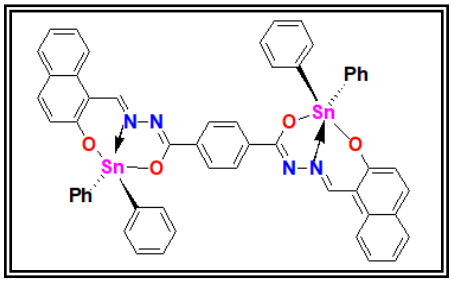

Preparation of **5** was accomplished following the same procedure of **4** from terephthalohydrazide 0.05 g (0.25 mmol) and 2-Hydroxy-1-naphthaldehyde 0.08 g (0.51mmol) more dibutyltin oxide 0.14mg (0.51 mmol) to 180°C for 30 min. Yield: 0.26g (0.25 mmol, 98%). Yellow solid. M.P. 336°C IR_{umax} (ATR) 3065 (C-H ArH), 2326 (O-C=N), 1580 (C-N-N-C), 1596 (C=N), 1582 (C=N-N=C), 715 (C-H ArH) UV/vis ($CHCl_3$) λabs/max (nm) [$^{\varepsilon}$max *10^4 (M^{-1} cm^{-1})]: 453 [0.07] Fluorescence ($CHCl_3$): λ_{fluor} (nm): 491 ^{1}H RMN (9.78 [s, 2H, $^{3}J(^{1}H\text{–}^{119}Sn)$ = 56 Hz H-11],], 8.39 (s, 4H, ArH, H-14), 8.09 - 8.12 (d, *J*=12 Hz, 2H, H-9), 7.91-7.93 (d, *J*=8 Hz, 2H, H-4), 7.73-7.78 (d, *J*= 8.0Hz, 2H, H-6), 7.54 (t, *J*= 16 Hz, 2H, H-8), 7.46 (t, *J*= 8Hz 2H, H-7), 7.42-7.43 (d, ^{3}J= 8.0 Hz, 2H, H-3),7.91 (s, 8H, ^{3}J = 7.2 Hz, H-o), 7.43 (s, 8H, ^{3}J=

8.0 Hz, H-m), 7.45 (s, 4H, ^{3}J=8.0 Hz,H-p ^{13}C RMN (100.61 MHz, CDCl3) δ= 136.39 (H-o,), 130.76 (H-m), 133.94 (H-p), 137.39 (C-i) 107.82(C1, 1C), 169.94 (C2, 1C), 119.75 (C3, 1C), 141.44 (C4, 1C), 127.61 (C5, 1C), 127.61 (C6, 1C), 123.54 (C7, 1C), 124.62 (C8, 1C), 129.37 (C9, 1C), 134.00 (C10, 1C), 157.98 (C11, 1C), 167.85 (C12, 1C), 139.13 (C13, 1C), 128.45 (C14, 1C) ^{119}Sn RMN (100.7 MHz, C6D6) δ: -328.69 HRMS (APCI/TOF-Q) m/z: Calcd. For $C_{37}H_{37}NO_2Sn$ [M^+] 1046.0900 Found: 1047.1009 u.m.a. (Error: -0.8524 ppm)

4.10.4. Synthesis of 1, 3, 5-Benzene-tricarbohydrazide (8).

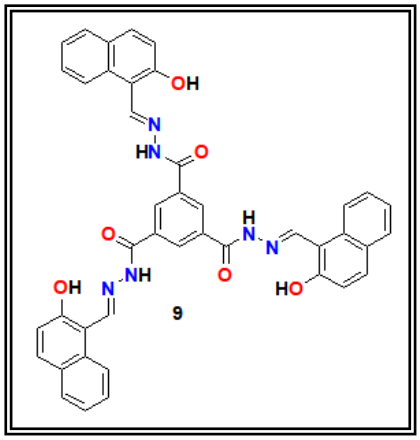

9

Preparation of **8** was accomplished following the same procedure of **3** from 1,3,5-benzenetricarboxylic 0.100 g (0.39 mmol) and 2-hydroxy-1-naphthaldehyde 0.2047 g (1.18 mmol). Yield 0.17 g (83 %) M.P. >400 °C $IR_{\upsilon max}$ (ATR): 3312-3118 (s, N-H), 3115-2900 (s, O-H), 1641 (s, C=O), 1625 (m, C=N) 12.70 (s, 2H, OH), 12.62 (s, 2H, CH), 9.57 (s, 2H, NH), 8.88 (d, *J*=8.0 Hz, 2H, Np), 7.95-7.98(d-d, *J*=7.6 Hz, 2H, Np), 7.91-7.92 (d-d, *J*=7.6 Hz, 2H, Np) 7.63 (d, *J*=8.8 Hz, 2H, Np) 7.43-7.44(dd, 3H4, J = 7.6 Hz) , 7.25-7.28 (dd, 3H1, J = 8.8 Hz). EM (TOF) Calcd. For $C_{42}H_{30}N_6O_6Sn$ [M^+] 714.2227 [M+] Found: 715.2299 PPM error: -0.0874

4.10.5. Synthesis of Tri(2-hydroxy-1-naphthaldehyde) 1, 3, 5- Benzene-tricarbohydrazide. Tri-n-butyltin (IV) 9.

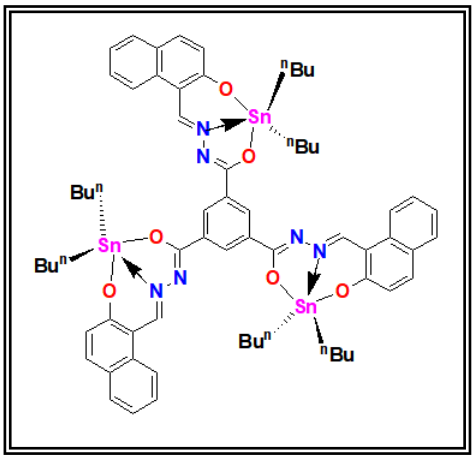

Preparation of **4** was accomplished following the same procedure of **9** from 1,3,5-benzenetricarboxylic acid trihidrazide 0.05 g (0.19 mmol) and 2-Hydroxy-1-naphthaldehyde 0.10 g (0.59mmol) more dibutyl tin oxide 0.14 g (0.59 mol) to 190°C for 30 min. Yield: 0.25g (0.18 mmol, 93%) as bright yellow solid. M.P. 86 °C $IR_{\upsilon max}$ (ATR) 3058 (C-H ArH), 2338 (O-C=N) 1608 (C=N), 776 (C-H ArH) UV/vis ($CHCl_3$) λabs/max (nm) [$^{\varepsilon}$max *10^4 (M^{-1} cm^{-1})]: 446 [0.08] Fluorescence ($CHCl_3$): λ_{fluor} (nm): 486 ^{1}H RMN (400.13 MHz, $CDCl_3$, 25°C) δ= 9.73 [s, 2H, $^3J(^1H–^{119}Sn)$ = 44.88Hz H-11], 8.85 (s, 4H, ArH, H-14), 8.03 - 8.05 (d, *J*=8 Hz, 2H, H-9), 7.68-7.70 (d, *J*=8 Hz, 2H, H-4), 7.61-7.63 (d, *J*= 8.0Hz, 2H, H-6), 7.46 (t, *J*= 16 Hz, 2H, H-8), 7.24 (t, *J*= 16Hz, 2H, H-7), 6.88-6.90 (d, *J*= 8.0 Hz, 2H, H-3),1.29-1.34 (t, 6H, 3J = 7.2 Hz, CH_3- γ), 0.78-0.83 (m, 4H, CH_2- δ), 1.50-1.54 (t, 4H, 3J = 7.2 Hz, CH_2- α), 1.60-1.68 (m, 4H, 3J = 7.2 Hz, CH_2- β) ^{13}C RMN (100.61 MHz, CDCl3) δ= 13.41 (δ, CH_3,), 26.64 [Cγ, $^3J(^{13}C-^{119}Sn)$ = 81.44 6Hz] , 27.04, [Cβ, $^2J(^{13}C-^{119}Sn)$ = 34 Hz], 22.28 [Cα, $^1J(^{13}C-^{119}Sn)$ = 594/567 Hz], 107.22 (C1, 1C), 169.00 (C2, 1C), 119.31 (C3, 1C), 136.75 (C4, 1C), 127.30 (C5, 1C), 128.97 (C6, 1C), 123.18 (C7, 1C), 124.53 (C8, 1C), 129.30 (C9, 1C), 134.17 (C10, 1C), 157.35 (C11, 1C), 168.06 (C12, 1C), 134.01 (C13, 1C),

128.30 (C14, 1C) ^{119}Sn RMN (128.0 MHz, C6D6) δ: -192.30) EM (TOF) 966.2261 [M+] Found: 967 .226181 PPM error: 0.1445

4.10.6. Synthesis of Tri(2-hydroxy-1-naphthaldehyde) 1, 3, 5- Benzene-tricarbohydrazide. Tri-n- diphenyltin (IV) ***10****.*

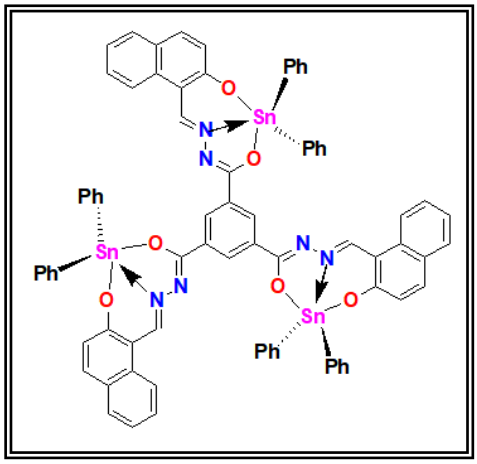

Preparation of **4** was accomplished following the same procedure of **10** from 1,3,5-benzenetricarboxylic acid trihidrazide 0.05 g (0.19 mmol) and 2-Hydroxy-1-naphthaldehyde 0.10 g (0.59mmol) more diphenyltin oxide 0.7mg (0.59 mmol) Yield: 0.28g (0.18 mmol, 95%) 180°C for 25 min. of **10** as a yellow solid. M.P. 336°C IRυmax (ATR) 3055 (C-H ArH), 2313 (O-C=N), 1580 (C-N-N-C), 1580 (C=N), 773 (C-H ArH) UV/vis (CHCl3) λabs/max (nm) [εmax *104 (M-1 cm-1)]: 442 [0.07] Fluorescence (CHCl3): λfluor (nm): 482 1H RMN (9.90 [s, 2H, 3J(1H–119Sn) = 56 Hz H-11], 9.25(s, 4H, ArH, H-14), 8.16 - 8.18 (d, J=8 Hz, 2H, H-9), 8.01 (d, J=8 Hz, 2H, H-4), 7.73-7.90 (d, J= 8.0Hz, 2H, H-6), 7.55 (t, J= 16 Hz, 2H, H-8), 7.34 (t, J= 8Hz 2H, H-7), 7.28-7.31 (d, 3J= 8.0 Hz, 2H, H-3),7.99 (s, 8H, 3J = 7.2 Hz, H-o), 7.45 (s, 8H, 3J= 8.0 Hz, H-m), 7.47 (s, 4H, 3J=8.0 Hz,H-p 13C RMN (100.61 MHz, CDCl3) δ= 136.39 (H-o,), 129.15(H-m), 130.76 (H-p), 137.40 (C-i) 107.58(C1, 1C), 169.78 (C2, 1C), 119.60 (C3, 1C), 141.43 (C4, 1C), 127.62 (C5, 1C), 129.35 (C6, 1C), 123.55 (C7, 1C), 124.64 (C8, 1C), 129.54 (C9, 1C), 134.00 (C10, 1C), 157.88 (C11, 1C), 167.72 (C12, 1C), 139.13 (C13, 1C), 127.51 (C14,

1C) 119Sn RMN (100.7 MHz, C_6D_6) δ: -328.69 HRMS (APCI/TOF-Q) m/z: Calcd. For C78H54N6O6Sn3 [M+] 1530.1171 Found: 1531.1243 u.m.a. (Error: -0.0003 ppm)

4.11. Synthesis under microwave irradiation.

The organotin compounds **4**-**5** and **9**-**10** were synthesized under microwave irradiation and condensation reaction for comparison purposes as is indicated in the Scheme 3.

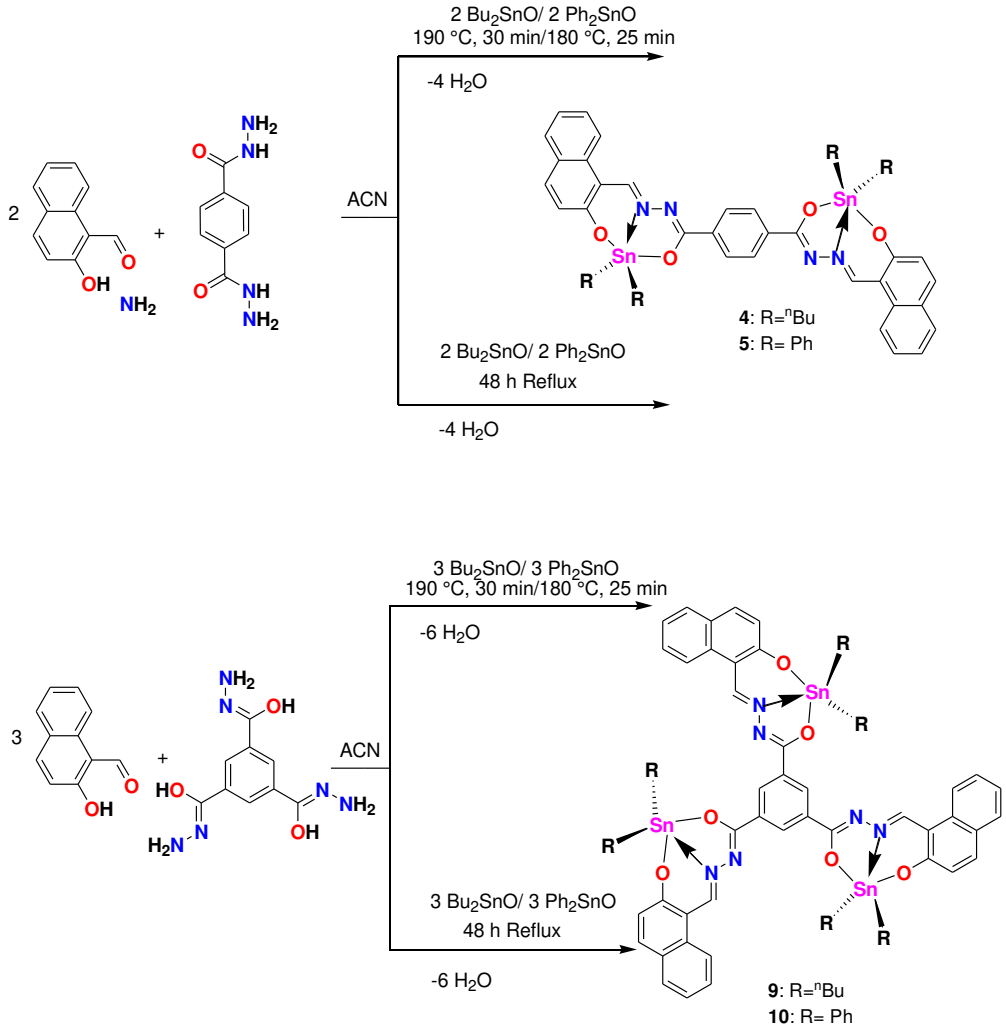

Scheme 3. Rutes of synthesis for comparison purposes of the new organotin compounds.

4.12. Disposal of waste generated.

Hazardous wastes generated in the condensation reactions and microwave irradiation as well as for the work up acetonitrile, as well as for the work up: hexane, acetone, ethyl acetate, were collected in the container C, which is assigned for halogen free-solvents. Waste of solvents like chloroform and dichloromethane were collected in container D, which is assigned for halogen containing solvents.

5. RESULTS AND DISCUSSION.

5.1 Synthesis.

We carried out the synthesis of organotin compounds **4**-**5** and **9**-**10** (Figure **7**) by multicomponent reaction through irradiation with terephthalohydrazide/1,3,5-Benzenetricarboxylic Acid Trihydrazide, 2-hydroxynaphtalehyde, and diphenyl/dibutyltin oxide in stoichiometric ratio (1:2:2) for **5** and **6**, (1:3:3) for **11** and **12** in acetonitrile for 48 hours and yields reaction of 75-76 % The products were obtained after filtration reaction crude. The compounds were recrystallized in chloroform.

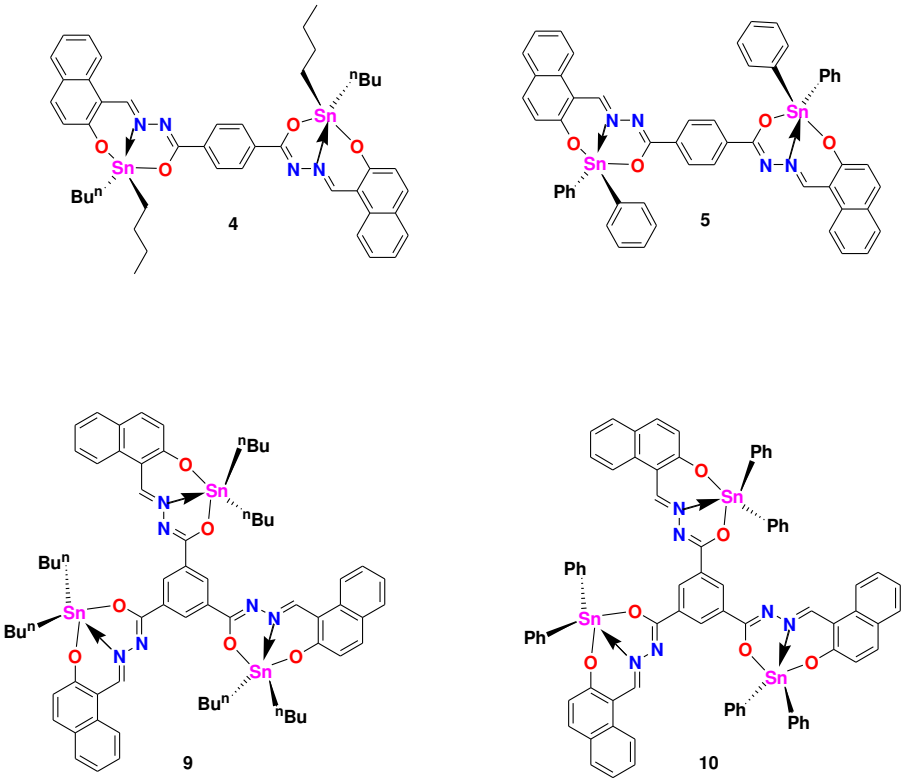

Figure 7. Organotin compounds **4**-**5** and **9**-**10.**

All compounds were completely soluble in common organic solvents such as dichloromethane, chloroform, and tetrahydrofuran and partially soluble in methanol and ethanol, while ligand **3** and **8** just in dimethyl sulfoxide. The high solubility of the ligands in a polar solvent, is due to the presence of functional groups like hydroxyl (-OH), and amino ($-NH_2$), that makes the molecules more polar and presents more affinity for polar solvents like DMSO.

The organotin compounds were obtained in suitable yields after 48 h. Better yields and time reactions were determinate for tin compounds **4**-**5** and **9**-**10** when

the microwave irradiation is used. A comparison about both methods are summarized on Table 1.

Table 1. Comparison of the time reaction and yields from different methods of compounds **4**-**5** and **9**-**10**.

Comp	Yield [%]		Reaction time [min]	
	Conve	Microw	Conve	Microw
4	85	96	2880	20
5	86	98	2880	30
9	84	93	2880	30
10	85	95	2880	25

The reaction yields were increased around 91 to 98%. The most important change was, the reaction time which decreased around of 90 times in comparison with the conventional synthesis, in addition, the solvent used is reduced and with the multicomponent method the complex can be carried out in a single step.

5.2 Chemical structures elucidation.

5.2.1. Analysis of NMR data.

^{1}H-NMR spectra confirmed the formation of Schiff bases for the **3** and **8** (See Appendix) with signals for H-11 at 9.51 and 10.52 ppm respectively, which are according to reported.[36] In the range 9.51 to 9.57 ppm and 12.70 to 12.75 and 12.37 to 12.62 ppm were assigned to OH and NH protons, these signals are

displaced to high δ values due to highly electronegative of atom oxygen and nitrogen. The Figure 8 shows ^{1}H-NMR spectra for **3** as example.

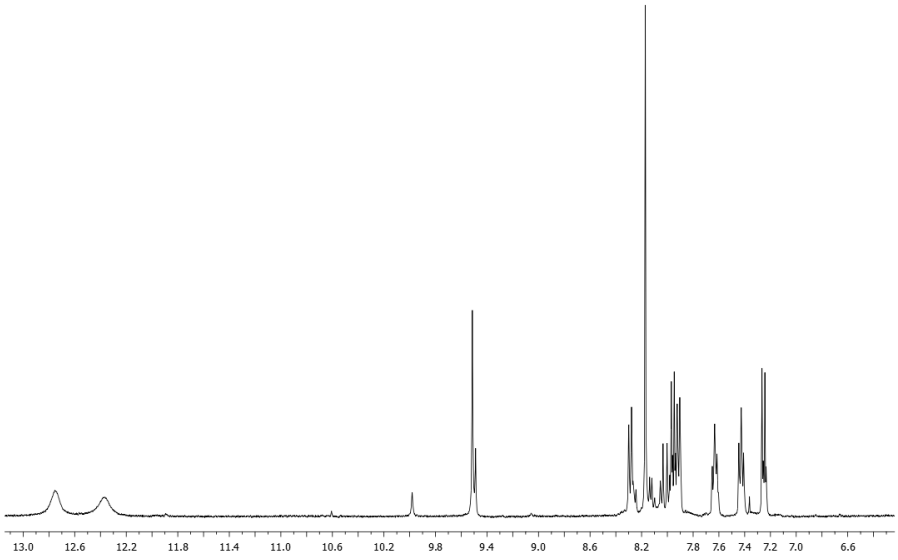

Figure 8. ^{1}H NMR spectrum of ligand **3.**

By comparison, the ligands and organotin compound, we can see the signal 11 in the spectrum shift to lower more frequencies from 9.73 to 9.90 ppm with a constant couple from $^{3}J(^{1}H,^{119}Sn)$ = 45 to 56 Hz[37] for the compounds. This signal is typical from an imine proton according to the reports from Santillan *et al*.[38] this is due to the existence of the N→Sn coordination bond evidenced by ^{119} Sn NMR spectra indicative of pentacoordinate tin atoms.[39] (Figure 9 and 10)

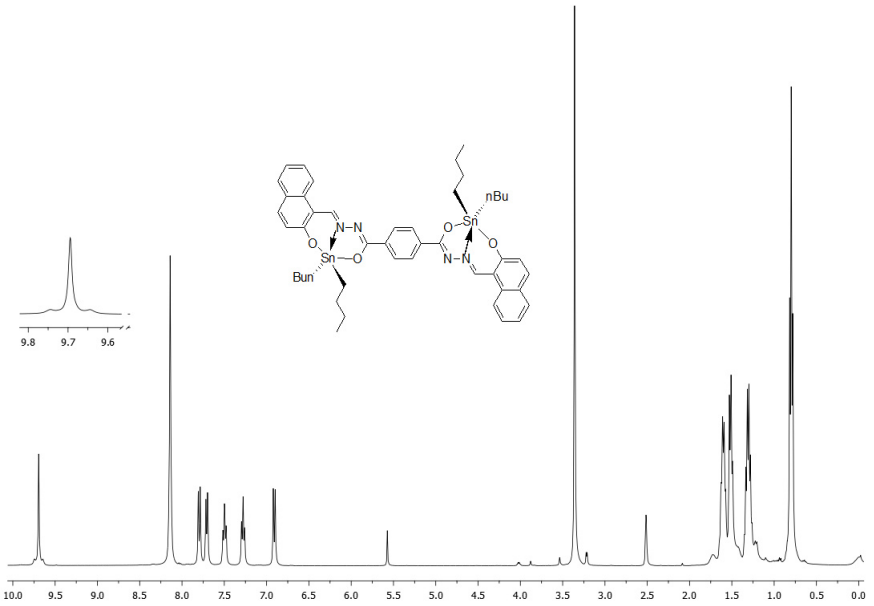

Figure 9. ^{1}H NMR spectrum of organotin compound **4**.

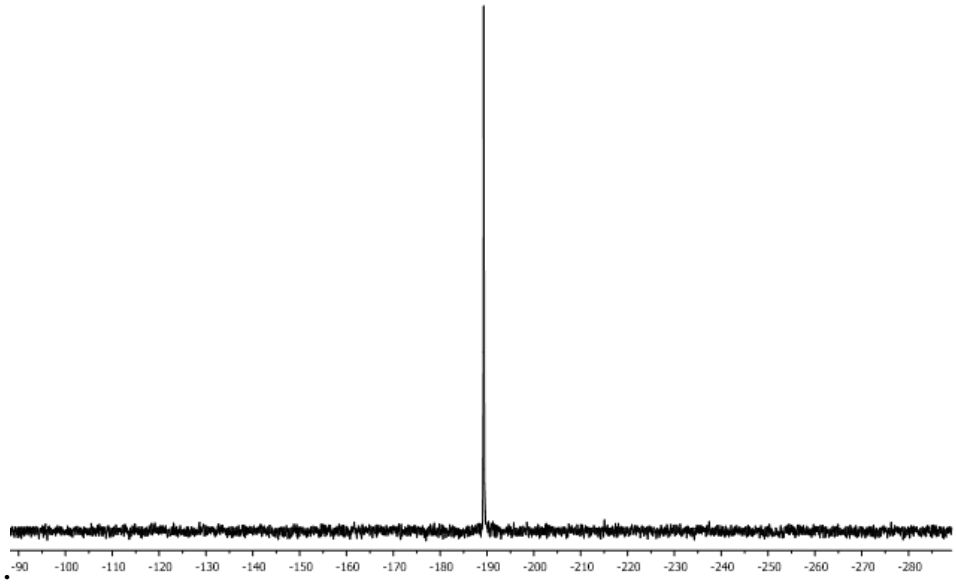

Figure 10. ^{119} Sn NMR spectrum of organotin compound **4.**

In addition, a singlet for 14 indicates the protons the ring aromatic central around from 8.14 to 9.25 ppm that integrates for 4 and 3 hydrogens for complex

with symmetry C2 and C3 respectively. The signals for the substituents $^{n}Bu_2SnO$ appear in the range aliphatic the spectrum while the substituents Ph_2SnO in the range aromatic. The coupling the ortho protons due to the approach the tin atom is appreciated. The Table 2. shows in resume these signals.

Table 2. Signals for the protons $^{n}Bu_2SnO$ and Ph_2SnO.

Comp	**CH_2-α**	**CH_2-**	**CH_2-**	**CH_3-**
4	1.55-	1.65-	1.35-	0.85-
5	-	7.91	7.43	7.45
9	1.50-	1.60-	1.29-	0.78-
10	-	7.99	7.45	7.47

In the ^{13}C NMR spectra the signals for C-11 (C=N) around to 157 ppm with a constant couple ^{2}J (^{13}C, ^{119}Sn) from 67 to 79 Hz, the signal for C-14 corresponds to the signal from 127.51 to 129.34 ppm. In addition, the four signals for chain of dibutyltin α, β, γ and δ are the region aliphatic, for the phenyls, the signals are in the region aromatic, C-ipso, C-ortho, C-meta and C-para with the respectively constant couple with allow assign the signals. Electronic density of ring aromatic is affected by *ortho* and *para* carbons. The chemical environment of the carbons coordinated with the tin atom of this is different with respect to the carbonyl of the ligand, although the effect deprotection is small indicates that the effect is coordinated with the tin atom. The dates for ^{13}C RMN are in the Table 3.

Table 3. Chemical shifts of groups linked to tin atom $^{n}Bu_2SnO$ and Ph_2SnO.

Comp	C-α/C-i	C-β/C-	C-γ/C-	C-δ/C-
4	1.55-	1.65-	1.35-	0.85-
5	-	7.91	7.43	7.45
9	22.28	27.04	26.64	13.41
10	137.39	136.39	130.76	133.94

5.2.2. Analysis of IR.

The IR spectral analysis realized in solid state (See Appendix), showed the imine (C=N) stretching vibration bands for ligands to 1625 cm^{-1} while for the compounds the range from 1600 to 1608 cm^{-1}. This shift is due to the coordination of the imine nitrogen to the central tin atom;[40] therefore, we can conclude there is a decrease in force when the new dative link is formed. In addition, for the ligand, the stretching vibration bands of N–H, O–H and C=O disappear from the spectra of complexes due to the deprotonation of the –OH by the coordination with the central atom, and C=O confirm that the ligand coordinates with the tin in the enol form. Besides, we can see the presence of a C=N–N=C group[41] for the complex around to 1599-1585 cm^{-1}. The stretching vibration bands of N–H, O–H and C=O. (Table 4)

Table 4. **IR data of ligands and compounds in cm^{-1}**

	3	**4**	**6**	**8**	**9**	**1**
C=	1622	16	1	162	1	1
N-	3318-			331		
O-	3250-			325		
C=	1642			163		
C-	3066-	30	3	306	3	3
C-	3056	29		162	2	
O-	2313	23	2	231	2	2

5.2.3. High resolution mass spectrometry analysis.

The mass spectra of the molecules (See Appendix), were obtained by time of flight method (TOF). The high-resolution mass spectrum confirms the expected molecular ion peak (**3**: 534.2267, **4**: 967.2261, **5**: 1047.1009, **8**: 715.2299, **9**: 1410.3049, **10**: 1531.124357)

The compounds **5** and **10** showed the peak base corresponds to the molecular ion peak and it is consistent with the theoretical molecular mass, for **3** and **8** the ion peak correspond to the loss one tin and its butyl chain. Besides, the isotopic distribution of parent ions in the spectra demonstrated the presence of two atoms of tin in the organotin 4. The comparison of predicted theoretical and

experimental isotopic distributions of spectra for compound 4 is given in Figure 11. For the trinuclear compounds the signals for three tin atoms can be observed (See Appendix)

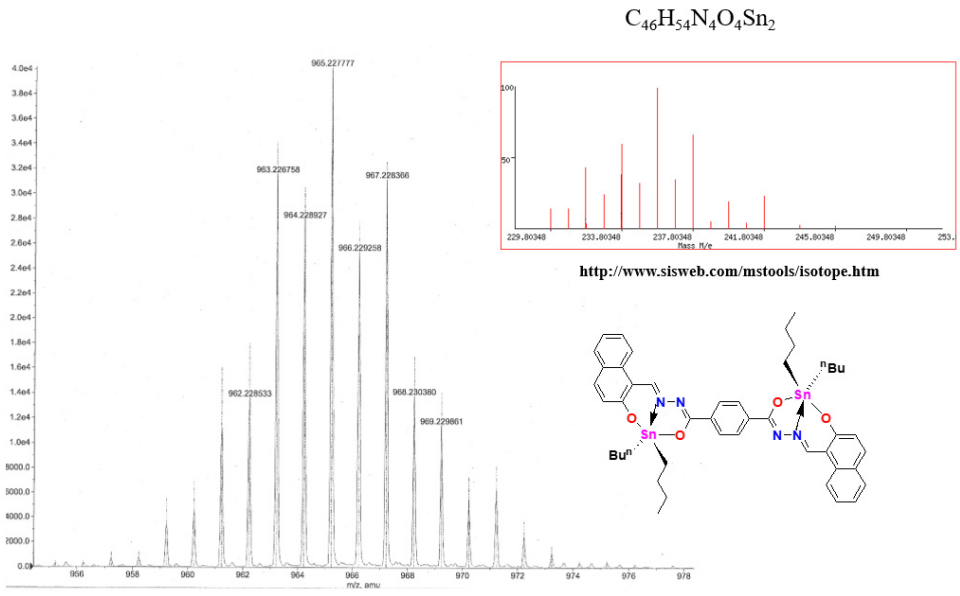

Figure 11. Isotopic pattern of compound **4.**

5.2.4. X-ray single analysis.

The structure of compounds **4** (See Appendix) and **5** are represented by the ellipsoid plot. (Figure 12). Crystal data were determined by single crystal X-ray diffraction analysis (Table 5). Selected bond length and angles are listed in Table 6. The structures of compounds **4** and **5** belong to the system triclinic space group P-1

The structures **4** and **5** contains binuclear diorganotin structure with trans conformation, the oxygen atoms are in axial position **4**: Sn-O1 2.092(2), Sn-O2 2.136(2) Å , (**6**: Sn-O1 2.0688(11), Sn-O2 2.1205(11) Å and nitrogen atom forms a coordination bond with the tin atom in an equatorial position, the central tin atoms are five-coordinated with distorted trigonal bipyramidal molecular geometry (O–Sn–O range angle **4**:1554.35°, **5**: 156.00°, C–Sn–C **4**: 128.6°, **5**: 123.84°), results from strained five-membered Sn–N–N–C–O chelate ring. The coordinate bonds N→Sn is a length the **4**: 2.161(2) Å, **5**: 2.1409(13) Å. for **4** and **5** respectively, these bonds are shorter that similar molecules reported.[42]

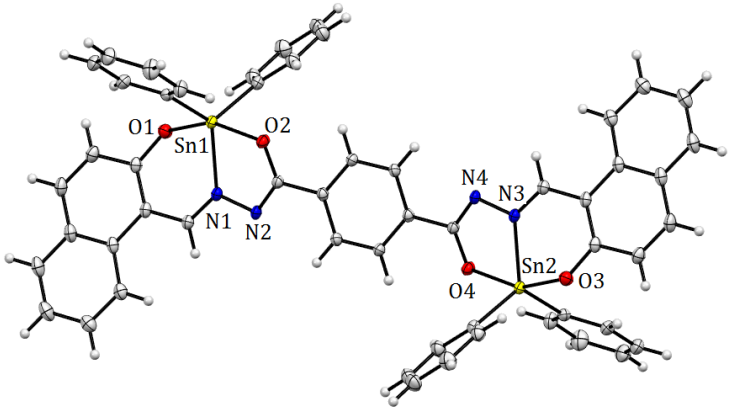

Figure 12. Molecular structure of **5.**

Additionally, the X-ray structure provide the molecular constitution with a planar system and show π-stacking as a dimer with a π-π distance of 3.47 Å (Figure 13). Moreover, the compound **5** shows the formation of a 1D chain through C-H(19)•••π-system (C-27) 2.851 Å intermolecular interactions In general, the crystallographic data obtained are comparable with related organotin complexes.[43]

Table 5. **Crystal data of compounds** 4 **and** 5**.**

	4	**5**
Empi	$C_{46}H_{54}N_4O_4Sn_2$	$C_{54}H_{38}N_4O_4S$
Form	964.31	1044.26
Tem	293(2)	293(2)
Wav	0.71073	0.71073
Cryst	Triclinic	Triclinic
Spac	P-1	P-1
a, Å	9.1440 (6)	9.1150 (8)
b, Å	10.8028 (7)	10.5354 (9)
c, Å	12.6767 (8)	12.3958 (11)
α	75.878 (2)	80.286(2)
β	71.479 (2)	71.486(2)
γ	68.949 (2)	68.711(2)
V, $Å^3$	1096.12 (12)	1055.35(16)
Z	1	1
$\rho_{calc,}$	1.461	1.643
μ,	1.185	1.239
2θ	2.852-27.098	3.376-
Inde	$-11 \leq h \leq 11$,	$-12 \leq h \leq 13$,
	$-13 \leq k \leq 13$,	$-15 \leq k \leq 15$,
	$-16 \leq l \leq 16$	$-17 \leq l \leq 17$
No.	11740	14656
No.	4823	6385
[R_{int}]	0.0215	0.0185
Goo	1.079	1.057
*R*1,	0.0337/0.0886	0.0216/0.054
*R*1,	0.0410/0.0945	0.0239/0.055

Table 6. Selected bond distances (Å) and angles (º) of compounds **4** and **5**.

bond	4	5	Angles	4	5
Sn(1)-	2.	2.14	O(1)-Sn(1)-	154.	156.0
Sn(1)-	2.	2.12	O(1)-Sn(1)-	98.5	97.86
Sn(1)-	2.	2.06	O(2)-Sn(1)-	95.6	96.61
Sn(1)C(	2.	2.10	O(1)-Sn(1)-	93.8	96.05
Sn(1)-	2.	2.12	O(2)-Sn(1)-	97.1	91.64
N(1)-	1.	1.30	O(1)-Sn(1)-	82.0	
N(2)-	1.	1.31	O(2)-Sn(1)-	73.0	73.69
C(2)-	1.	1.32	C(16)-	110.	117.9
C(1)-	1.	1.43	C(20)-	120.	117.7
C(12)-	1.	1.30	C(16)-	128.	123.8
N(1)-	1.	1.39			

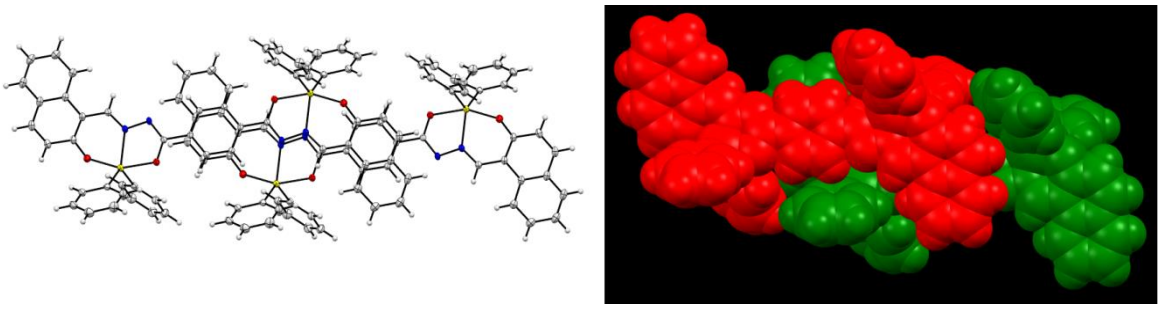

Figure 13. Molecular structure of **5** showing intermolecular interactions.

5.2.5. Optical properties.

The intrinsic photophysical properties of complexes were studied in chloroform and collected in Table 7. The ligands **3** and **8** are only soluble in DMSO, so its photophysical properties in solution were not investigated. The Figure 14 shows the absorption fluorescence spectra of tin complexes in chloroform. Compounds present two UV peaks (**4** and **5**/**9** and **10**) at 338/335 nm and at 346/350 nm, which are ascribed to intraligand electronic transitions and two peaks in the visible at 442/453 nm and 472/484 nm. This main peak nm is due to the HOMO-LUMO electronic transition of ligand-to-metal type and is found with no significant shift between the two complexes indicating that the phenyls and butyls ligands do not participate in the electronic delocalization of the

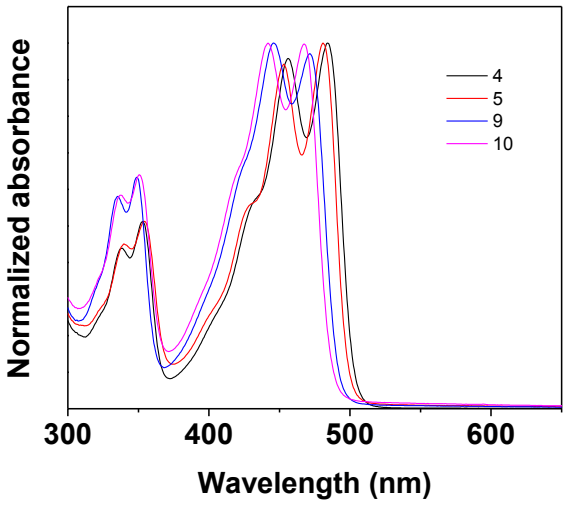

Figure 14. UV-vis of organotin compounds.

HOMO and LUMO orbitals, as previously found for other Sn complexes. The other peak in the visible around 442 at 456 nm can be associated with a vibrionic replica with spacing of 27 nm with respect to the (0,0) excitonic peak. The optical band gap was almost equivalent, ~2.5 eV, that belongs to the semiconducting range

Table 7. Photophysical properties of organotin derivatives **5**, **6** and ligand **4**.

		λ_{abs} (nm)	ε*	Eg (eV)	λ_{em} (nm)	$\Delta\nu$ (cm^{-1})	ϕ (%)	τ (ns)	Knr 10^9 s^{-1}	Krad 10^9 s^{-1}*
3	powder									
4	$CHCl_3$	337, 353, 456,**483**	$7.89*10^4$ M^1 cm^{-1}	2.45	495, 528	502	35.0	1.82	0.19	0.36
5	$CHCl_3$	337, 353, 452, **479**	$4.27*10^4$ M^1 cm^{-1}	2.49	488, 523	385	49.5	2.13	0.23	0.24
8	powder									
9	$CHCl_3$	337, 353, 446,**472**	$6.84*10^4$ M^1 cm^{-1}	2.51	486, 517	610	52.39	0.17	0.17	0.15
10	$CHCl_3$	337, 353, 442, **468**	$2.12*10^4$ M^1 cm^{-1}	2.54	482, 512	620	51.68	0.16	0.16	0.15

*calculated on the bold marked wavelength

.

The fluorescence spectra are quite mirror-like with respect to the visible part of the absorption spectra, presenting two peaks; a maximum at 486/495 nm and a replica 528/523 nm being the spacing equal to 33/35 nm, similar to the values found in the absorption spectra. (Fig. 15a). The corresponding excitation spectra are identical and match well the absorption spectra. Moreover (Fig. 15b)., the fluorescence spectra do not change with the excitation wavelength (Fig. 16). From all these results, it is deduced that there is only one emitting state.

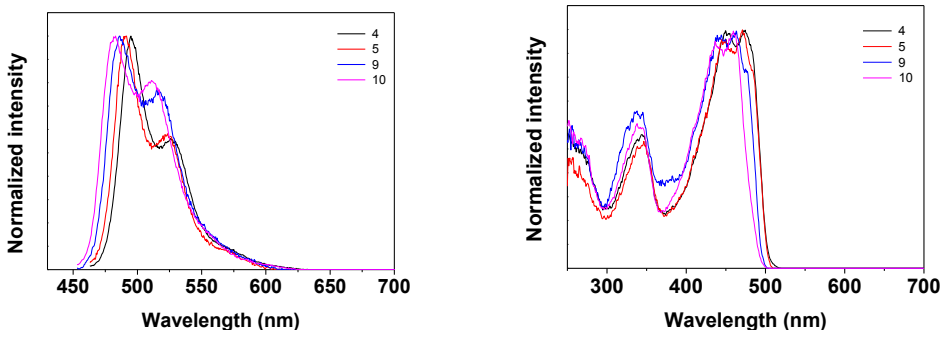

Figure 15. a) Emision espectra and b) excitation spectra of organotin compounds.

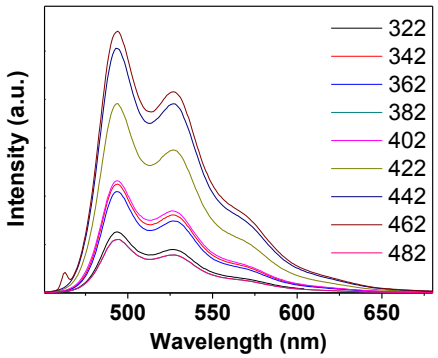

Figure 16. Excitation spectra of organotin compounds.

In general, the optical properties are similar to those previously reported for mononuclear Sn complexes derived from [N-(2-Oxido-1-naphthaldehyde)-4-hydroxybenzyhydrazidate][44] but with redshifts in the absorption and emission maxima indicating an increase in the effective conjugation length, i.e the complexes Sn units are electronically interacting. The fluorescence quantum yields are also in the same range, with even shorter Stokes' shifts Δ. The extremely small Δ values reveal that the geometry is maintained after excitation. The deviation from the unity for the fluorescence quantum yield is thus expected to be mainly due to competitive processes different from internal conversion. It is evident that there is a large overlapping between the absorption and emission spectra. This suggests that the emitted light can be re-absorbed. Intersystem crossing to triplet states can be also possible. The fluorescence decays can be well fitted by a monoexponential curve with lifetime τ of ~ 2ns (Fig. 17).

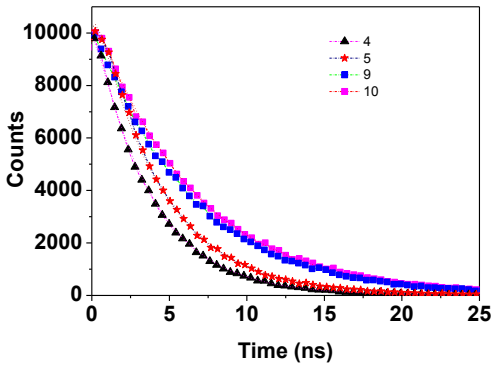

Figure 17. Fluorescence decays spectra of organotin compounds.

Due to the good quantum yields and previous results reported for other Sn complexes,[22,45] the feasibility of obtaining good optical quality films for optoelectronic applications was investigated.

5.2.6 Thermal analysis.

Simultaneous analysis of thermal stability of tin compounds **4**-**5** and **8**-**10** were determined by differential thermal analysis (DTA) and thermogravimetric analysis (TGA) in the temperature range 25 to 600 °C under a nitrogen atmosphere. The melting transition (Tm) and decomposition temperature (Td5) are summarized in Table 8. The Figure 18 show the decomposition temperature curves for the compounds which exhibited thermal stability in the range of 210-308 °C. which is a requirement for those tin compounds that wants to be deposited by thermal evaporation.

Table 8. Thermal data (°C) of organotin derivatives **5** and **6**.

Compound	T_o	T_{d5}	T_{max}	T_m	T_f
4	281	329	382	172	635
5	299	356	386	336	637
9	278	321	396	86	639
10	310	348	398	340	630

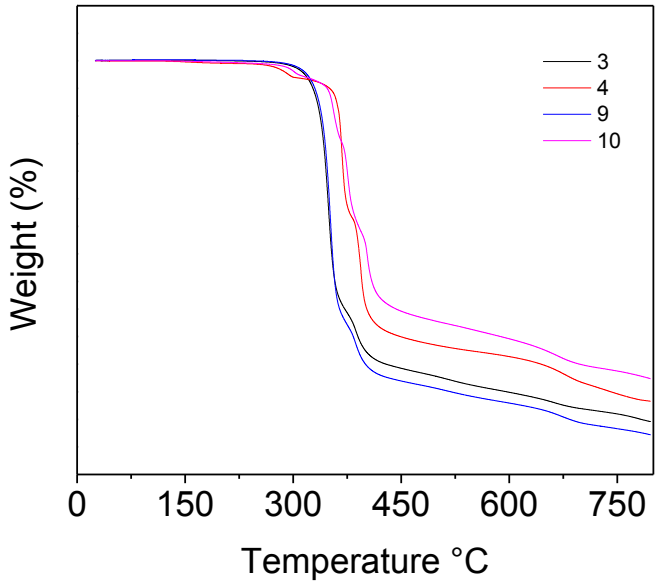

Figure 18. TGA thermograms of tin compounds.

5.2.7 Characterization of film.

The shape of the absorption peaks is the same as that of the solutions, having visible absorptions with the typical appearance of an excitonic spectrum and weaker UV bands. There is a bathochromic displacement of the maxima, in all cases, with respect to the solutions, which is consistent with what are known as solid state effects, i.e. the presence of intermolecular interactions. Unfortunately complexes **5** and **10** could not form thin films of the thickness that is required for light emitting diodes or solar cells (100-150 nm) as its solubility is limited to 5 g/L. On the contrary, complex **4** and **9** can be dissolved in concentrated solutions (5-30

g/L) from different solvents (chloroform, dichloromethane, THF, chlorobenzene). (Fig 19.)

The UV-Vis spectra in films (Figure 24) are similar to those studied in solution but the maxima are slightly red shifted, which is due to intermolecular interactions occurring in solid state. (Table 7)

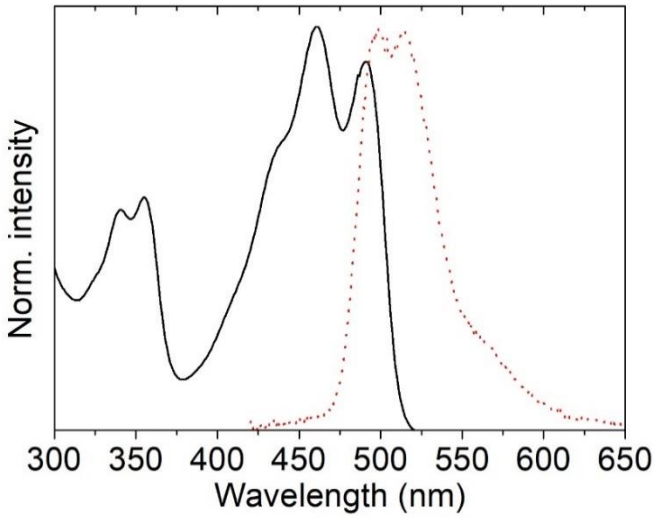

Figure 19. UV-vis (solid line) and fluorescence (dotted line) spectra of a spun film of organotin compound **5**.

5.2.8. Atomic force microscope.

The morphological study of the films was done by AFM in tapping mode, as can be seen in figure 13. The thickness of the film for **4** was around 100 nm and is observed, a homogeneous layer with agglomerates of different morphology and size that persist in areas of 5 * 5 μm^2, giving a roughness in this area of 1188 nm, a

little higher than that observed on the compound **5**. The section study gives a thickness of 139.4 nm, more akin to the desired thickness for diodes. (Figure 20)

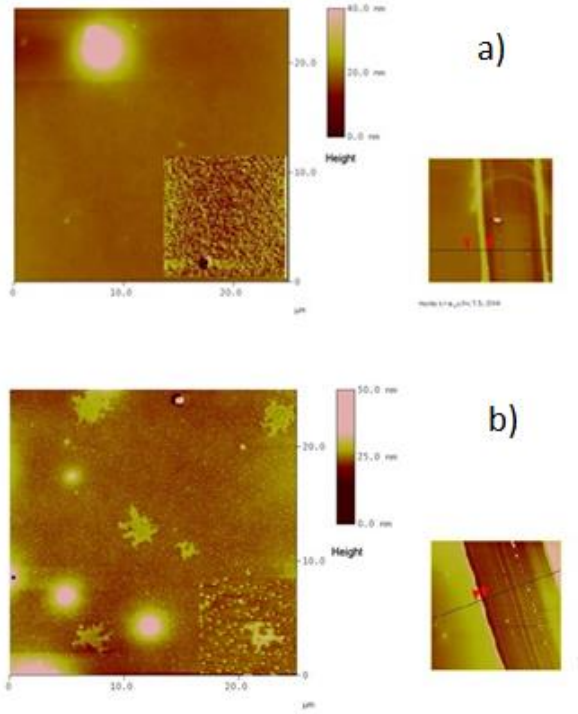

Figure 20. AFM of organotin compound **4** in a) $CHCl_3$. b) C_6H_5Cl.

5.2.9. Cyclic voltammetry.

The calculated electrostatic potential map (EPM) of ligand **4** and Sn-complexes **5**, **6** is shown in Figure 21. The ligand exhibits an inhomogeneous electrostatic distribution map (in green) all along the structure. The greatest surface of electronegative charge (in red) susceptible to redox process is mainly located on both –OH's of the anthracenes and slightly on one of the nitrogens of the azine group (=N-N=), in contrast the lowest electronegative charge (in blue) is mainly

found on the central phenyl. Interestingly, when ligand is complexed with Sn, either with butyls or phenyls, the EPM images show that the greatest surface of negative or electron rich regions is distributed on the aryls, on the -O and N- coordination center, while the lowest electrostatic potential surface is located around the -Sn- coordination center, meaning that their redox behavior and contribution is lower with respect to the entire conjugation part, likely because Sn imparts an electron donor character. As a term of comparison, the analogue Sn-mononuclear complex **I** [45], shows that the great surface of negative charge is concentrated around the -C-O-phenyl, -C-O-anthracenyl and on one of the coordination nitrogen Sn←-N=N-, while a slight EPM is distributed (yellow) on the conjugated aryls.

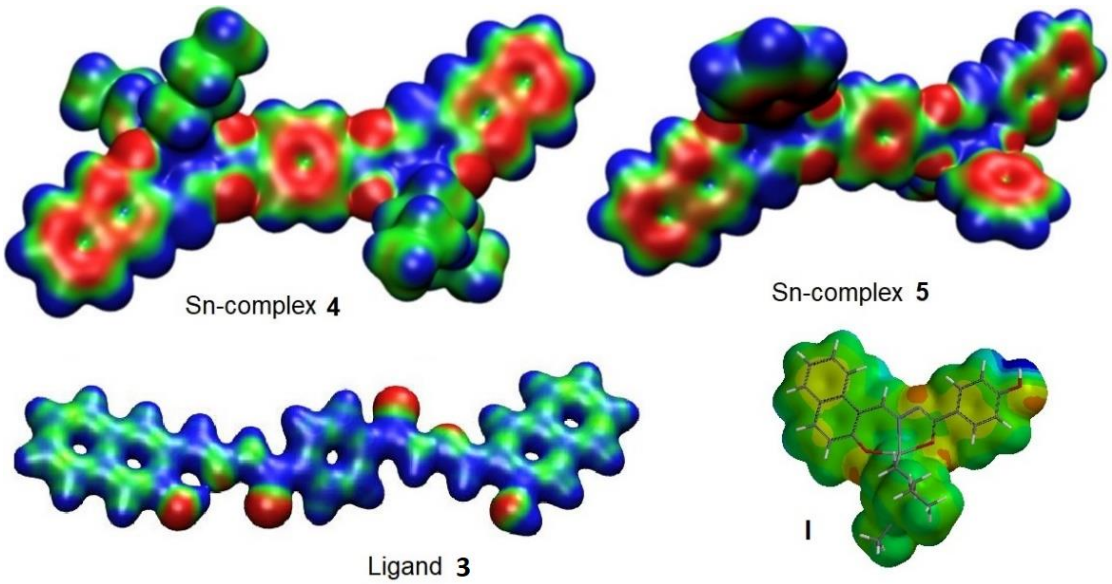

Figure 21. Electrostatic potential map (EPM) of binuclear Sn-complex 5 and 6 and their corresponding ligand 4. EPM of mononuclear Sn complex I ([N-(2-Oxido-1-naphthaldehyde)-4-hydroxybenzyhydrazidato] di-nbutyltin) is given as comparison purposes.

All the complexes are electroactive in acetonitrile either in forward direction (from -3 to +3V) or separately analyzed (0 to +3 V and 0 to -3 V). In order to better understand the electrochemical behavior of these complexes, Figure 21 shows the voltammogram for **5**, together with the mononuclear complex **I**[45] as term of comparison. We have found that the Sn-mononuclear complex I exhibits at least four distinguishable oxidation peaks, whereas three reduction peaks are well defined. From the molecular structures and EPM images, we may consider the -C-O-aryls, =N-N=, aryls functional groups to be susceptible to redox processes. Where, the metal ion and its coordination with the azine group could rather be associated with the oxidation processes. In Figure 22, the first peak at +1.08 V was associated with the loss of electrons of both the Sn and =N-N=, since we previously found that the oxidation of the azine group appears for free ligand at +0.9 V.[46] Similarly, in the reduction process, the first peak of the reduction processes at -0.66 V is associated with the reduction of both, the Sn and its coordination with the azine because the corresponding free ligand reduction of the azine to (-NH-NH-) is found between -0.9 V and -1.0 V.

In contrast, voltammograms of complexes **4**, **5** disclose: no significant change in both E_{red} potentials as is observed in the inserted Table of Figure 22; this behavior is in accordance with what was observed by UV/Vis spectroscopy, i.e. there is no marked difference in the electronic properties of the complexes by changing the butyls per phenyls. The voltammogram shows only one weak oxidation peak around +0.8 V, assigned to the Sn oxidation, and another one,

almost perceptible, at +1.20 V, which is assigned to the loss of electrons of =N-N=, and the more intense peaks are found at +2.27 and +2.53 V, assigned to the conjugated aryls that become more difficult either to oxidize or reduced. The presence of only one peak in the voltammograms for the Sn, suggests that both atoms are electronically interacting, while their cathodic shift, with respect to the mononuclear **I** is due to the effect of an increase in the conjugation length, such as was also observed by UV-Vis spectroscopy. From the E_{ox} and E_{red} potentials, the HOMO (5.6 eV) and LUMO (3.5 eV) values were calculated for both compounds giving an electrochemical band gap of Eg = 2.0 eV, values that are quite consistent to those obtained from the theoretical calculations (HOMO 5.5 eV and LUMO 2.2 eV, Eg = 3.2 eV), while the optical band gaps determined in $CHCl_3$ are of Eg =2.1 eV; in the range of semiconductor materials.

The ligand **8** and the trinuclear compounds (**9** and **10**) has the same behavior that the binuclear compounds and the respect ligand. (Table 9) This is observed in the voltamperogram (See Appendix)

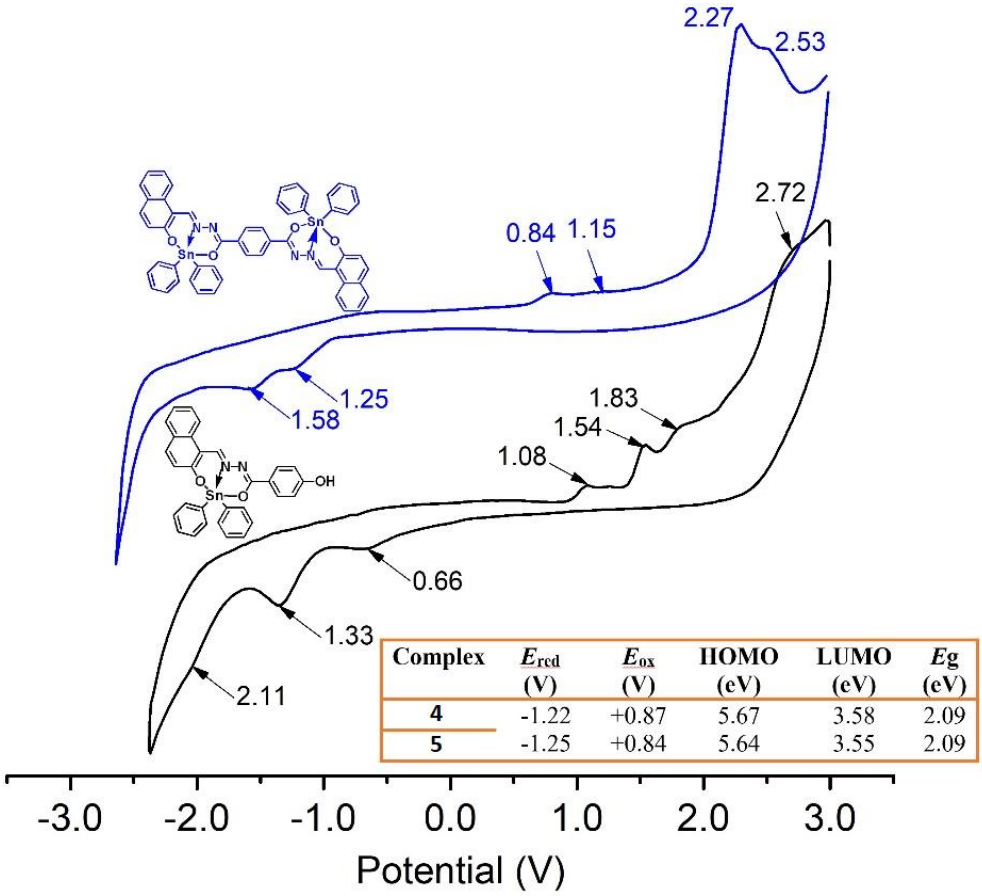

Complex	E_{red} (V)	E_{ox} (V)	HOMO (eV)	LUMO (eV)	Eg (eV)
4	-1.22	+0.87	5.67	3.58	2.09
5	-1.25	+0.84	5.64	3.55	2.09

Figure 22. Cyclic voltammograms of binuclear Sn complex **6** and of mononuclear Sn complex **I** ([N-(2-Oxido-1-naphthaldehyde)-4-hydroxybenzyhydrazidato] di-nbutyltin) in 0.1 mmol acetonitrile, at scan rate of 50 mV/s, V vs Ag/AgCl and using GC as working electrode. The inserted table summarises the electrochemical parameters determined for both binuclear complexes.

Table 9. **Dates of Cyclic Voltammetry for all the molecules**

Compound	E_{red}	E_{ox}	Ip	Ea	Eg
3	-0.7485	+0.96	5.4	3.7	1.7
4	-1.22	+0.87	5.6	3.5	2.0
5	-1.25	+0-84	5.6	3.5	2.0
8	-0.97	+0.95	5.4	3.4	2
9	-1.23	+0.52	4.9	3.2	1.7

10	-1.10	+1.55	6.0	3.3	2.7

5.2.10. Scanning tunneling microscopy (STM)

Both binuclear complexes were investigated at atomic level by STM. After having deposited a drop of the 2.8 mM solution on the highly oriented pyrolytic graphite (HOPG), a pulse of 2-6 V was immediately applied in order to induce the self-assemble monolayer (SAM) at the interface HOPG/TCB. Figures 23**a,c** show the mesoscopic STM images, while those obtained at high resolution are shown in Figure 23**b**,**d**, respectively. It can be seen, that at mesoscopic scales complex **4** does not cover large surface areas as complex **5** does. In fact, **4** self-organizes in randomly oriented microdomains, while **4** sponteaneusly arranges into a well-defined molecular layer. However, both complexes pack tightly on the surface, forming long lamellar structures, with differences in the lamellar stacking because of the change in the ligand (butyl or phenyl) but always adopting a face-on arrangement,[47] where the conjugated backbones are flat-lying on the HOPG surface, likely due to the π-π interaction of the aryls with the HOPG. The average lamellas distance, Figure 23**b,d** for complex **4** is of 2.39 ± 0.14 nm, and 2.52 ± 0.10 nm for complex **5.** This value fits well the theoretical molecular length in their most extended conformation (=2.69 nm), which was obtained for the equilibrium

geometries through density functional theory. Within the lamellas, a spacing of 0.84 ± 0.07 nm for **4** and of 1.58 ± 0.15 nm for **5** was determined according to their profiles, (See Appendix). In this case, the difference with the theoretical value (i.e, 1.37 nm corresponding to the alkyl-alkyl spacing for **4** and 1.46 nm that is the phenyl-phenyl distance for **5**) is more significant. This suggests that the molecules stack with the butyls/or the phenyls ligands interdigitated as is sketched in Figure 22**e,f**. Complex **5** presents a are more extended separation because of the major steric volume of the phenyl with respect to the butyl ligands of complex **4**. The 2D unit cell parameter of a monoclinic type cell for Sn-complex **4**,

Figure 23e, was of a = 0.99, b = 2.76 nm and $\gamma = 83^{\circ}$, and of monoclinic type cell for Sn-complex **5**, Figure 23f, was of: a = 1.46, b = 2.54 nm and $\gamma = 88^{\circ}$.

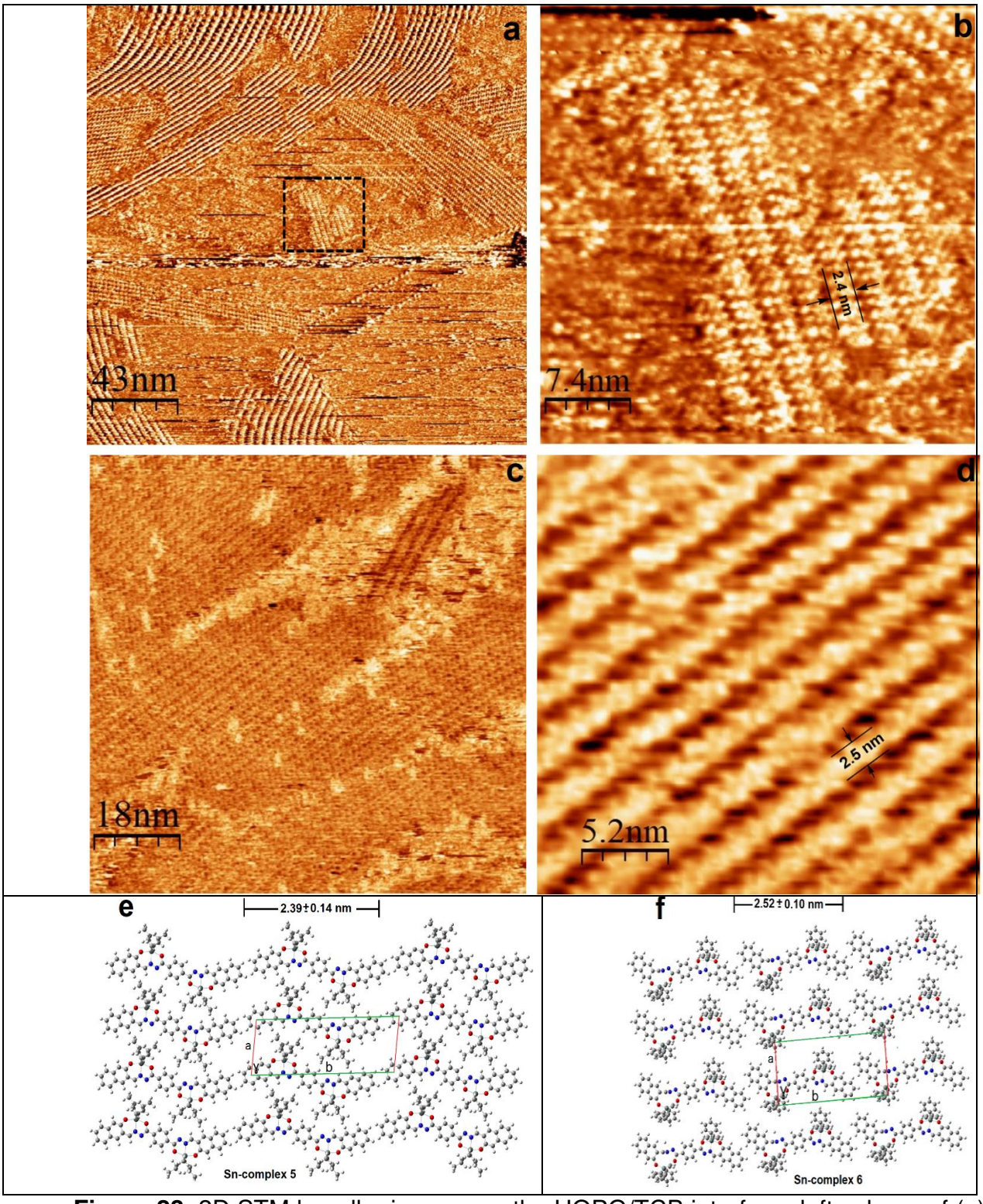

Figure 23. 2D STM lamellar images on the HOPG/TCB interface, left column of (a) 4: Vbias = -740 mV, It = 90 pA and (c) 5: Vbias = -830 mV, It = 110 pA. Right

column, high resolution STM images of **4**: Vbias = -740 mV, It = 90 pA and (c) **5**: Vbias = -830 mV, It = 110 pA. Right column, high resolution STM images of (b) **4**: Vbias = -740 mV, It = 90 pA and (d) **5**: Vbias = -830 mV, It = 110 pA. The 2D cell parameters for **4** are a = 0.99 nm, b = 2.76 nm, γ = 83º, for **5** a = 1.46 nm, b = 2.54 nm, γ = 88º.

5.2.11. Characterization of the diode.

The OLED type device was assembled as described in the part experimental. Figure 21 shows a typical current density curve (J) - voltage (V) and a luminance curve (L) -voltage (V), observing a density of current (2.7 mA/cm^2) and a relatively low luminance (7.75X10 $^{-05}$ cd/m^2). In this can be seen a peak of current at Vp = 14.5 V, this effect is characteristic of the so-called tunnel diodes, this indicates that as the potential barrier decreases the probability of the charges going through that barrier increases, so the effect increases of tunnels, the decrease of the potential barrier, may be due to the proximity between electrodes (thin film), the chemical structure of the molecules and their conformation in solid state, but as noted by AFM the film is not so thin to produce tunnel effect, which would indicate that it is produced by the conformational arrangement in the solid state of the molecule.

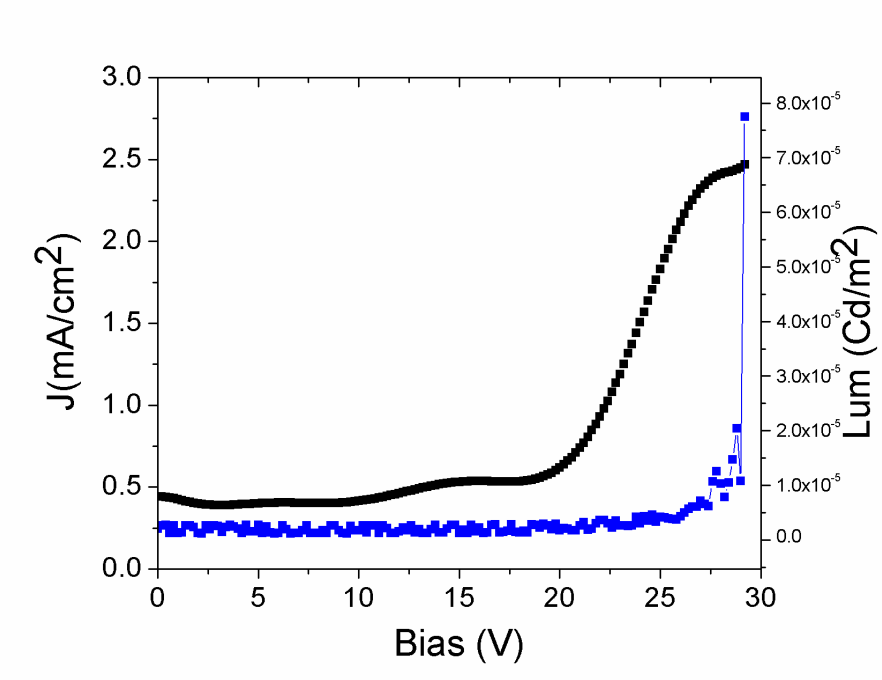

Figure 24. Curve current density (J) -voltage (V) and luminance (L) -voltage (V) for a configuration ITO/PEDOT:PSS / **4** /Al OLED

5.2.12. Solar cell

As an additional contribution, an assembly of a solar cell with mixture in PCBM. As in the diode, the photovoltaic behaviour is low obtaining efficiencies in the order of 0.007 ± 0.00006%, with very low saturation currents ranging from 0.08 to 0.11 mA/cm^2 with an average of 0.09 ± 0.02 mA/cm^2, the voltage in Open circuit goes from 0.30 to 0.33 V making the device a reproducible experiment. As for the FF is also low and can improve with the increase in the amount of $PC_{61}BM$ because although we are talking about photogeneration, the curve does not reach

its total rectification, this could be improved by changing the $PC_{61}BM$ ratio in the device. (Figure 25)

In the Table 11 shows the parameters obtained of the characterization of solar cells.

Table 10. Values obtained in solar cell.

Jsc (mA/cm^2)	Voc V	FF	n%
0.11	0.3	0.23	0.008
0.08	0.38	0.22	0.007

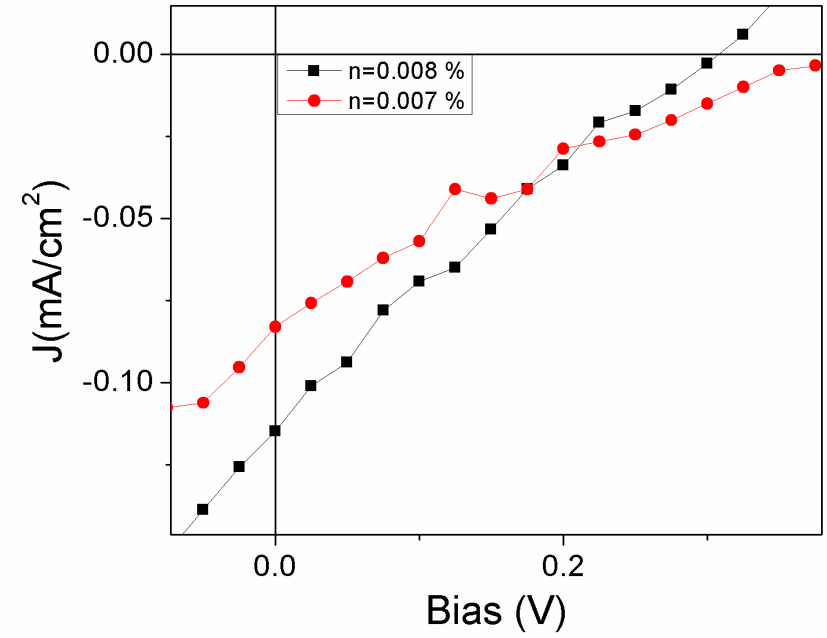

Figure 25. Curve I-V for ITO/PEDOT:PSS/**4**:PC61BM/FM.

5.2.13. Multi-Stimuli Responsive Fluorescent Materials.

In addition, our research group are interested in multi-stimuli responsive fluorescent (MSRF) materials, due to their interesting application in sensors, optical devices, drug delivery, and cell imaging[48] The study was carried out altering their photophysical properties upon application external stimuli such as: temperature and mechanochromism.

The binuclear complexes were studied in photophysical properties at different temperatures from – 40 to 40°C and that the absorption properties suggest electronic interaction between the two Sn units, energy transfer from one unit to the other is likely possible. On the other hand, another possible cause is induced non radiative losses because of intramolecular rotation, as found for other Schiff bases complexes. [49] To support this hypothesis, fluorescence spectra were recorded in the temperature range -10 to 40 °C. Figure 26 reports the spectral evolution for **4** (See Appendix, for **5**) as an example, where it can be observed a gradual increase of the emission intensity by lowering the temperature confirming this no-radiative loss.

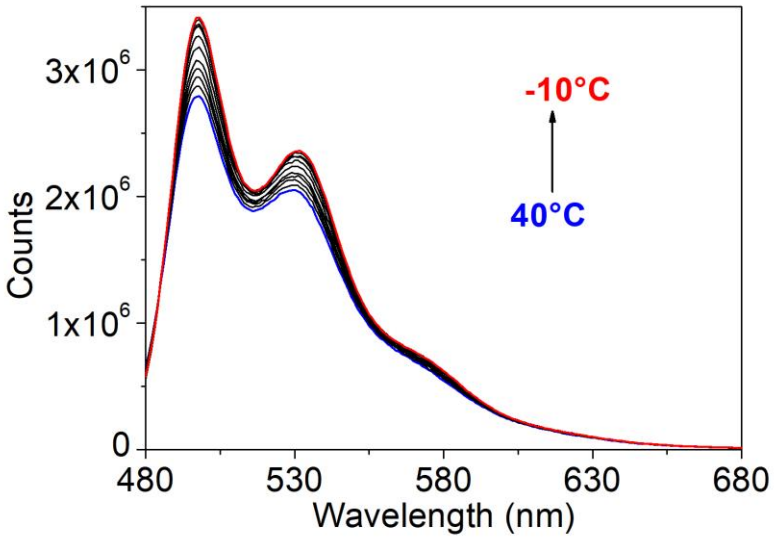

Figure 26. Fluorescence spectra of organotin compound **4** in chloroform at different temperatures.

Due to the good quantum yields and previous results reported for other Sn complexes,[50],[51] the feasibility of obtaining good optical quality films was investigated. Complex **5** unfortunately could not form thin films of the thickness, (100-150 nm) as its solubility is limited to 5 g/L. On the contrary, complex **4** can be dissolved in concentrated solutions (5-30 g/L) from different solvents (chloroform, dichloromethane, THF, chlorobenzene). Based on the thickness and roughness values, 10g/L chlorobenzene solution was used for the preparation of the films. The AFM study shows the coexistence of a flat surface with some aggregates with different morphology and that persist even in small areas. (See Appendix)

As the fluorescence quenching is very large, and aggregates were observed in the AFM study, aggregation studies were carried out in THF/water mixtures (**4** and **5** are soluble in THF but unsoluble in water) increasing the water content from 0 to 90% with a 10% volume percent increase. Figure 27 reports the study on complex **4 (5,** See Appendix**)** as example; the fluorescence intensity decreases with an increasing water content to 90 %. The aggregation caused quenching (ACQ)[52] is consistent with the strong π-π stacking interactions observed in the crystallographic study for the single crystal and that are expected to increase as the non-solvent content increases.

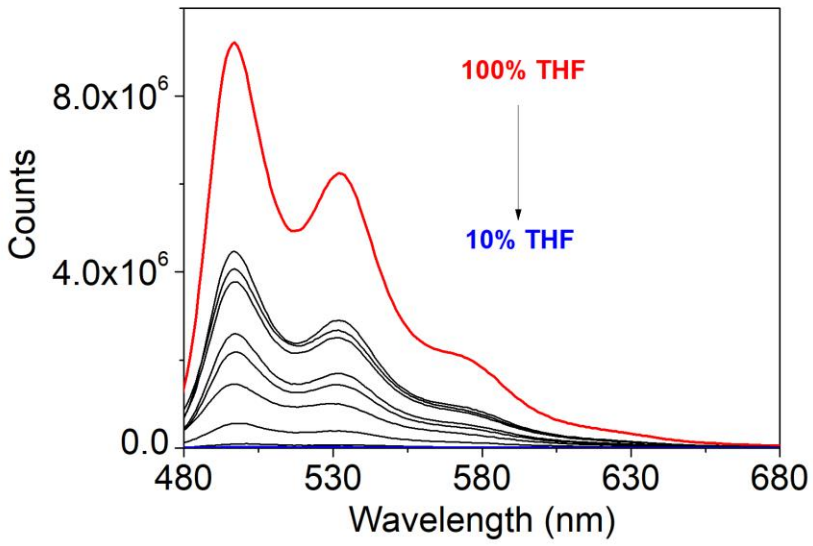

Figure 27. Emission spectra of **4** THF/water mixtures with different water fractions. From top to bottom: 100, 90, 80, 70, 60, 50, 40, 30, 20, 10% THF

Due to the good quantum yields and previous results reported for other Sn complexes,[53],[54] the feasibility of obtaining good optical quality films was previously investigated were by AFM study (See Appendix) showed the coexistence of a flat surface with some aggregates with different morphology and that persist even in small areas.

The Stokes's shift value is very small suggesting very minor influence of internal conversion but possible self-absorption. Nevertheless, the fluorescence quantum yield is ~500 fold quenched with respect to the solution.

In order to investigate if this behavior was retained in bulk, powders were also analyzed. Figure 28 presents the UV-Vis absorption (a) and emission (b) spectra of complexes **4** and **5.** The optical properties of the ligand **4** are also shown, as comparative term.

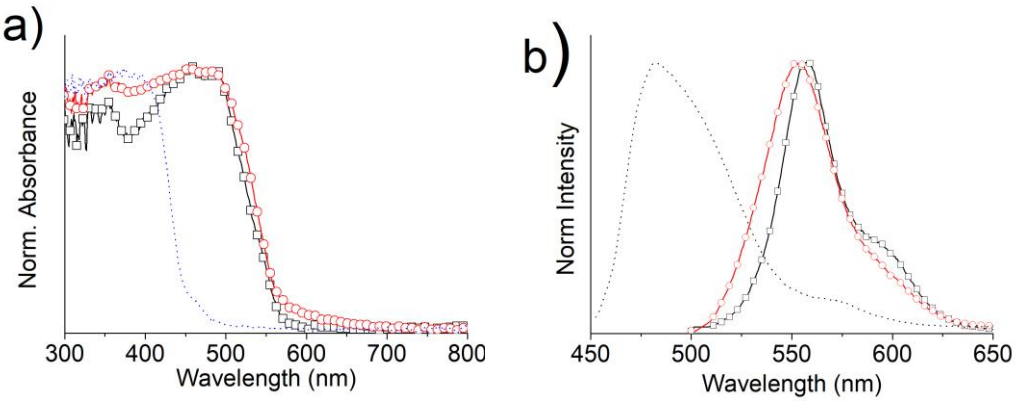

Figure 28. Powder a) UV-vis and b) fluorescence spectra of organotin compounds **4** (squares), **5** (circles) and the ligand **3** (dotted lines).

Both the absorption and emission spectra of the tin complexes in powders maintain spectral features similar to those of the solutions, but red shifted of almost 10 nm for the UV-Vis and 50 nm for the fluorescence maxima. This behaviour is consistent with intermolecular interactions that are likely more important for the excited than the ground state. The UV-Vis spectrum of the ligand **4** presents a broad band at around 400 nm, due to the π-π^* electronic transitions of the conjugated Schiff base, which gives rise to a very broad emission band at 482 nm.

For the stimuli in solid state we can see that the materials present a change in its coloration in a reversible manner in response to heating and cooling cycles. We can see a change that the materials present an increase in the emission intensity in heating.[57] (Figure 29a). The coloration from the compounds in UV-vis and Uv-light at 25°C, 160°C and after cooling (Figure 29b and 29c), i.e. The phenomenon of thermochromism is given by the chemical equilibrium between the "keto" and an "enol" form, by means of an intramolecular transfer of protons, with the increase in temperature, the "keto-enol" equilibrium moves towards the form "Keto", which absorbs at longer wavelengths, and thus produces a continuous deepening of colour over a wide temperature range.

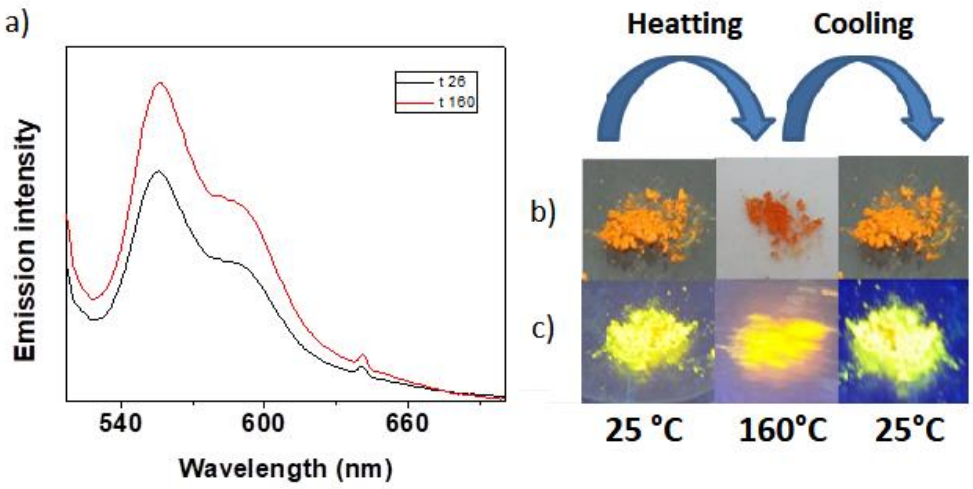

Figure 29. a) Emission spectra of compound **4** in solid state at different temperature. b) Fluorescence image of compound **4** at 25°C, 160°C and after cooling under Vis light. c) under UV light.

Interestingly, even if the fluorescence intensity decreases, the emission properties of the complexes are still detectable even after 10 tons of pressure or after grinding and do not exhibit changes in the maximum positions, i.e. there is no mechanochromism. Figure 30 reports the fluorescence spectra of **5** before and after the 10 tons, where the inserted photos show that the powder preserves the same (orange) colour under visible light and (yellow) upon UV excitation; after 10 tons. This is in agreement with the fact that the crystallographic structure of the compounds is maintained as found in the XRD studies (Figure 31) The XRD studies of the others molecules can be observed in the Appendix.

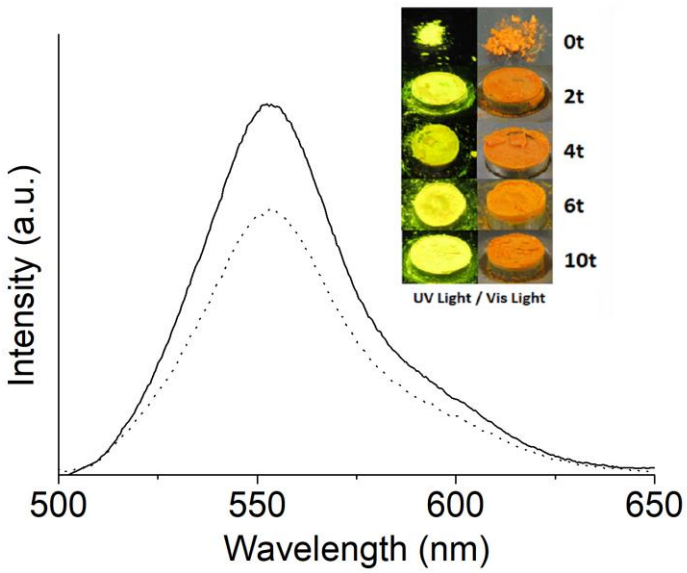

Figure 30. Powder absorption (left) and fluorescence (right) spectra of organotin compounds **5** before (solid line) and after (dotted line) 10 tons of pressure. Inserted figure: photos of the powder at different pre4ssures under visible and UV light.

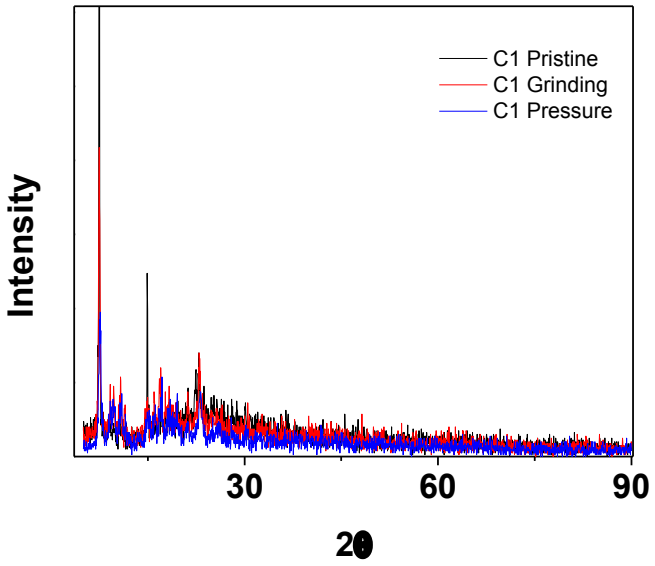

Figure 31. XRD of compound **4** to pristine, grinding and pressure.

.

Studying the thermochromic properties, the compounds were ground for 2 min on a mortar,[58] we can see the compounds respond to mechanical stimuli such as friction. The compounds low lost luminescent without changing colour, in the emission spectrum show a decrement and blueshift around to 10 nm this is likely that molecular interactions are partially destroyed, but there is not quenching in the molecule. (Figure 32)

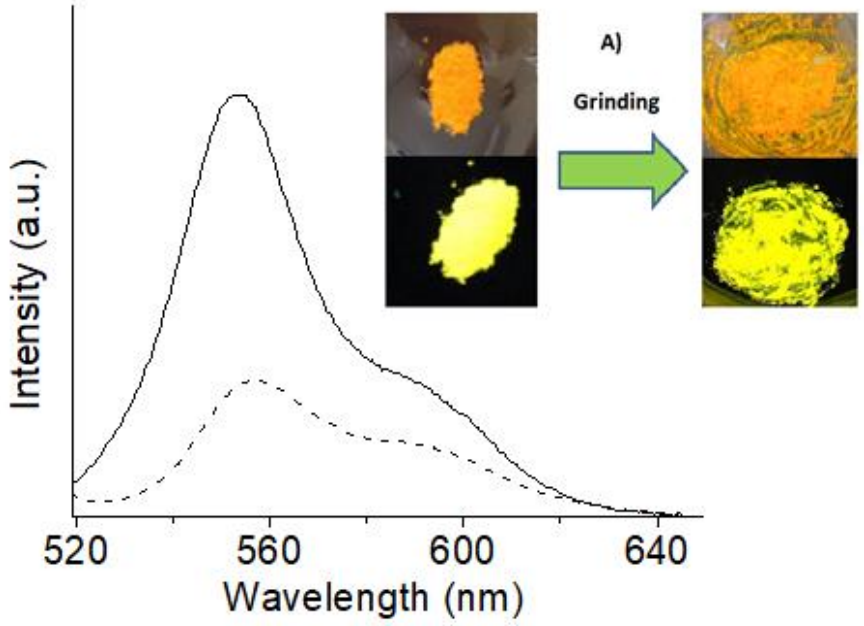

Figure 32. A) Fluorescence image of **4** and under grinding before (solid line) and after (dotted line) Inserted figure: photos of the powder at different pressures under visible and UV light.

6. CONCLUSION

Four tin complexes (**4**-**5**, **9**-**10**) and their respective Schiff bases (**3**-**8**) were prepared by microwave-assisted synthesis from 20 to 30 min; in one step by multicomponent method proceeded very fast and cleanly. The reaction times decreased around of 95 times in comparison with the conventional synthesis.

The organotin compounds were fully characterized by spectroscopic and spectrometric method obtaining the expected compounds. The crystal structures were obtained for single crystal x-ray diffraction analysis, where it was observed that binuclear compounds present two tin atoms with a trans conformation (centrosymmetry) in the skeleton and a N→Sn coordination lengths, the crystal system is triclinic and special group P-1 for the two binuclear compounds.

The absorption, fluorescence emission and lifetimes for the compound were studied in solution, except their ligand. The absorption spectra for (**4**-**5**, **9**-**10**) revealed a maximum absorption around 468 to 483 nm in the ultraviolet region

Fluorescence emission showed a mainly peak around at 482 to 495 nm and a replica around 512 to 528 nm being the spacing approximately 36 nm, like the values found in the absorption spectra.

An increase in quantum yield of fluorescence was observed around from 34 to 52%, in comparation with others studied in the research group, this is explained

based on the change of the aminophenol to hydrazone derivatives due to the effective conjugation length by the two complexed Sn units are electronically interacting. On the other hand, another possible cause is induced non radiative losses because of intramolecular rotation, as in another Schiff bases complexes reported.

The simultaneous thermal analysis under nitrogen of molecules showed that the complexes have high decomposition temperatures.

The electroluminescent device type OLED fabricated using **4** as an emitter and electron transport, displayed an luminance of 7.7x 10 -5 cd / m2 at 29 V. In addition, due to its low fluorescent quantum yield in powder, **4** have a poor electroluminescence performance.

As additional contributions to this work, a second application was made. due to the similar assembly when performing an OLED and a solar cell, we proceeded to make the device where its curve I-V shows efficiencies of .008% compared to literature is three orders greater than cells of Schiff bases reported by kaya and collaborators.

Multistimulus studies were carried out for tin complexes for biological applications or as sensors where it could be observed that they could be good candidates for these applications. In addition, now there are no reports of luminescent tin compounds with these applications, so is opened an interesting area for potential study these compounds.

7. APPENDIX

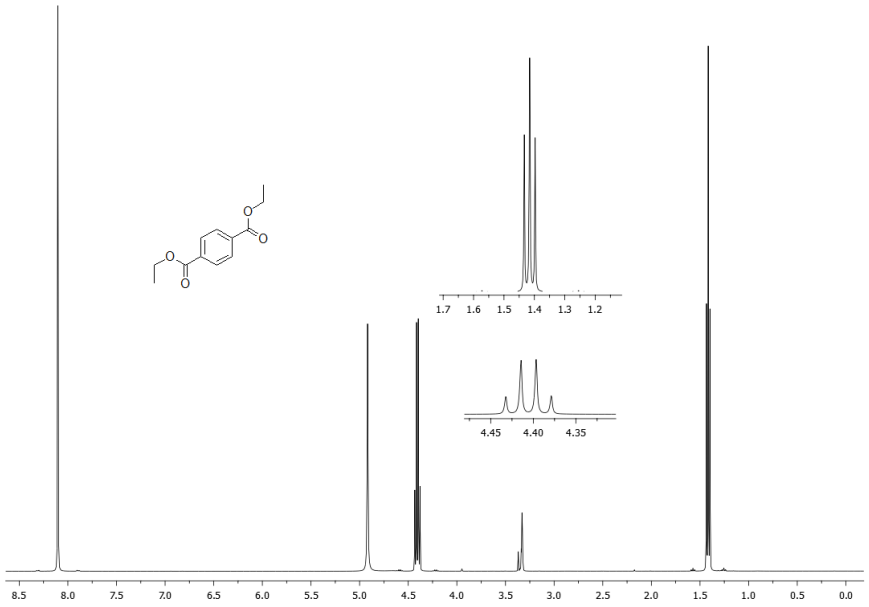

Fig. S1. ^{1}H NMR ($CDCl_3$) spectrum of **1.**

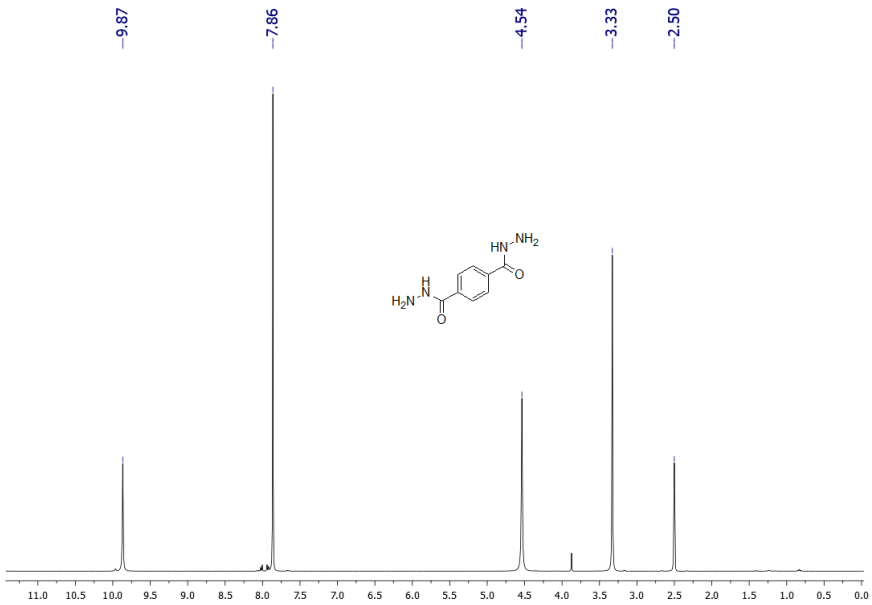

Fig. S2. ^{1}H NMR ($CDCl_3$) spectrum of **2.**

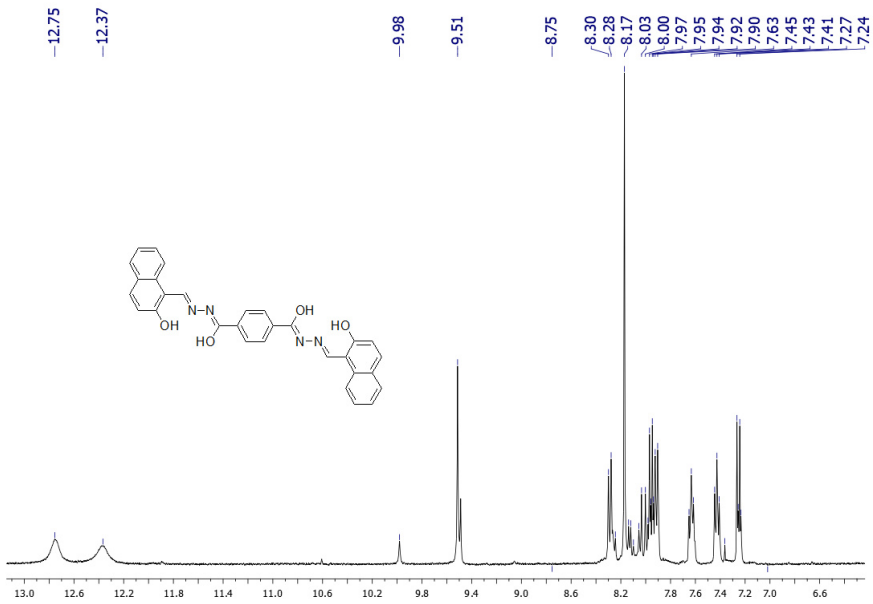

Fig. S3. ^{1}H NMR ($CDCl_3$) spectrum of ligand **3**.

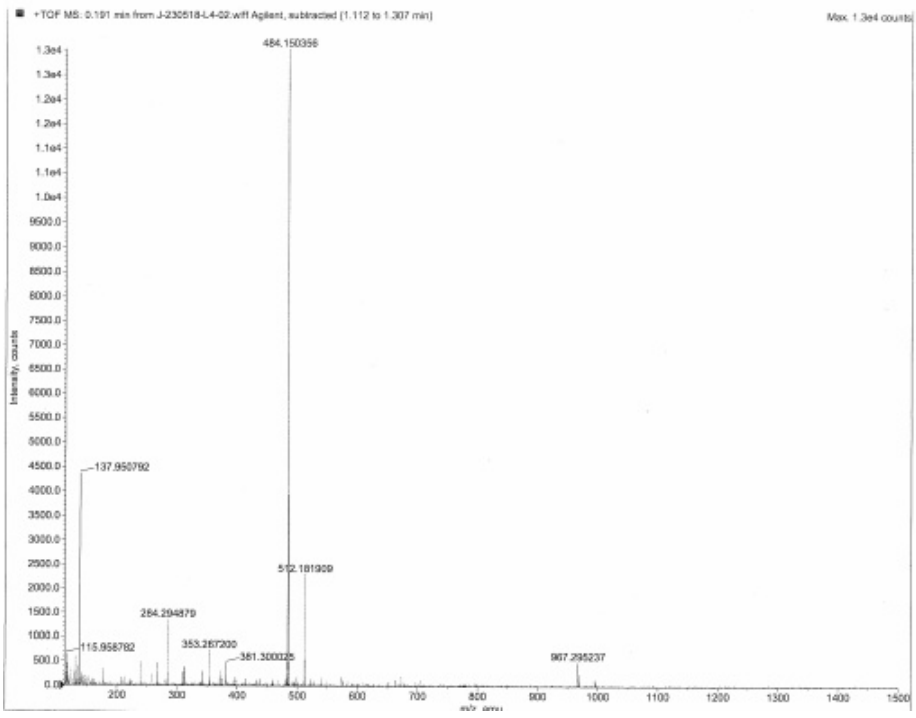

Fig. S4. Mass spectrum of ligand **3**.

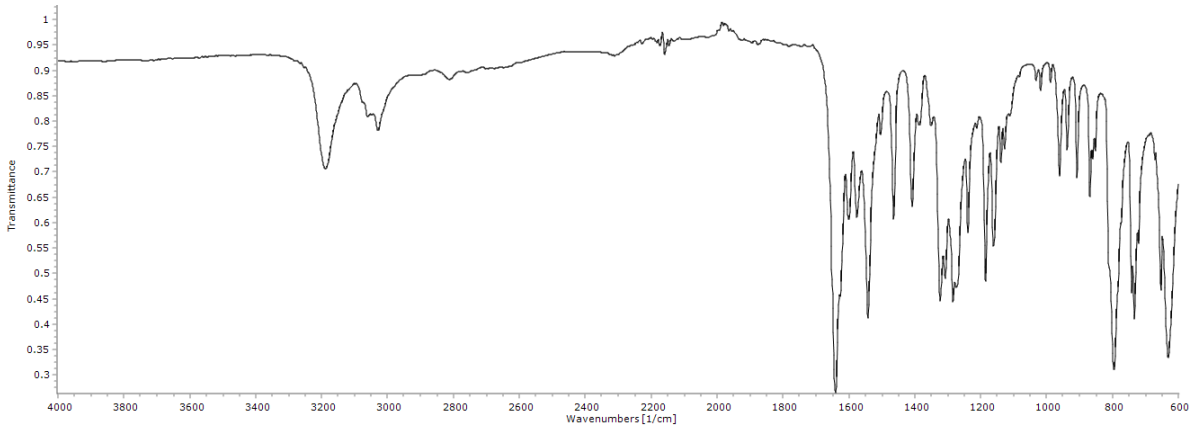

Fig. S5. Infrared spectrum of ligand **3**.

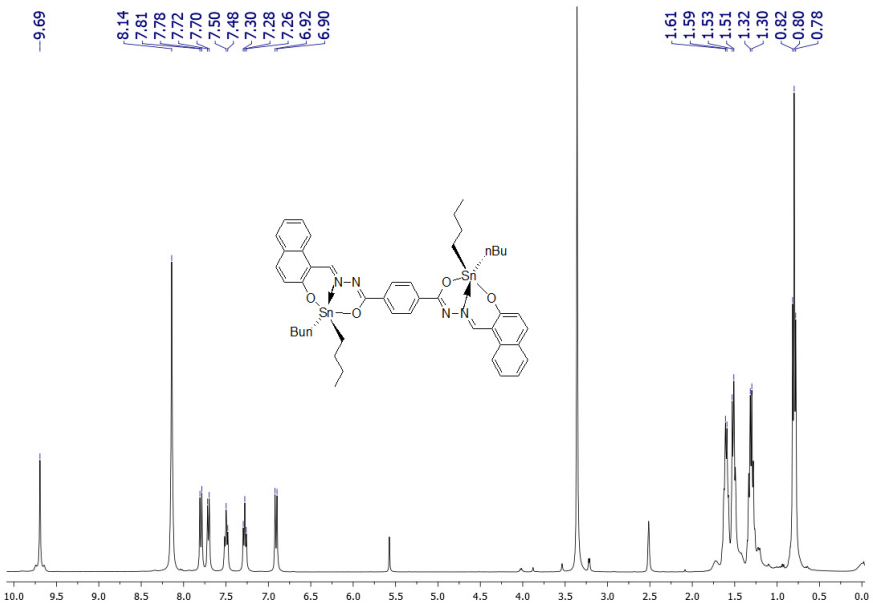

Fig. S6. ^{1}H NMR ($CDCl_3$) spectrum of compound **4**.

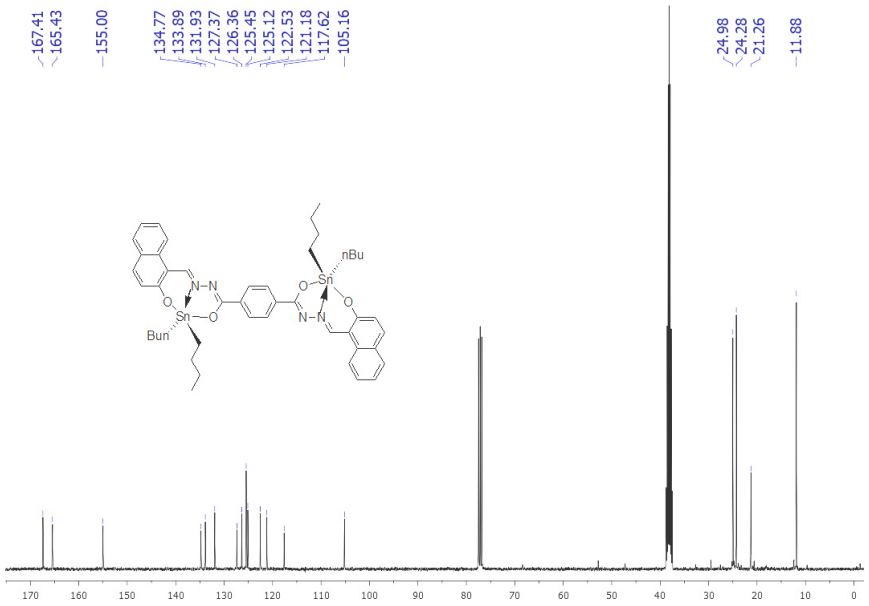

Fig. S7. ^{13}C NMR ($CDCl_3$) spectrum of compound **4.**

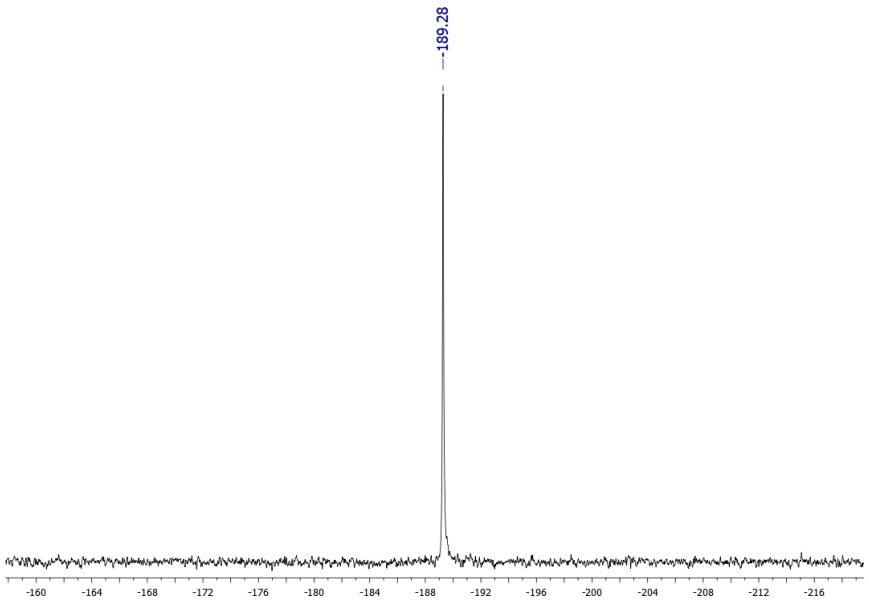

Fig. S8. ^{119}Sn NMR ($CDCl_3$) spectrum of compound **4.**

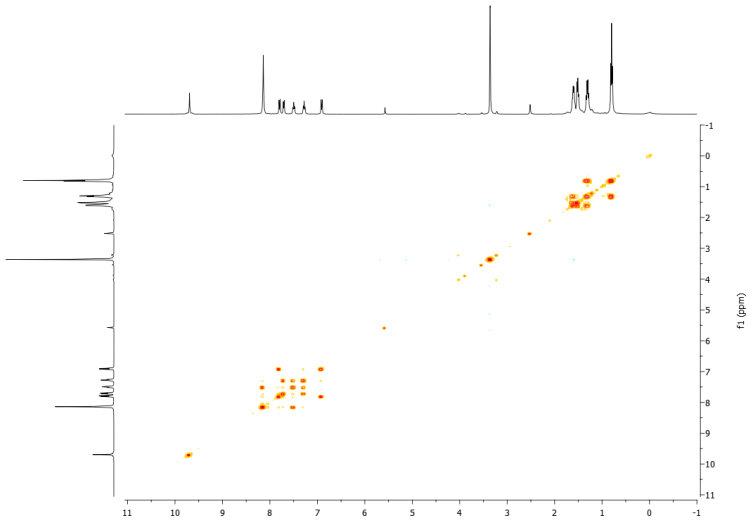

Fig. S9. COSY ($CDCl_3$) spectrum of organotin compound **4.**

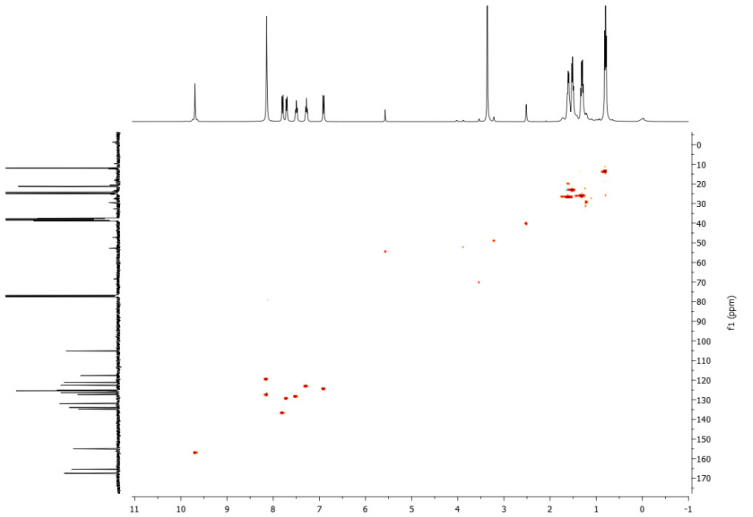

Fig. S10. HETCOR ($CDCl_3$) spectrum of organotin compound **4**.

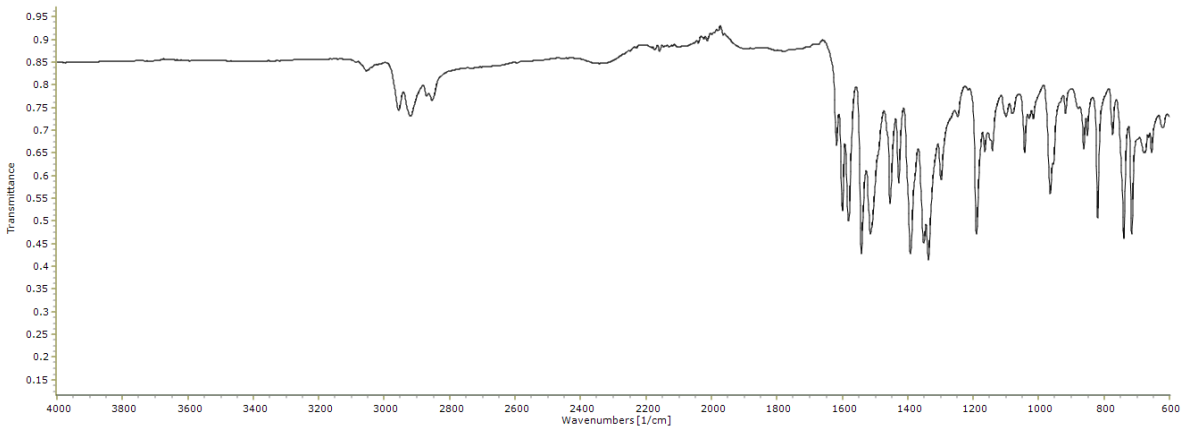

Fig. S11. Infrared spectrum of compound 4.

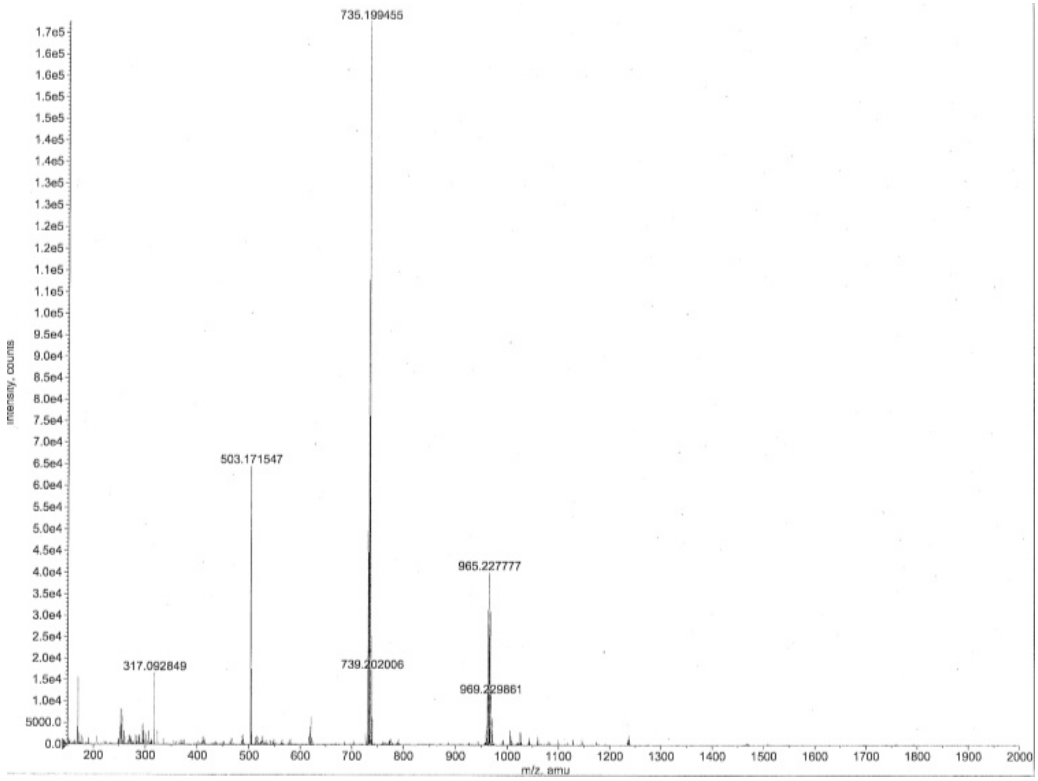

Fig. S12. Mass spectrum of compound **4**.

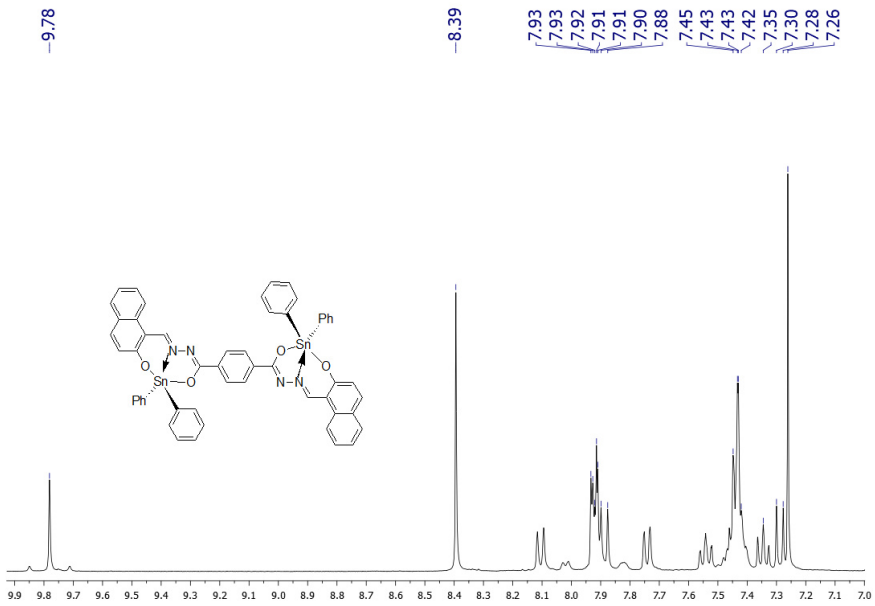

Fig. S13. ^{1}H NMR ($CDCl_3$) spectrum of compound **5.**

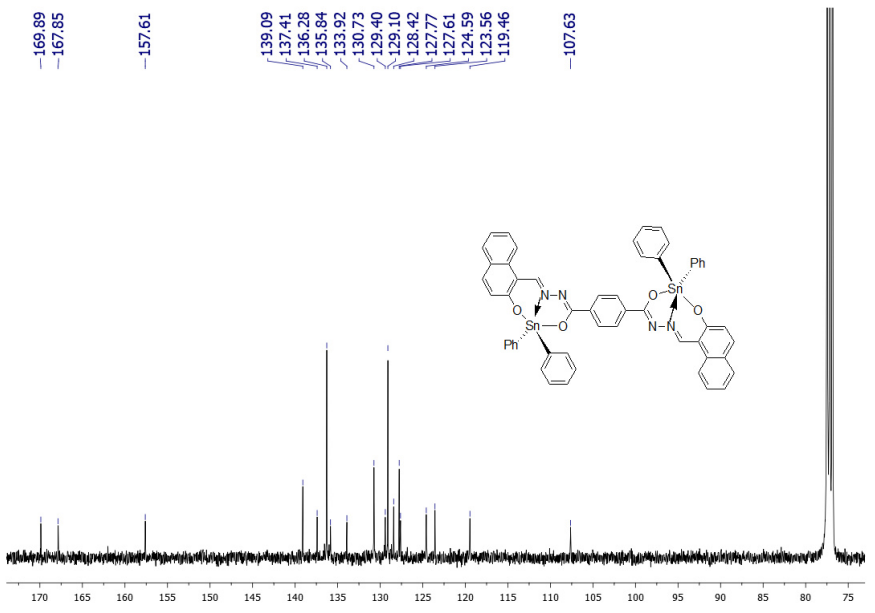

Fig. S14. ^{13}C NMR ($CDCl_3$) spectrum of compound **5.**

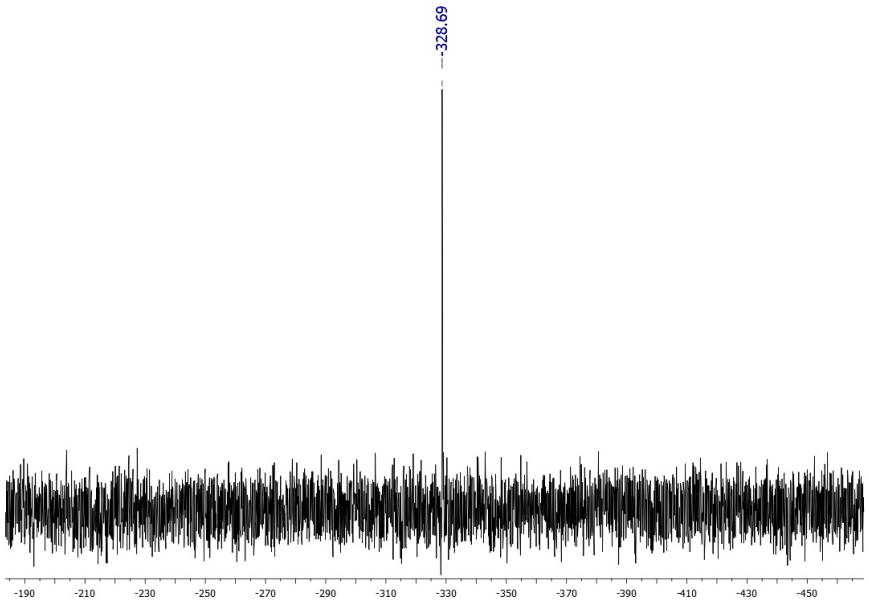

Fig. S15. ^{119}Sn NMR ($CDCl_3$) spectrum of compound **5**.

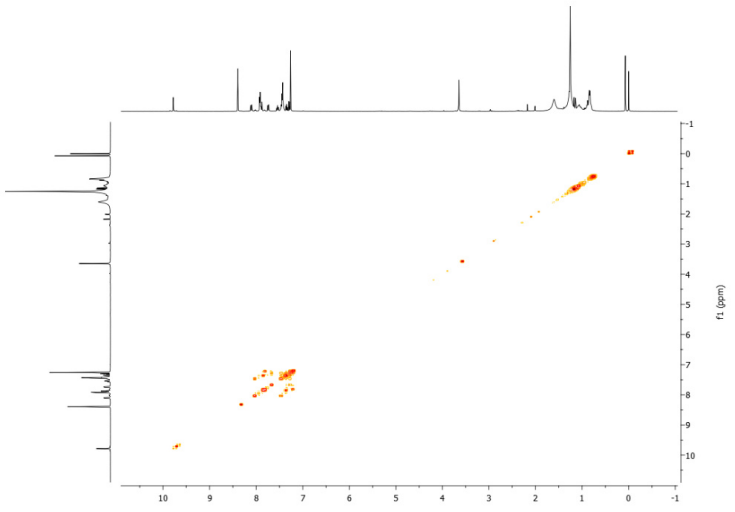

Fig. S16. COSY ($CDCl_3$) spectrum of organotin compound **5.**

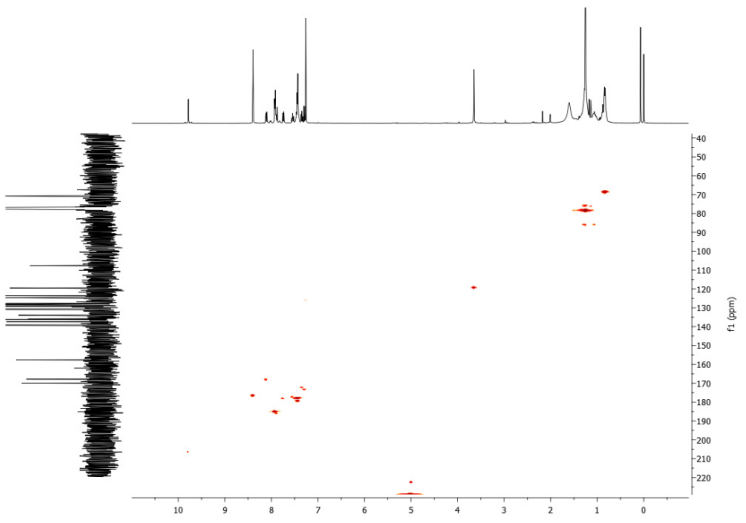

Fig. S17. HETCOR ($CDCl_3$) spectrum of organotin compound **5.**

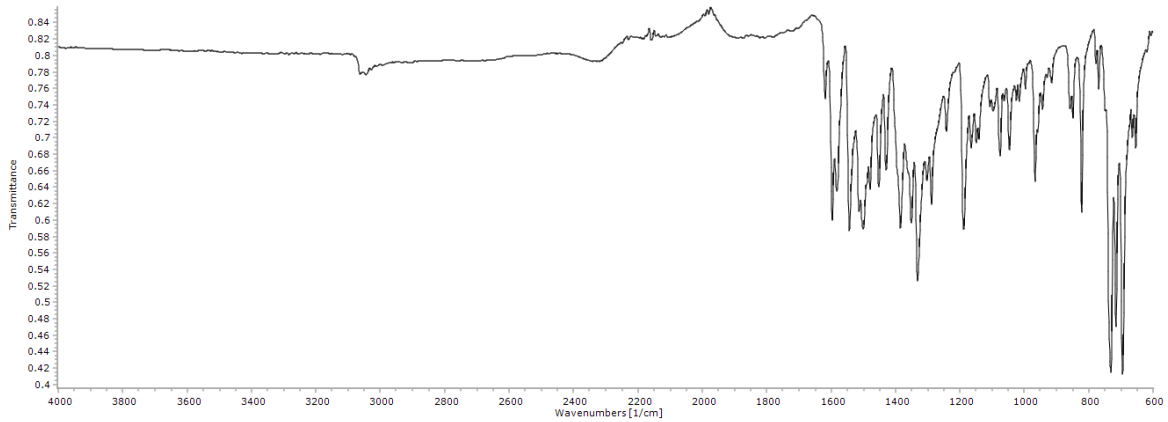

Fig. S18. Infrared spectrum of compound **5**.

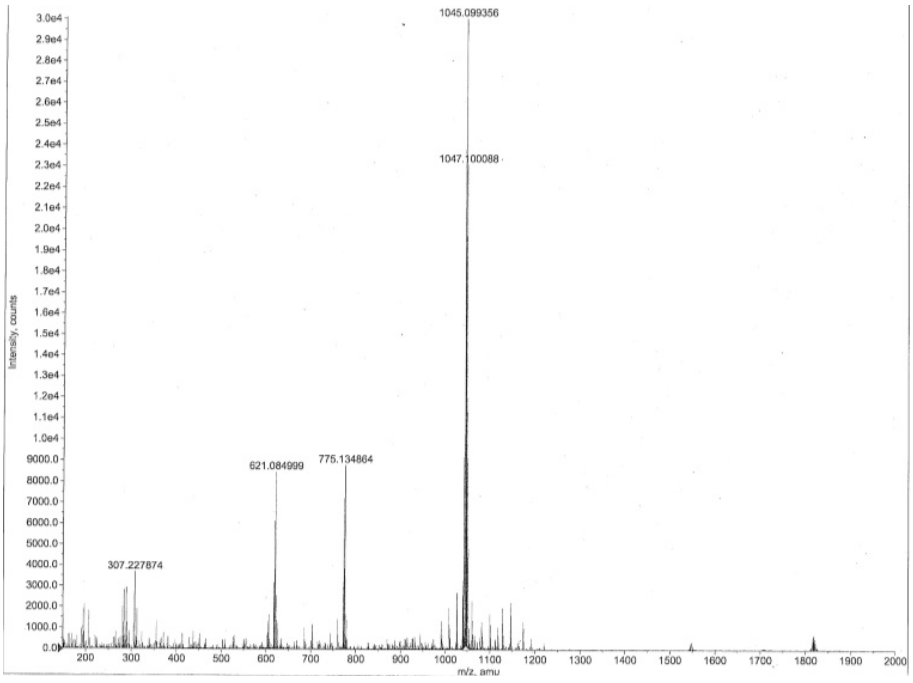

Fig. S19. Mass spectrum of compound 5**.**

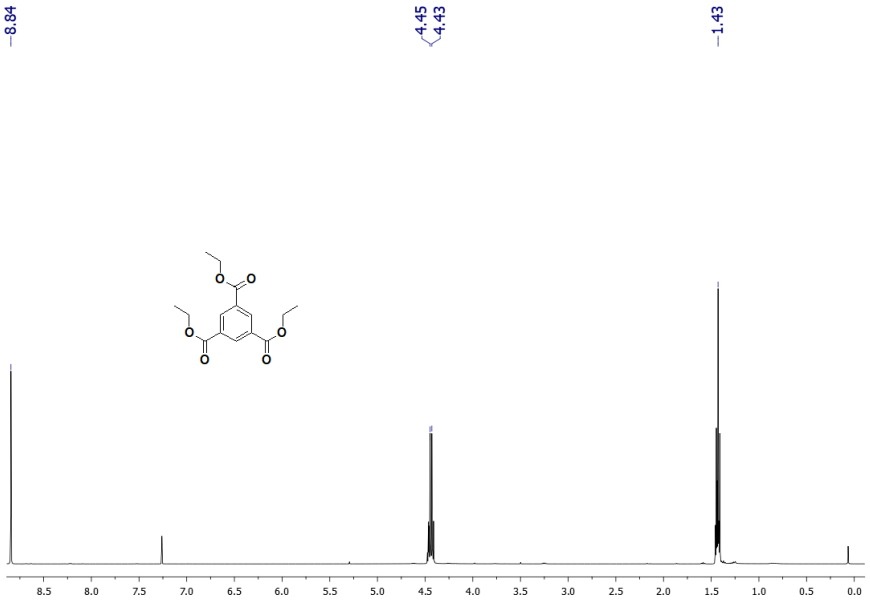

Fig. S20. ^{1}H NMR ($CDCl_3$) spectrum of **6**.

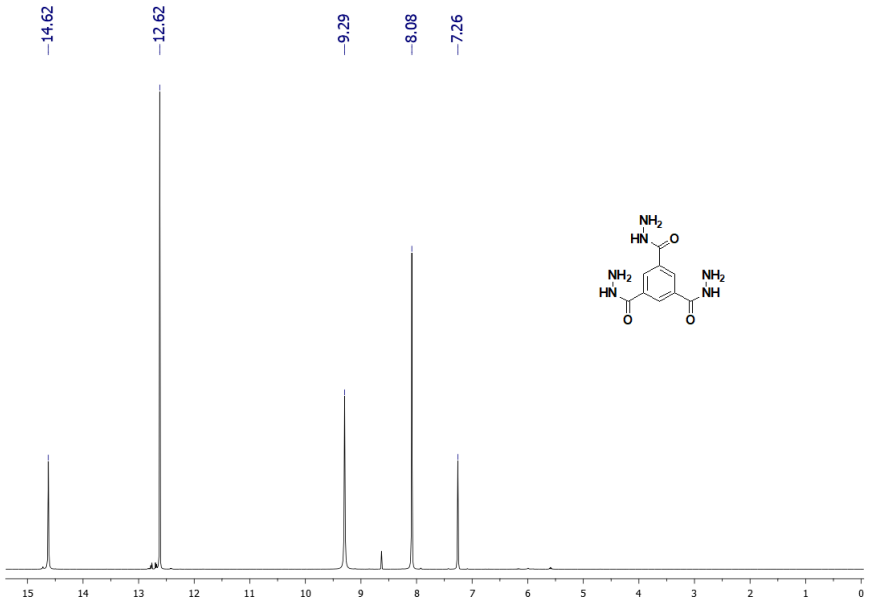

Fig. S21. ^{1}H NMR ($CDCl_3$) spectrum of **7.**

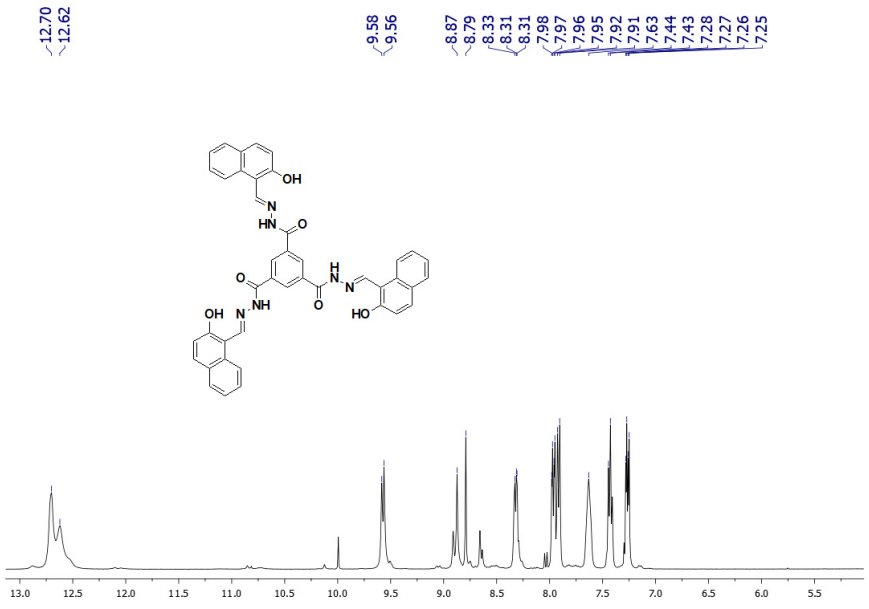

Fig. S22. ^{1}H NMR ($CDCl_3$) spectrum of ligand **8**.

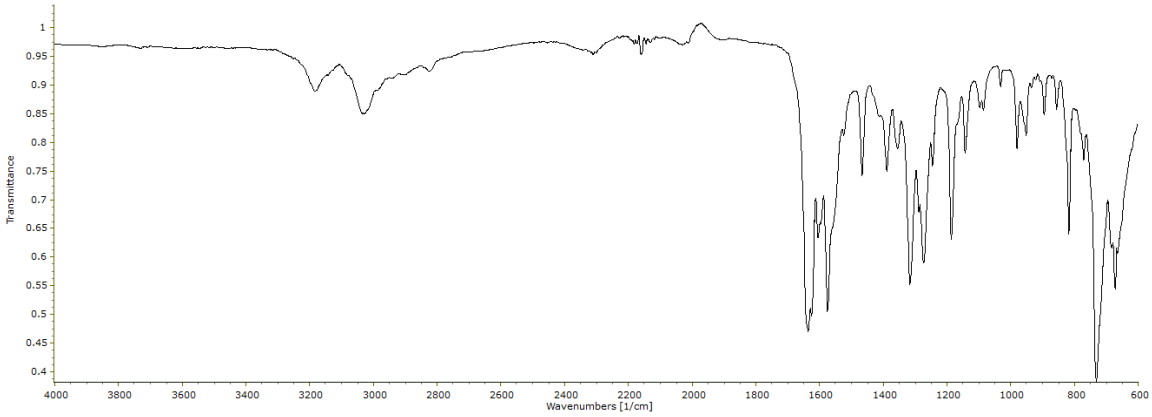

Fig. S23. Infrared spectrum of ligand **8**.

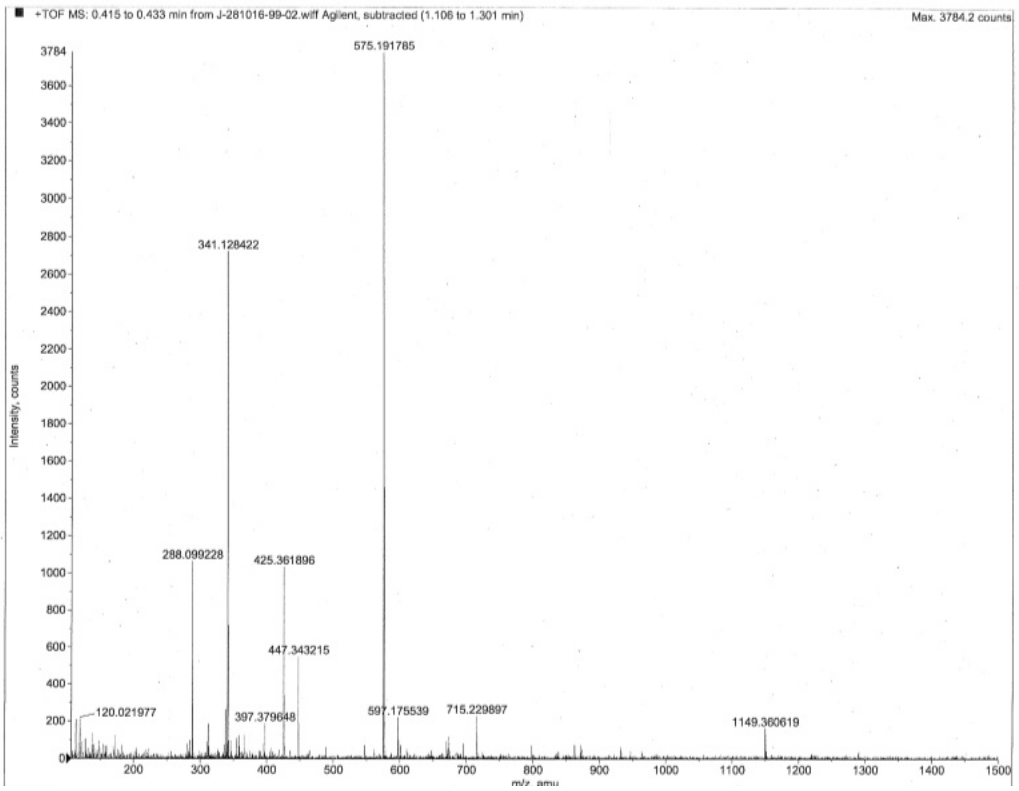

Fig. S24. Mass spectrum of ligand **8**.

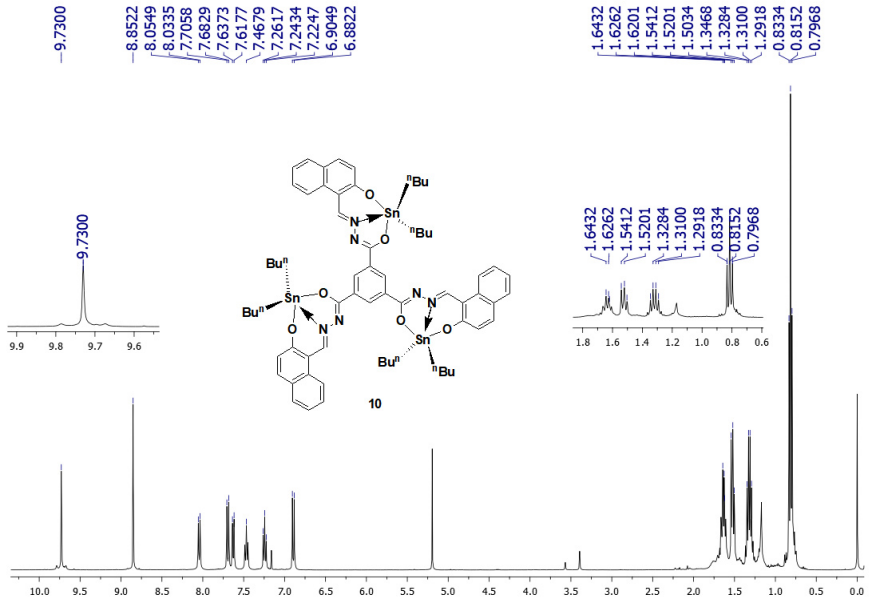

Fig. S25. ^{1}H NMR ($CDCl_3$) spectrum of compound **9.**

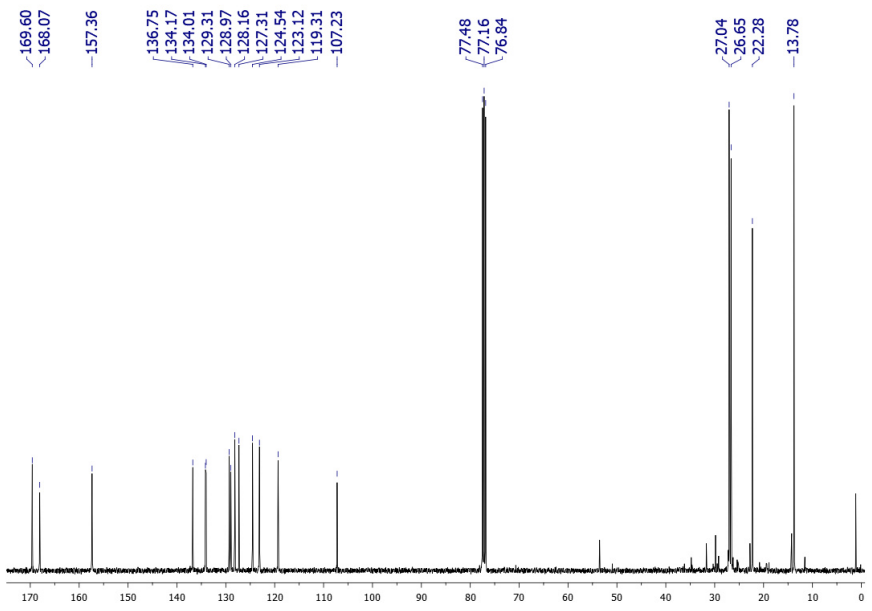

Fig. S26. ^{13}C NMR ($CDCl_3$) spectrum of compound **9.**

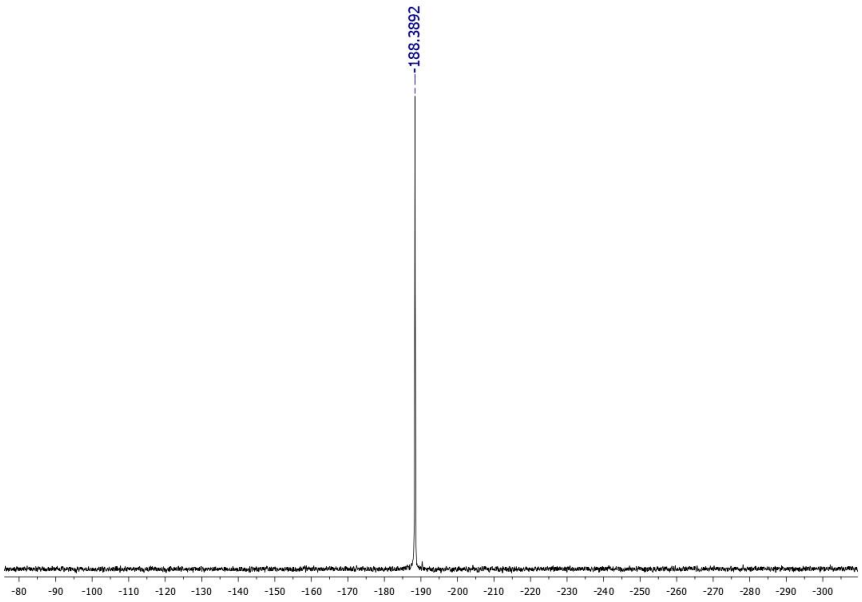

Fig. S27. ^{119}Sn NMR (CDCl3) spectrum of compound **9**.

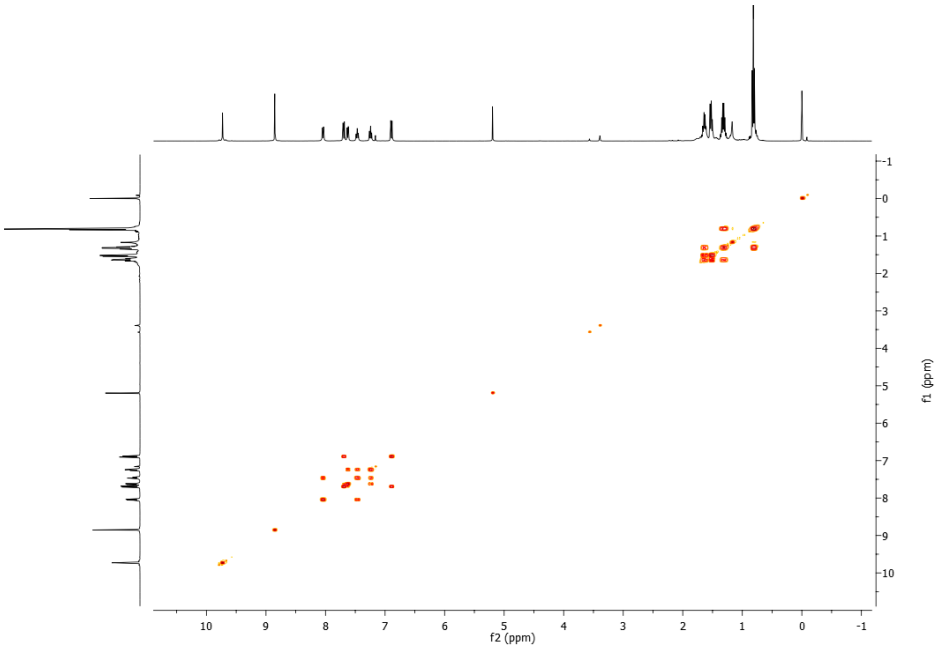

Fig. S28. COSY ($CDCl_3$) spectrum of organotin compound **9.**

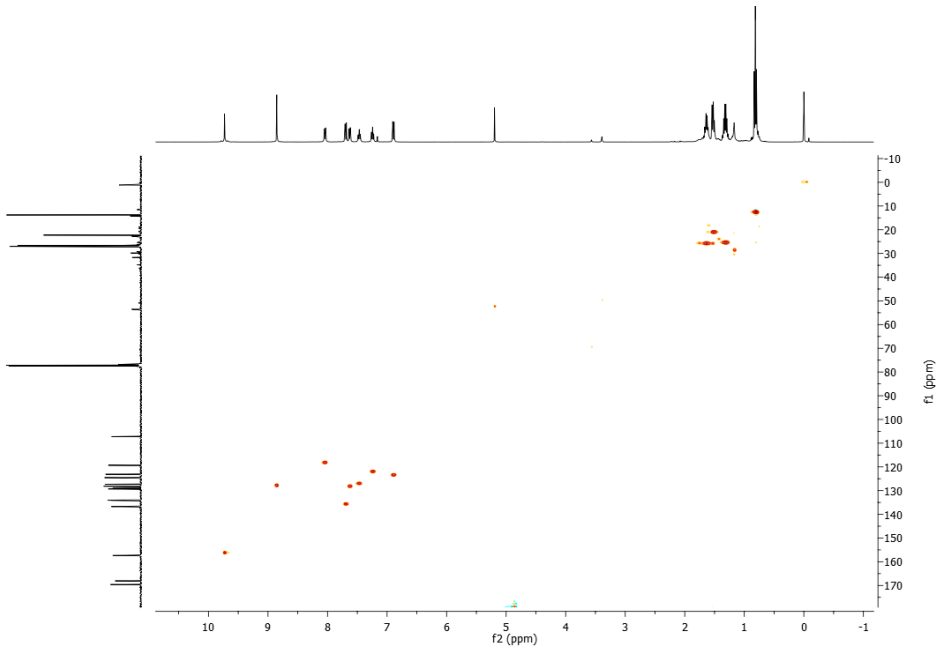

Fig. S29. HETCOR ($CDCl_3$) spectrum of organotin compound **9.**

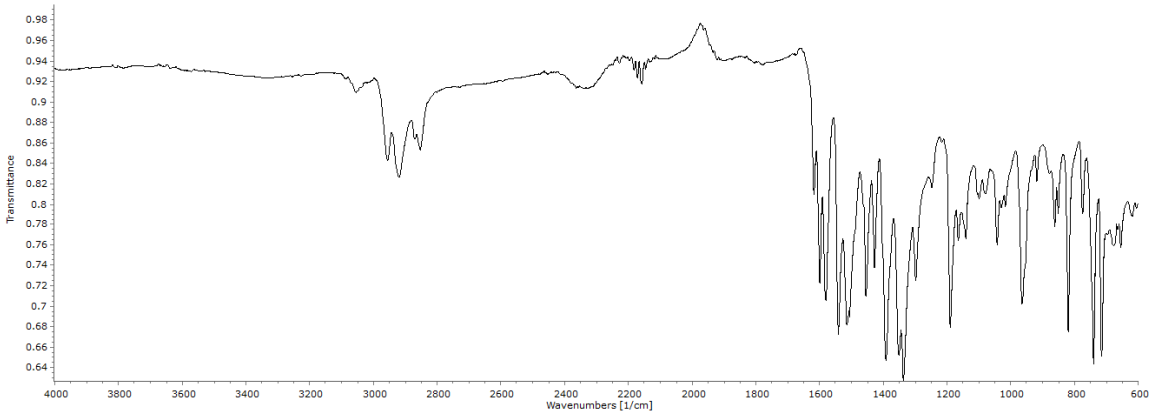

Fig. S30. Infrared spectrum of compound **9**.

Fig. S31. Mass spectrum of compound **9**.

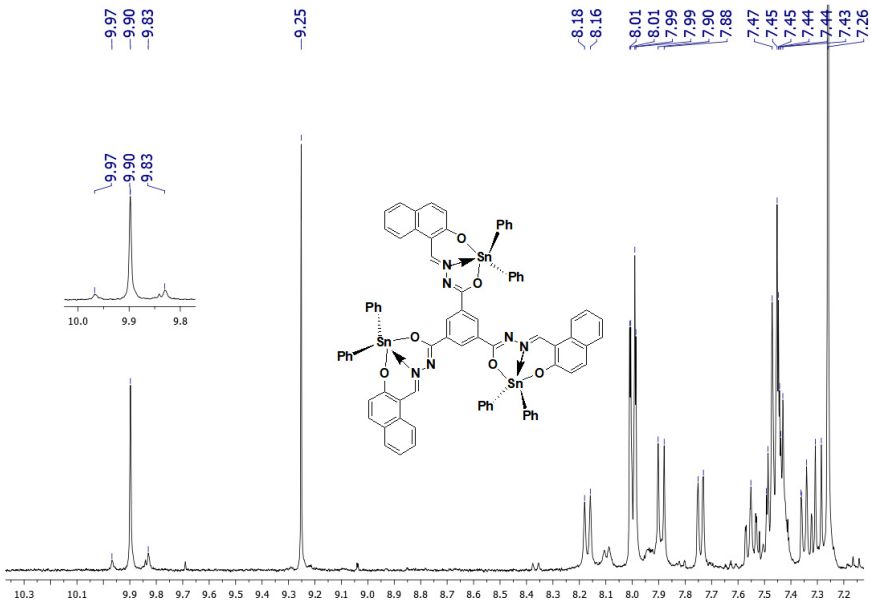

Fig. S32. ^{1}H NMR ($CDCl_3$) spectrum of compound **10**.

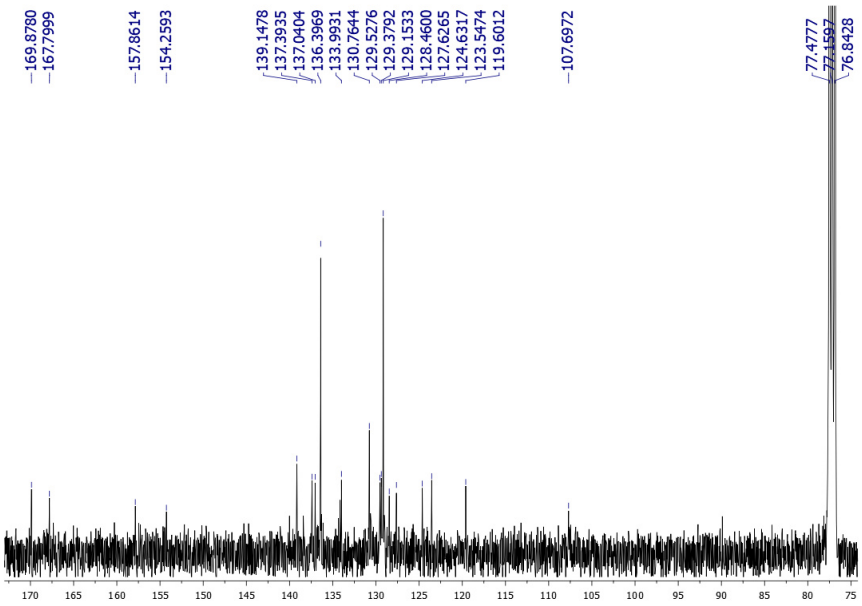

Fig. S33. ^{13}C NMR ($CDCl_3$) spectrum of compound **10.**

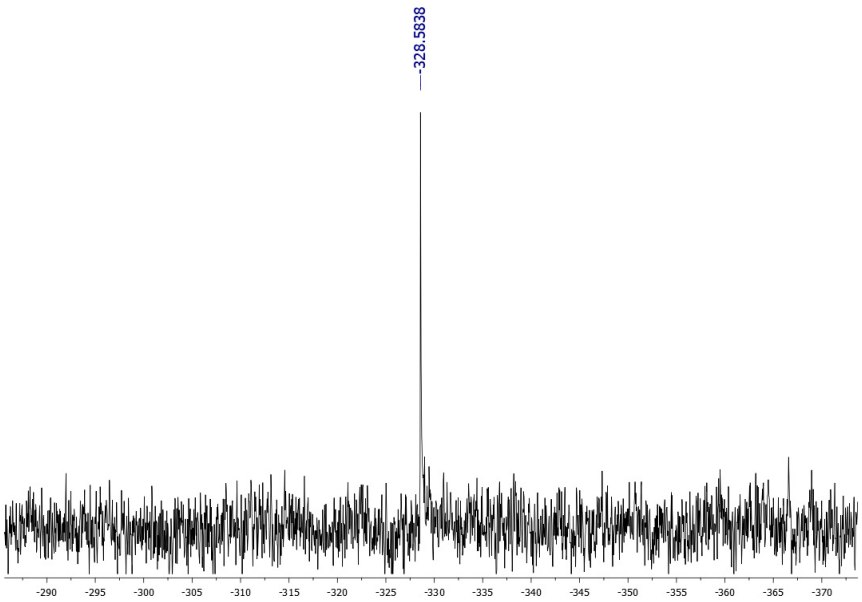

Fig. S34. ^{119}Sn NMR (CDCl3) spectrum of compound **10**.

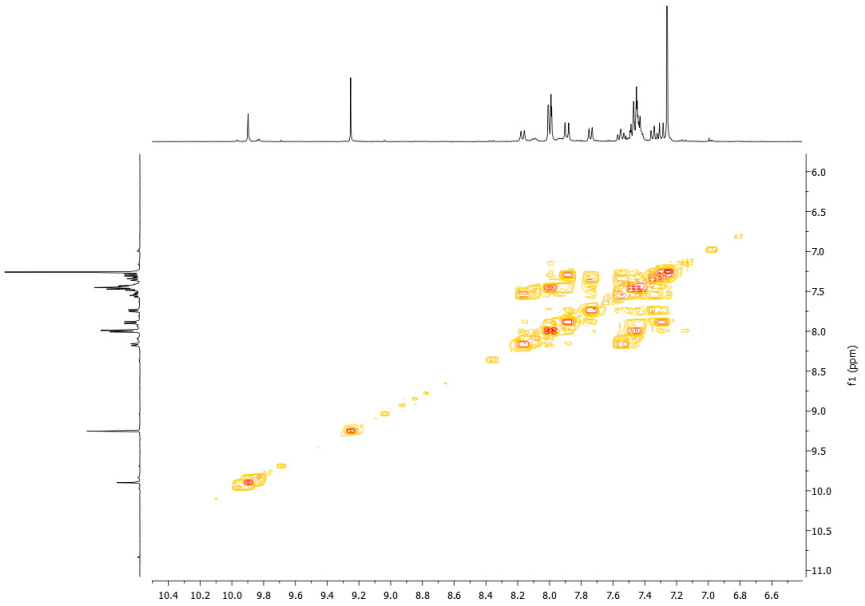

Fig. S35. COSY ($CDCl_3$) spectrum of organotin compound **10.**

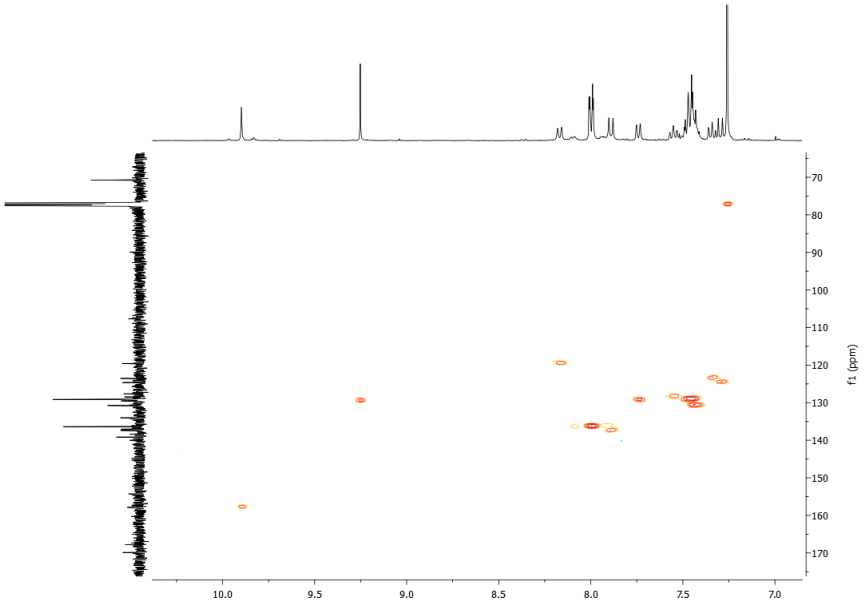

Fig. S36. HETCOR ($CDCl_3$) spectrum of organotin compound **10.**

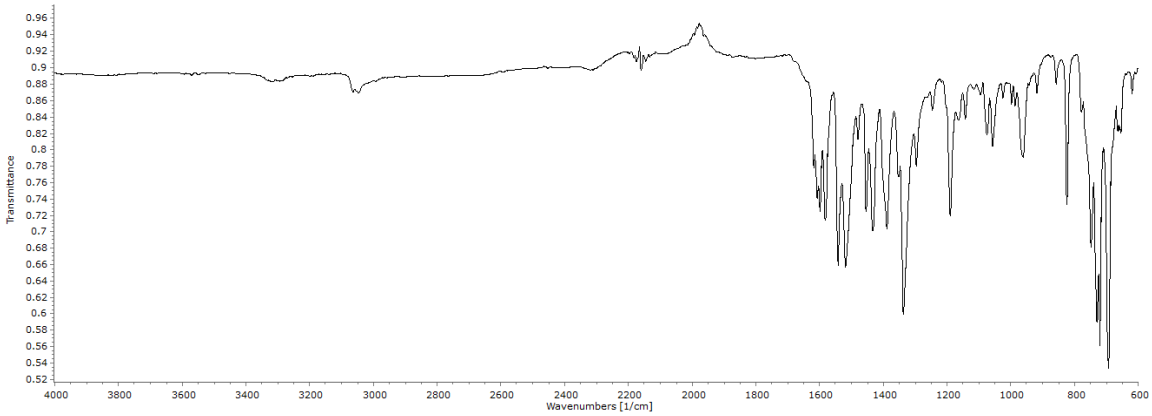

Fig. S37. Infrared spectrum of compound **10**.

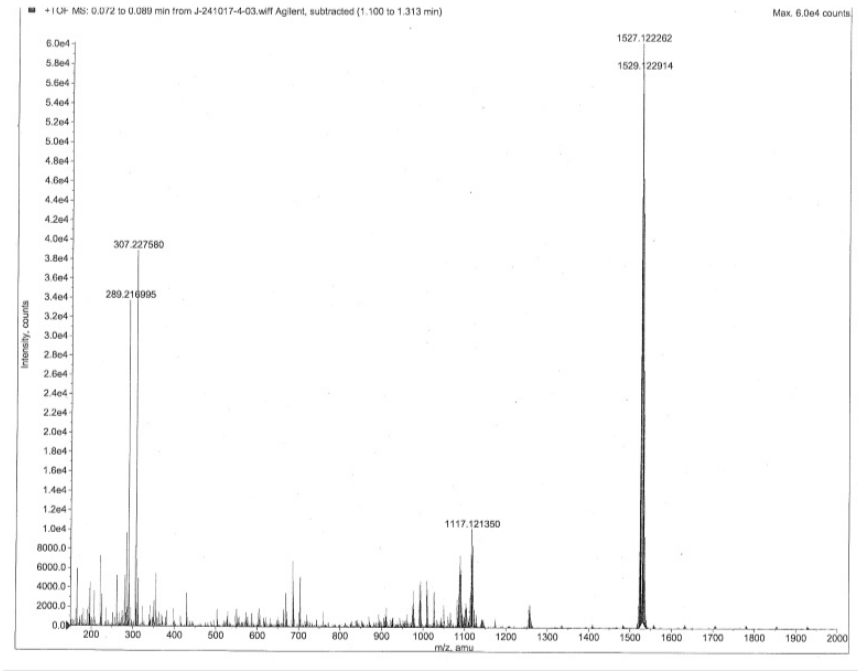

Fig. S38. Mass spectrum of compound **10**.

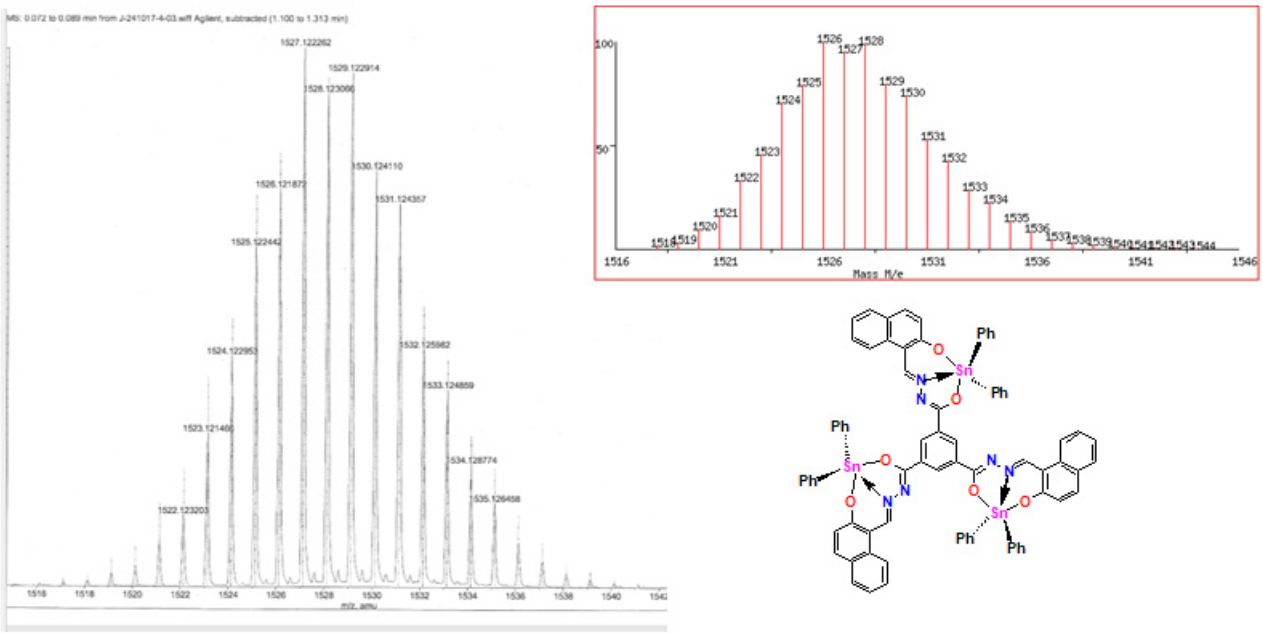

Fig. S39. Isotopic pattern spectrum of compound **10.**

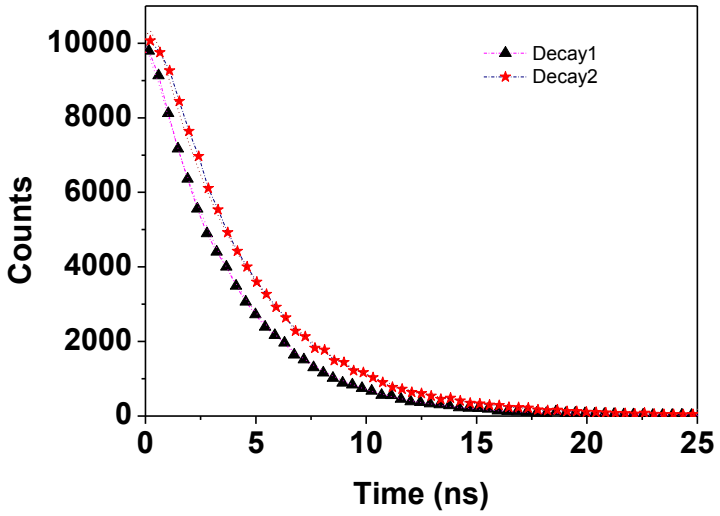

Fig. S40. TSPC data for **5**-**6** in $CHCl_3$ by exciting at 455 nm. Dotted lines: fitted curves. Symbols: experimental decays; triangles=**5**, bottom and triangles=**6**.

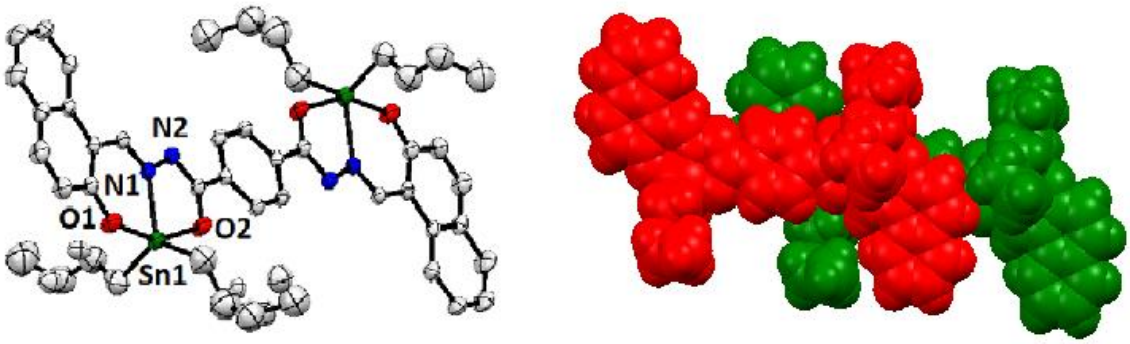

Fig. S41. Molecular structure of 5 **showing intermolecular interactions.**

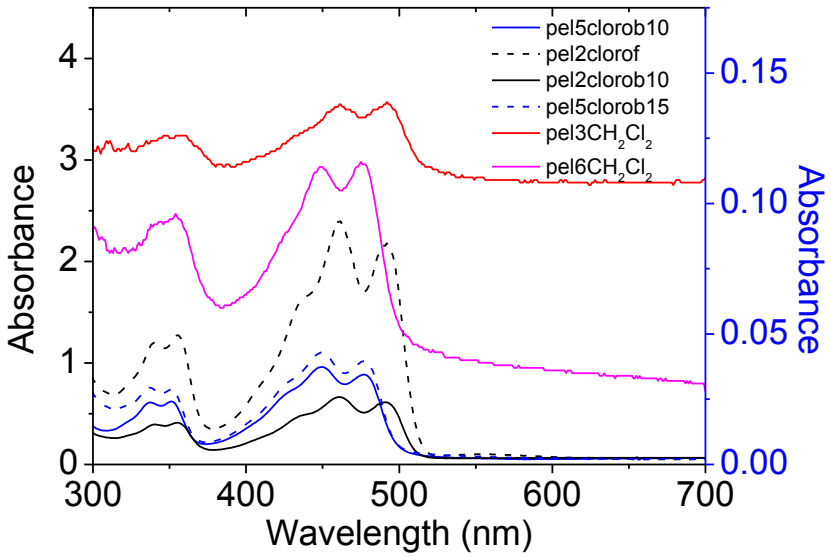

Fig. 42. Film absorption spectra of tin compounds.

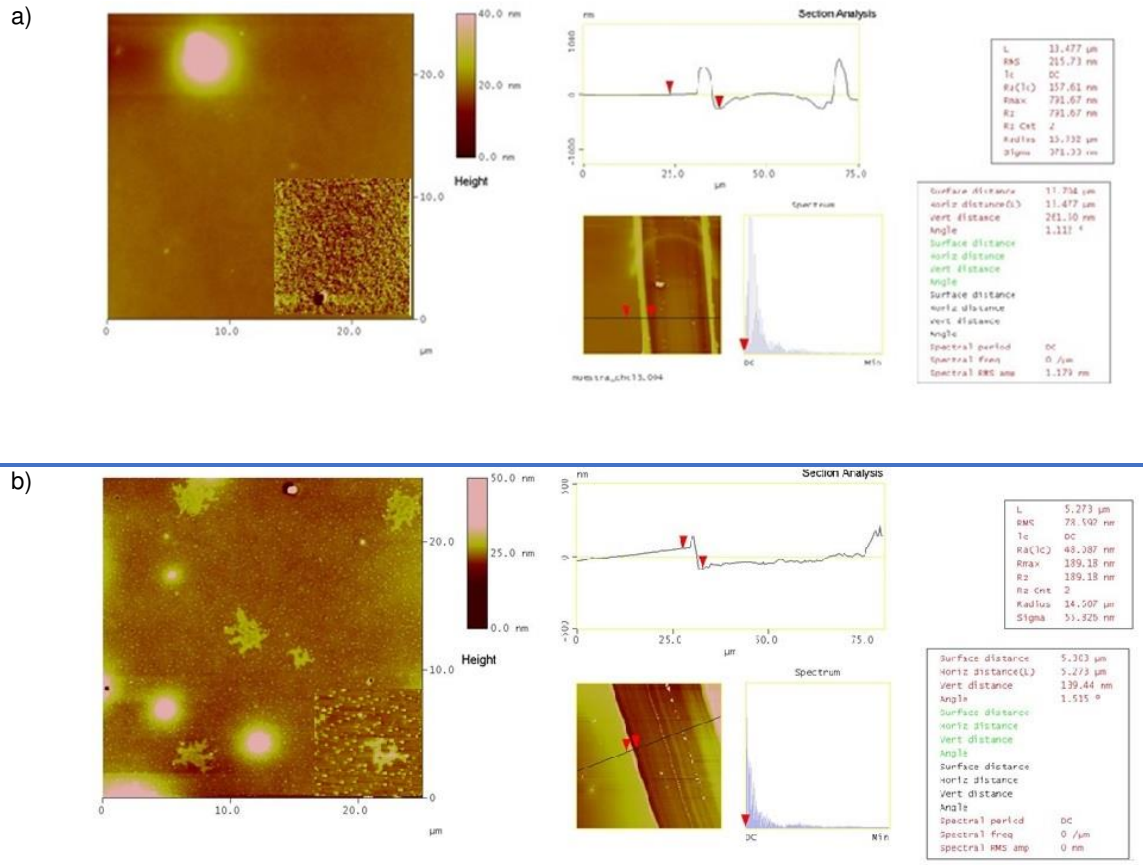

Fig. 43. AFM study of films of complex **3**. Left: Two-dimensional topographic images (25 * 25 main image and 5 * 5 μm2, inserted). Right: corresponding section analysis. A) film prepared from chloroform solution and b) chlorobenzene.

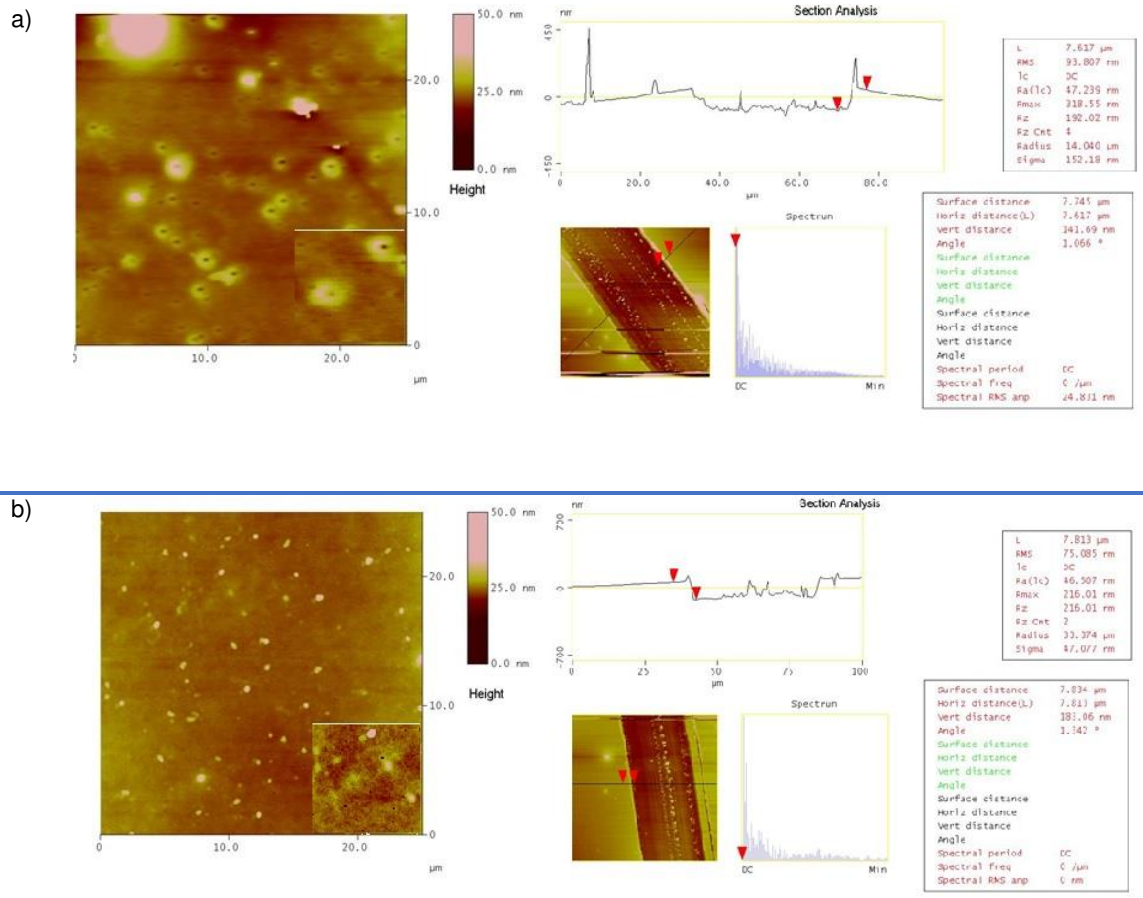

Fig. 44. AFM study of films of complex **5.** . Left: Two-dimensional topographic images (25 * 25 main image and 5 * 5 μm2, inserted). Right: corresponding section analysis. A) Film prepared from chlorobenzene solution 10 mg / mL (a) and 15 mg / mL (b)

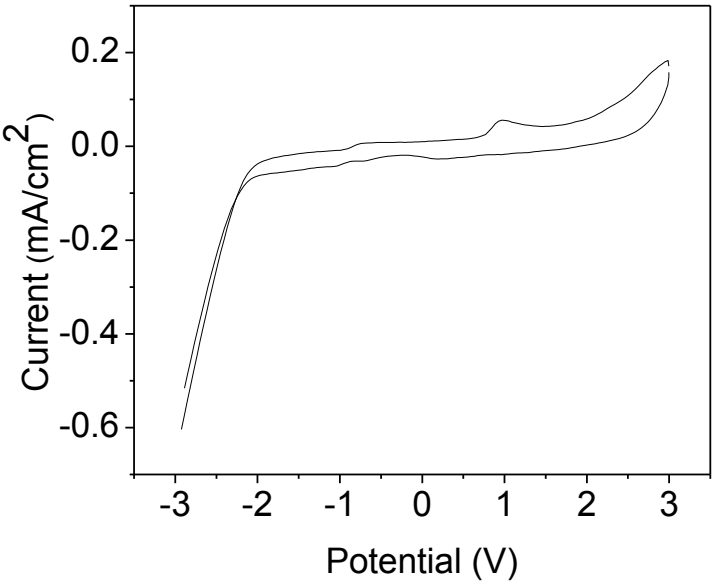

Fig. S45. Cyclic voltammetry ligand **3**.

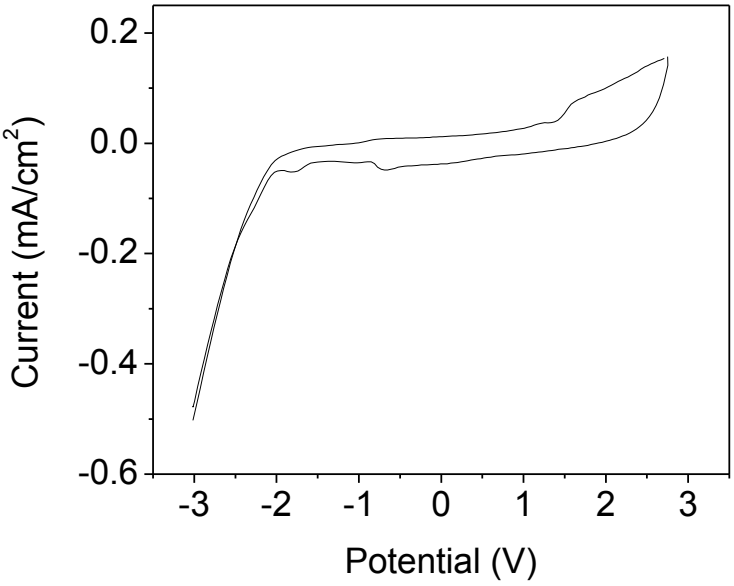

Fig. S46. Cyclic voltammetry compound **4**.

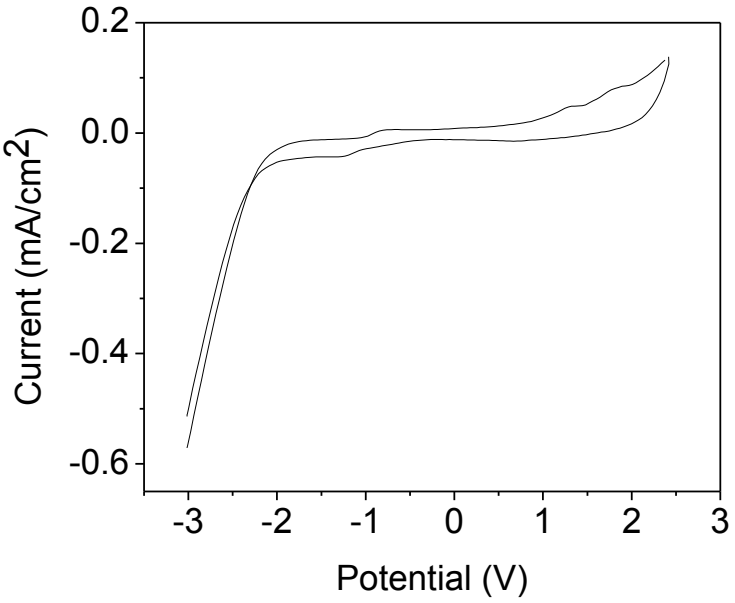

Fig. S47. Cyclic voltammetry compound **5**.

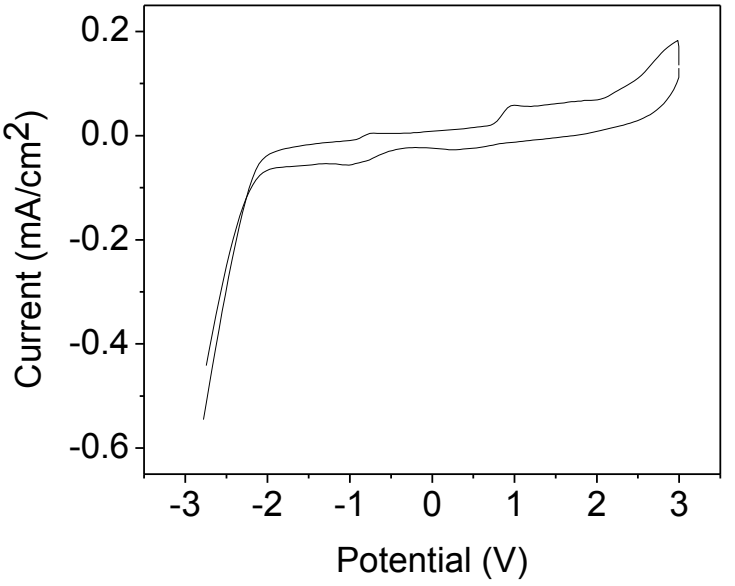

Fig. S48. Cyclic voltammetry ligand **8**.

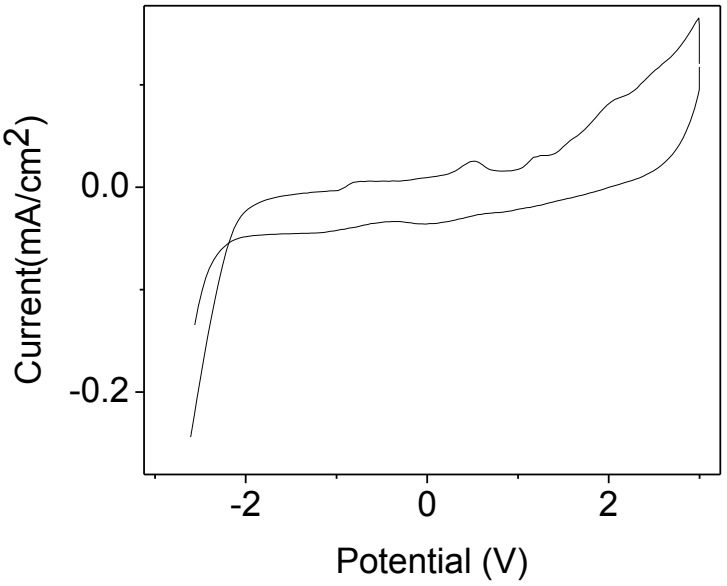

Fig. S49. Cyclic voltammetry compound **9**.

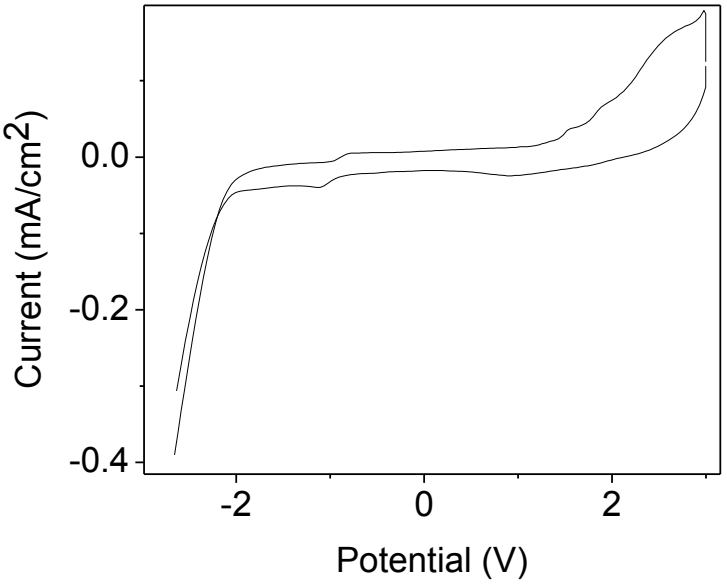

Fig. S50. Cyclic voltammetry compound **10**.

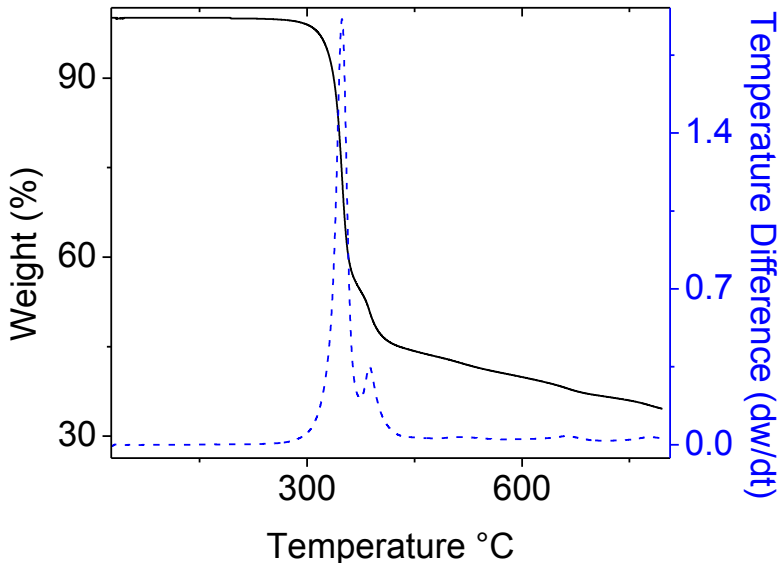

Fig. S51. Thermogravimetric Analysis of compound **5**.

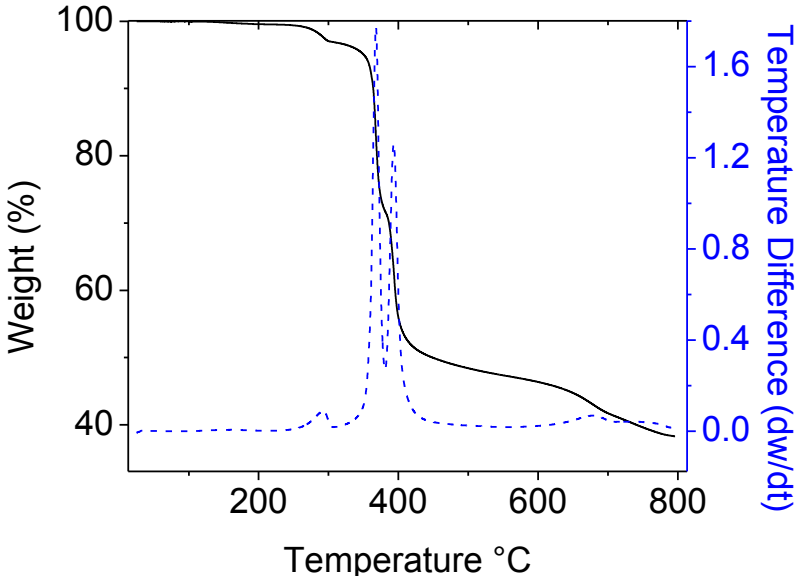

Fig. S52. Thermogravimetric Analysis of compound **5**.

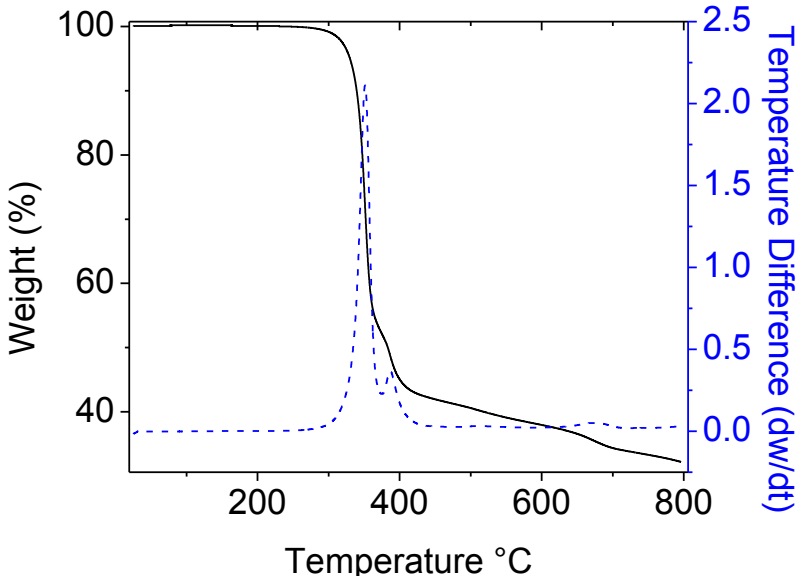

Fig. S53. Thermogravimetric Analysis of compound **9**.

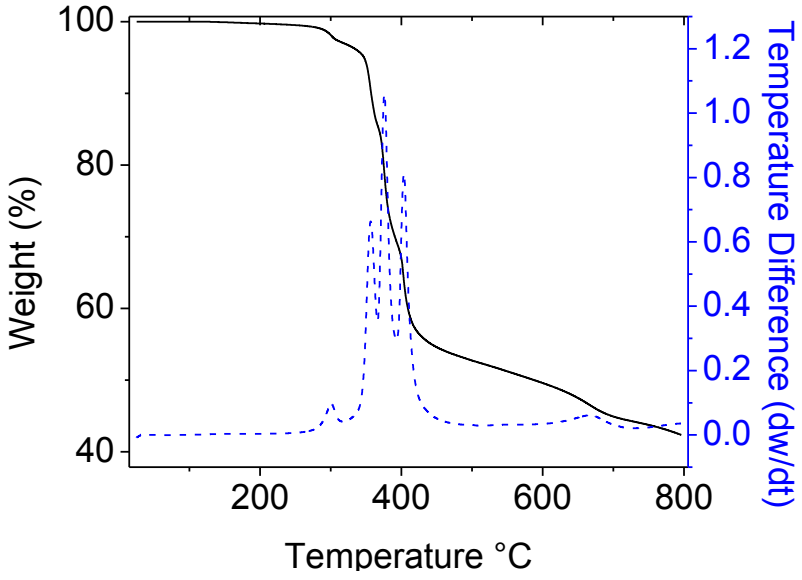

Fig. S54. Thermogravimetric Analysis of compound **10**.

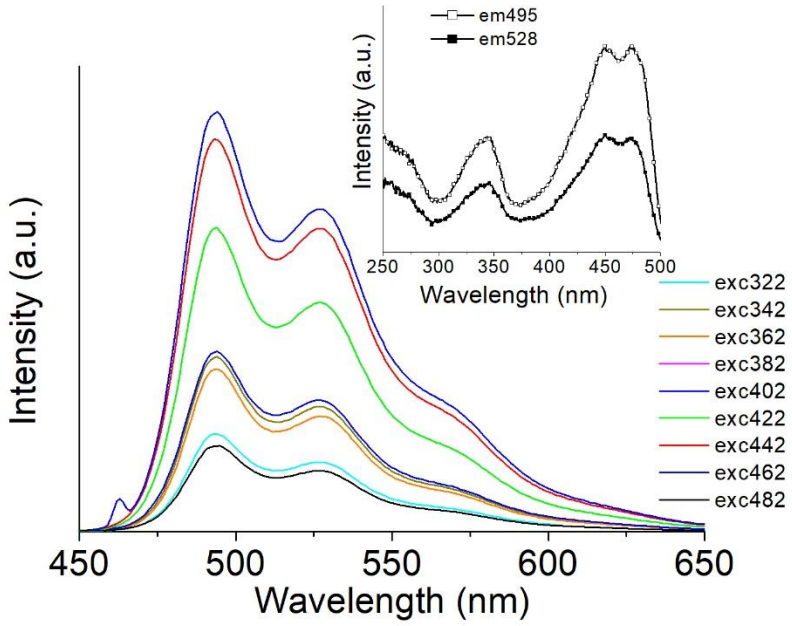

Fig. S55. Fluorescence spectra of organotin compound **5** in $CHCl_3$ at different excitation wavelength. Inserted figure: corresponding excitation spectrum by fixing as emission value, the peak at 495 nm or the shoulder at 528 nm.

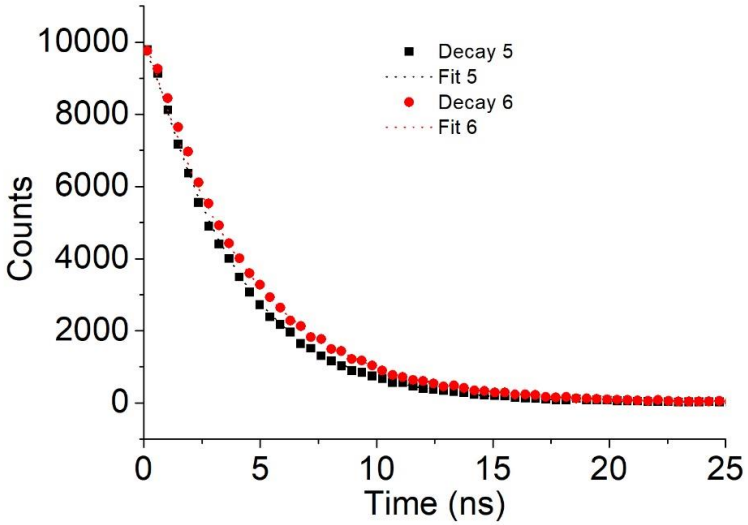

Fig. S56. TCSPC Fluorescence decay (symbols) and fit (dotted lines) of organotin compound **4** and **5** in $CHCl_3$.

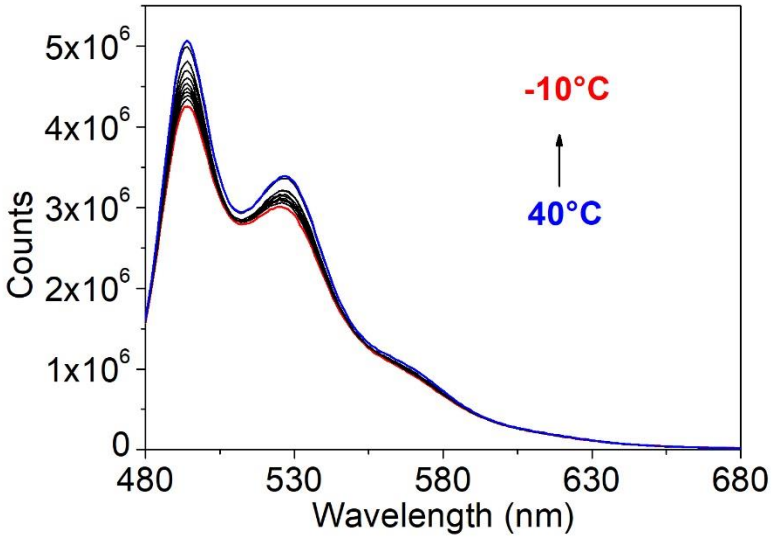

Fig. S57. Fluorescence spectra of organotin compound **5** in chloroform at different temperatures.

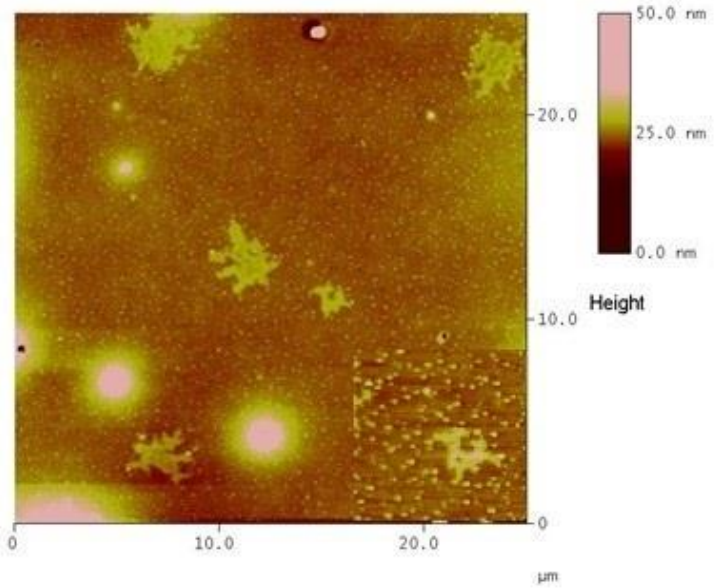

Fig. S58. Tapping AFM image of thin film prepared from chlorobenzene solutions of complex **4** in 25 μm*25 μm scanning area and (inset) 5 μm*5μm.

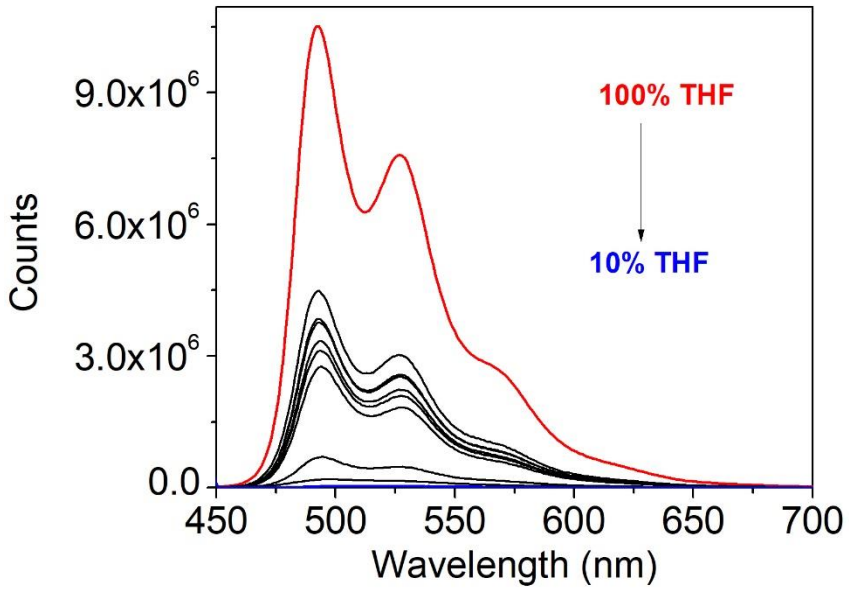

Fig. S59. Emission spectra of **5** in THF/water mixtures with different water fractions. From top to bottom: 100, 90, 80, 70, 60, 50, 40, 30, 20, 10% THF.

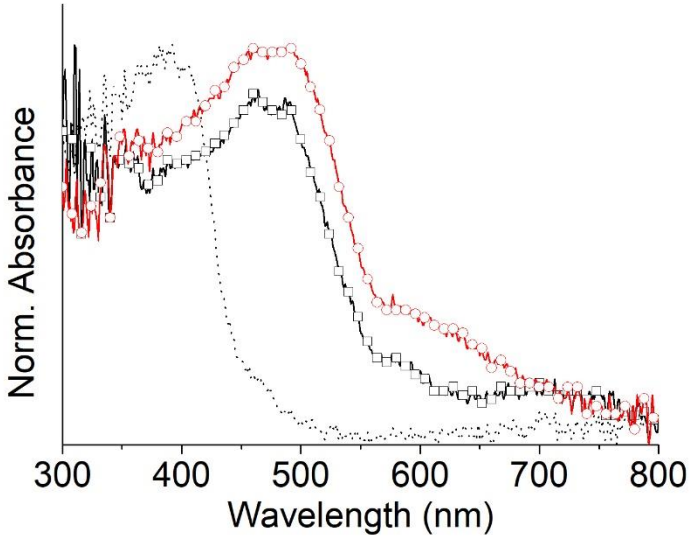

Fig. S60. Powder a) UV-vis spectra of organotin compounds **4** (squares), **5** (circles) and the ligand **3** (dotted lines) after 10 tons.

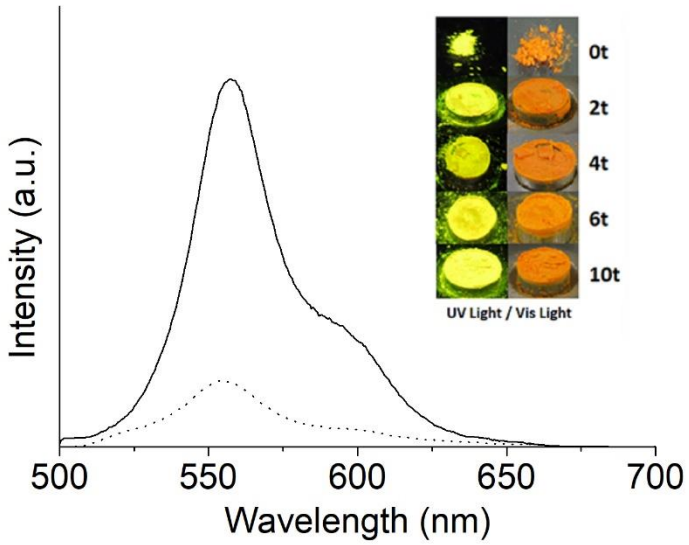

Fig. S61. Powder fluorescence spectra of organotin compounds **4** before (solid line) and after (dotted line) 10 tons of pressure. Inserted figure: photos of the powder at different pressures under visible and UV light.

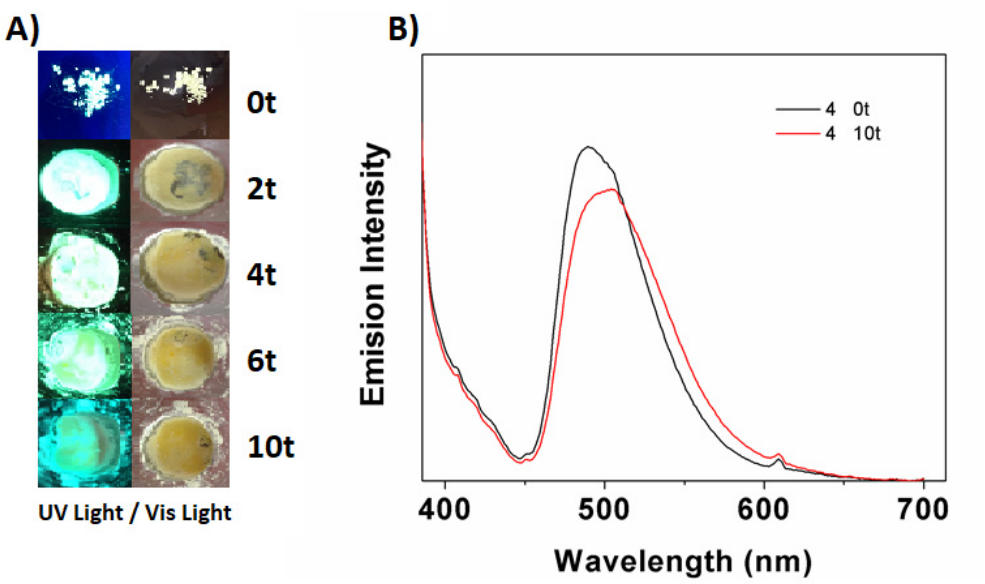

Fig. S62. A) Fluorescence image of **3** under pressure 0, 2, 4, 6 and 10 tons.

B) Emission spectra of **3** under pressure.

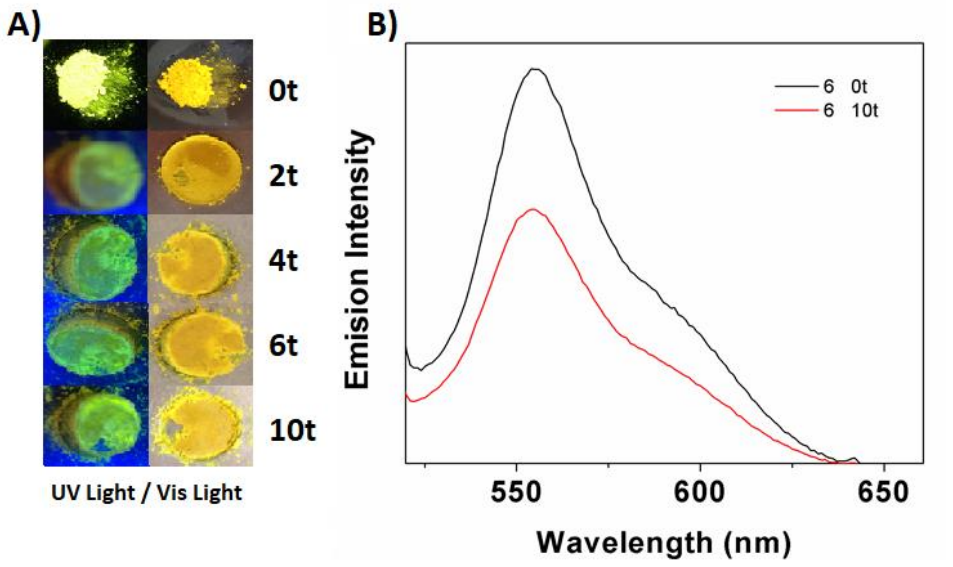

Fig. S63. A) Fluorescence image of **5** under pressure 0, 2, 4, 6 and 10 tons.

B) Emission spectra of compound **5** under pressure.

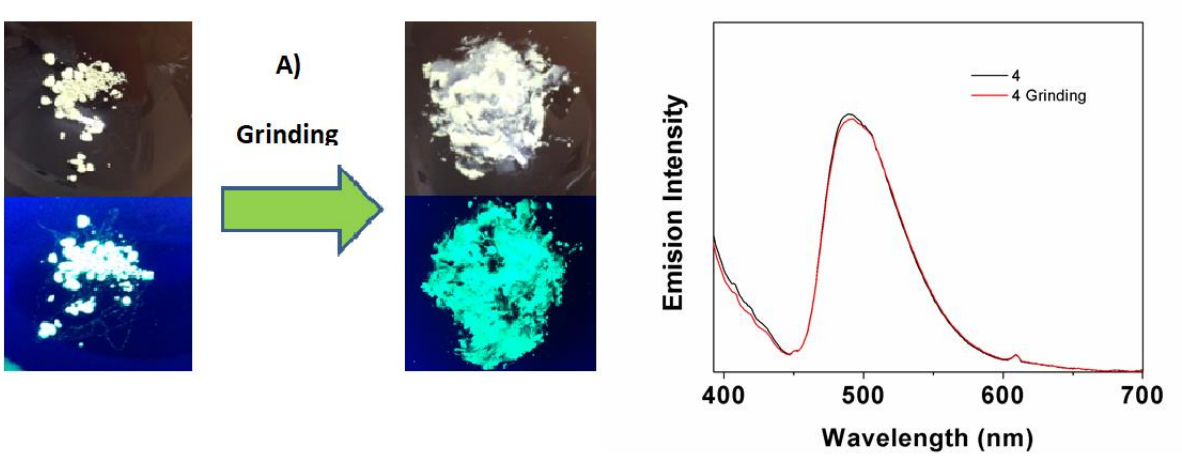

Figure S64. A) Fluorescence image of **3** and under grinding. B) Emission spectra of compound **3** and under grinding.

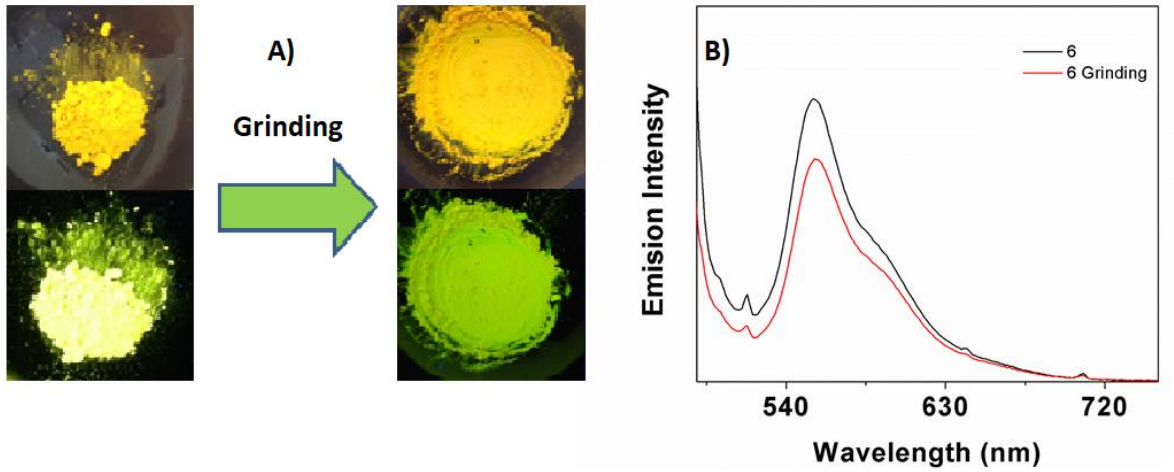

Figure S65. A) Fluorescence image of **5** and under grinding. B) Emission spectra of compound **5** and under grinding.

8. References.

[1] a) Turner J. A. "A realizable renewable energy future". *Science*. **1999**, 285, 687–689. b) Chow J., Kopp R. J., and Portney P. R. "Energy resources and global development". *Science*, **2003**, 302,1528-1531. c) Smalley R. E. "Future global energy prosperity: the terawatt challenge". *Mrs Bulletin*, **2005**, 30, 6, 412. d) Chu S., & Majumdar A. "Opportunities and challenges for a sustainable energy future". *Material Matters.* **2005**, 30, 412-17.

[2] CONUEE Proyecto nacional de eficiencia energética en alumbrado público Municipal. www.gob.mx/sener/documentos/proyecto-nacional-de-eficiencia-energetica-en-alumbrado-publico-municipal-proyecto-nacional.

[3] a) Pettinari C. "Special issue: recent advances in organotin chemistry". *J. Organomet. Chem.* **2006**, 691, 1435-36 b) Gielen M., Davies A. G., Pannell K., Tiekink E. Wiley. "Tin chemistry: fundamentals, frontiers, and applications". *Edit. Wiley*. **2009**. 752.

[4] Sedaghat T., & Rahmani M. "Synthesis and spectroscopic investigations of new schiff base complexes of tin (IV)" *Phosphorus Sulfur.Silicon Relat. Elements*. **2008**, 183, 1161-1167.

[5] Nath M. and Saini K. P. "Chemistry and applications of organotin(IV) complexes of Schiff bases". *Dalton Trans*. **2011**, 40, 7077-7121.

[6] Hui L., Junsheng Y., Nana W., Shuangling L. and Yadong J. "Fabrication and properties of do magnetron sputtered indium tin oxide on flexible plastic substrate". *J. Mater. Sci. Technol.* **2009**, 25,119-122.

[7] Shinar J. "Organic Light-Emitting Device" A Survey, Springer: Berlín, **2003**.

[8] Camp C., Andrez J., Pécaut J., Mazzanti M. "Synthesis of electron-rich uranium (IV) complexes supported by tridentate Schiff base ligands and their multi-electron redox chemistry". *Inorg. Chem.* **2013**, 52, 7078–7086.

[9] (a) Chen H., Chi Y., Liu C. S., Yu J.K., Cheng Y. M., Chen K. S. "Rational color tuning and luminescent properties of functionalized boron containing 2-pyridyl pyrrolide complexes". *Adv. Funct. Mater.* **2005**,15,567-574. (b) Cui Y., Liu Q., Bai D. R., Wen-Li J., Tao Y., Wang S. "Organoboron compounds with an 8-

hydroxyquinolato chelate and its derivatives: substituent effects on structures and luminescence". *Inorg. Chem.* **2005**, 44, 601-609. (c) Zhang H., Cheng H., Kaigi Y., Peng Z., Wenjing T., Wang Y. "Synthesis, structures, and luminescent properties of phenol-pyridyl boron complexes". *Inorg. Chem*. **2006**, 45, 2788-94.

[10] Costa R. D., Orti E., Bolink H. J. "Luminescent ionic transition-metal complexes for light-emitting electrochemical cells". *Angew. Chem. Int. Ed.* **2012**, 51, 8178-8211.

[11] You Y. G., Nam W. W. "Photofunctional triplet excited states of cyclometalated Ir (III) complexes: beyond electroluminescence". *Chem. Soc. Rev.* **2012**, 41, 7061-84.

[12] Vezzu D. A. K., Deaton J. C., Jones J. S., Bartolotti L., Harris C. F., Marchetti A. P., Kondakova M., Pike R. D., Huo S. "Highly luminescent tetradentate biscyclometalated platinum complexes: Design, synthesis, structure, photophysics, and electroluminescence application. *Inorg. Chem.* **2010**, 49, 5107-19.

[13] Otitoz K. J., Peters J. C. "Efficient luminescence from easily prepared three coordinate copper (I) aryl amidophosphines". *Chem. Commun*. **2010**, 46, 3690-92.

[14] Borsenberger P.M. and Weiss D.S., "Organic photoreceptors for Xerography" Marcel Dekker, New York, ***1998.***

[15] Wang L., Fine D., Sharma D., Trsi L., and Dodabalapur A. "Nanoscale organic and polymeric field-effect transistors as chemical sensors. *Anal. Bioanal. Chem.* **2006**, 384, 310-21.

[16] Sam-Shajing S., Niyazi-Serdar S. "Organic photovoltaics, mechanisms, materials and devices". CRC, Boca Raton, FL, **2005**.

[17] Hadziiannou G. and Van Hutten P. F. "Semiconducting polymers, Chemistry, physics and engineering". Wiley-VCH, Weinheim, **2000**.

[18] Park J.K., Kim W. S., Otgondemberel G., Lee B. J., Kim D. E., Kwon Y. S., "Photoluminescence and electroluminescence properties of organotin (IV) complexes". *Coll. Suf. A: Physico. Chem Eng*. **2008**, 321, 266-70.

[19] Tao X. T., Shimomura M., Suzuki H., Miyata S., Sasabe H. "Teravalent tin complex with high electron. affinity for electroluminescent applications". *Appl. Phys. Lett.* **2000**, 76, 3522-24.

[20] Fazaeli Y., Amini M. M., Najafi E., Mohajerani E., Janghouri M., Jalilian A. "Syntesis and characterization of 8-hydroxyquinoline complexes of tin(iv) and their application in organic light emitting diode". *J. Fluoresc.* **2012**, 22, 1263–1270.

[21] Zhou Y., Won J., Lee J. Y. and Richlter J. Y. "Studies leading to the development of a highly selective colorimetric and fluorescent chemosensor for lysine. electrochemiluminescence (ECL)". *Chem Rev.* **2004**,104, 3003–36.

[22] García-López M. C., Muñóz-Flores B. M., Jiménez-Pérez V. J., Moggio I., Arias E., Chan-Navarro R., Santillan R. "Synthesis and photophysical characterization of organotin compounds derived from Schiff bases for organic ligth emitting diodes". *Dyes and Pigments* **2014**, 106, 188-96.

[23] Jiménez-Pérez V. M., Berrones-Reyes J. C., García-López M. C., Muñoz-Flores B. M., Chan-Navarro R., Rasika Dias H. V., Moggio I., Arias E., Serrano-Mireles J. A. and Chavez-Reyes A. "New application of fluorescent organotin compounds derived from Schiff bases: synthesis, X-ray structures, photophysical properties, cytotoxicity and fluorescent bioimaging". *J. Mater. Chem. B*, **2015**, 3, 5731-574.

[24] Cantón-Díaz A.M. **2016**. Compuestos de Sn (IV) fluorescentes derivados de bases de schiff: síntesis, caracterización y fabricación de un dispositivo optoelectrónico. Tesis de maestría. Monterrey, Nuevo León, México. Facultad de Ciencias Químicas. Universidad Autónoma de Nuevo León. 148.

[25] García-López M.C.; Muñoz-Flores B. M., Chan-Navarro R., Jiménez-Pérez V. M. Moggio I., Arias E. Rodríguez-Ortega A., Ochoa M. E. "Microwave-assisted synthesis, third-order nonlinear optical properties, voltammetry cyclic and theorical calculations of organotin compounds bearing push-pull Schiff bases". *Org. Chem.* **2016**, 806, 68-76.

[26] Sheldrick. G. M. "A short history of SHELX". *Acta Cryst.* **2008**, 64, 112–122.

[27] Farrugia L. J. "WinGX suite for small-molecule single-crystal crystallography". *J. Appl. Crystallogr.* **1999**, 32, 837–8.

[28] Felouat A., D'Aléo A., Fages F. "Synthesis and Photophysical Properties of Difluoroboron Complexes of Curcuminoid Derivatives Bearing Different Terminal Aromatic Units and a meso-Aryl Ring". *J. Org. Chem*. **2013**, 78, 4446–4455.

[29] Williams A. T. R., Winfield S. A., Miller J. N. "Relative fluorescence quantum yields using a computer-controlled luminescence spectrometer". *Analyst*. **1983**, 108, 1067–1071.

[30] El-Daly S. A., El-Azim S. A., Elmekawey F. M., Elbaradei B. Y., Shama S. A., Asiri A. M. "Photophysical Parameters, Excitation Energy Transfer, and Photoreactivity of 1,4-Bis(5-phenyl-2-oxazolyl)benzene (POPOP) Laser Dye". *Int. J. Photoenergy*. **2012**, 12, 1–10.

[31] Horcas, I., Fernandez, R., Gomez-Rodriguez, J.M., Colchero, J., Gomez-Herrero, J., Baro, A.M., *WSXM:* A software for scanning probe microscopy and a tool for nanotechnology. *Rev. Scien. Instrum.*, **2007**, 78, 013705.

[32] Hosseini-Monfared H., Asghari-Lalami N., Pazio A., Wozniak K., Janiak C. "Dinuclear vanadium, copper, manganese and titanium complexes containing O,O,N-dichelating ligands: Synthesis, crystal structure and catalytic activity" *Inorg. Chem. Acta.* **2013**, 406, 241–250.

[33] a) Zhang X., Tang B., Zhang P, Li M., Tian W. L. "Synthesis and characterization of 1, 3, 4-oxadiazole derivatives containing alkoxy chains with different lengths" *Journal of Molecular Structure.* **2007** 846, 55–64 b) B. Lakshmi K., Shivananda N., Prakash G. A., Isloor A. M. and Mahendra K. N. " Synthesis and characterization of Schiff base metal complexes and reactivity studies with malemide epoxy resin" *Bull. Korean Chem. Soc.* **2012**, 33, 473-481.

[34] a) Jia, Lei *et al*. "Method for preparation of trimesoyl hydrazone derivatives and application as molecule probe for identifying fluorine ion. *From Faming Zhuanli Shenqing*, 103497121, 08 Jan 2014. b) Davis M. C. "Tricarbamate of 1,3,5-triaminobenzene via curtius rearrangement of trimesic acid and subsequent nitration". *Synthetic Communications.* 2007 37 1457-1462.

35] Yang C. C., Hsu C. J., Chou P. T., Cheng H. C., Su Y. O. and Leung M. K. "Excited State Luminescence of Multi-(5-phenyl-1,3,4-oxadiazo-2-yl)benzenes in an Electron-Donating Matrix: Exciplex or Electroplex?" *J. Phys. Chem. B* **2010**, 114, 756–768.

[36] Smith F. E., Hynes R. C., Ang T. T., Khoo L- E. and Eng G."The synthesis and structural characterization of a series of pentacoordinate diorganotin (IV) N-arylidene-α-amino acid complexes" *Can. J. Chem*. **1992**, 70, 1114-1120.

[37] Smith P. J. "Chemical Shifts of 119Sn Nuclei in Organotin Compounds. Annual Reports on NMR Spectroscopy", **1978**, 8, 291-370.

[38] Muñoz B., Santillan R., Rodriguez M., Méndez J., Romero M., Farfán N., Lacroix P., Nakatani K., Ramos G., Maldonado J. "Synthesis, cristal structure and non linearopticalproperties of boronatesderivatives of saliciyldeniminophenols". *J. Organomet. Chem*. **2008,** 690, 2351- 2357.

[39] Kumari R., Nath M. "Tri- and diorganotin (IV) derivatives of non-steroidal anti-inflammatory drug sulindac: Characterization, electronic structures (DFT), DNA binding and plasmid cleavage studies". *Appl. Organometal. Chem*. **2017**, 31, 3661.

[40] Dong H., Shao Y., Chen W. "Synthesis and characterization of di- and tri-organotin(IV) complexes with Schiff base ligand pyruvic acid 3-hydroxy-2-naphthoyl hydrazine" *Inorg. Chim. Acta.* **2006**, 356, 3330-3338.

[41] López-Torres E., Medina-Castillo A., Fernandez-Sanchez J. Mendiola A. "Luminescent organotin complexes with the ligand benzil bis(benzoylhydrazone)" *J.Organomet. Chem.* **2010**, 695, 2305-2310.

[42] Chow K. M., Lo K. M. "Synthesis, spectral characterization and crystal structures of benzyltin complexes with (E)-4-chloro-N0 -(2-hydroxy4-methoxybenzylidene)benzohydrazide". *Polyhedron.* **2014**, 81, 370–381

[43] a) Yin H. D. and Chen S. W. "Synthesis and characterization of organotin(IV) compounds with Schiff base of o-vanillin-2-thiophenoylhydrazone". *J. Organomet. Chem*. **2006**, 691, 3103–3110 b) Yamamura M., Albrecht M., Albrecht M., Nishimura Y., Arai T., Nabeshima T. Inorg. Chem. 53, 2014, 1355–1360

[44] Muñoz, B. M.; Cabrera, J.; Chávez-Reyes, A.; Rasika Dias, H. V.; Viñas, C.; Nuñez, R.; Jiménez-Pérez V. M. Organotin dyes bearing anionic boron clusters as cell-staining fluorescent probes, *Chem. Eur. J*. **2018**, 24, 5601.

[45] Cantón-Díaz, A. M.; Muñóz-Flores B. M.; Moggio I.; Arias E.; De León A.; García-López M. C.; Santillán R.; Ochoa M. E. and Jiménez-Pérez V. M. One-pot microwave-assisted synthesis of organotin Schiff bases: an optical and electrochemical study towards their effects in organic solar cell. *New J.Chem*. **2018**, 42, 14586.

[46] Chan-Navarro R., Muñoz-Flores B. M., Jimenez-Pérez V. M., Moggio I., Arias E., Ramos-Ortíz G., García-López M. C., Rosas-García V., Elizondo P., Rodríguez M. Optical and Nonlinear Optical Properties, Thermal Analyses, Cyclic Voltammetry, and Computational Studies: Green Synthesis Approach of Boronates derived from Schiff Bases. Int. J. Innov. Sci. Eng. Tech. 2014, 1, 462–475

[47] Yang H., Wang L., Zhang J., Yu X., Geng Y., Han, Y. Molecular packing and orientation transition of crystalline poly(2,5-dihexyloxy-p-phenylene), *Macromol. Chem. Phys*. **2014,** 215, 405-11.

[48] Ibarra-Rodríguez M., Muñoz-Flores B. M., Jiménez-Pérez V. M. "Multi-stimuli fluorescent behaviour of boron compounds derived from hydrazones in the solid state (thermochromism, vapochromism, and piezochromism): Synthesis, characterization, and photophysical studies" *J. Lumin.* **2018**,198, 342–349.

[49] Molina-Paredes A., Jiménez-Pérez V. M., Lara-Cerón J., Moggio I., Arias E., Santillán R., Sánchez M., Suacedo-Yañez A., Muñoz-Flores B. M. Fluorescent boron Schiff bases dyes for staining silk fibroin: Green synthesis, structural characterization, DFT, and photophysical properties. *App. Organomet. Chem.* Accepted.

50] García-López M. C., Muñoz-Flores B. M, Jiménez-Pérez V. M., Moggio I., Arias E., Chan-Navarro R., and Santillan, R. Synthesis and Photophysical Characterization of Organotin Compounds Derived from Schiff Bases for Organic Light Emitting Diodes. *Dyes and Pigm*. **2014**, 106, 188– 196.

51] Cantón-Díaz A. M., Muñoz B. M., Moggio I., Arias E., De León A., García-López M. C., Santillán R., Ochoa M. E. and Jiménez-Pérez, V. M. One-pot microwave-assisted synthesis of organotin Schiff bases: an optical and

electrochemical study towards their effects in organic solar cells. *New. J. Chem*., **2018**, 42, 14586– 96.

[52] a) Yan W., Wang L., Zheng J., Huang J., Zhang J., Zhou H., Wu J. and Tian Y. Aggregation-induced fluorescence behavior of triphenylamine-based schiff bases: the combined effect of multiple forces. *J. Org. Chem.* **2013**, 78, 10344−10359. b) Xiao-Feng M., Rui S., Jinghui C., Jiaoyan L., Fei G., Haifeng X., and Xiangge Z. Fluorescence aggregation-caused quenching versus aggregation-induced emission: a visual teaching technology for undergraduate chemistry students. *J. Chem. Educ*. **2016**, 93, 345−350.

[53] García-López M. C., Muñoz-Flores B. M, Jiménez-Pérez V. M., Moggio I., Arias E., Chan-Navarro. and Santillan, R. Synthesis and Photophysical Characterization of Organotin Compounds Derived from Schiff Bases for Organic Light Emitting Diodes. *Dyes and Pigm*. **2014**, 106, 188– 196

.

[54] Cantón-Díaz A. M., Muñoz B. M., Moggio I., Arias E., De León A., García-López M. C., Santillán R., Ochoa M. E. and Jiménez-Pérez, V. M. One-pot microwave-assisted synthesis of organotin Schiff bases: an optical and electrochemical study towards their effects in organic solar cells. *New. J. Chem*., **2018**, 42, 14586– 96.

[57] Seeboth A.and Lötzsch D. “Thermochromic and Thermotropic Materials”. *CRC Press*, **2013**.

[58] Butler T., Zhuang M., and Frase C. L. Color Tuning of Mechanochromic Luminescent β‑Diketones via Boron Coordination and Donor-Acceptor Effect. *J. Phys. Chem. C.* **2018**, 22, 19090-19099.

9. AUTOBIOGRAPHIC SUMMARY

M. en C. ARELLY MONTSERRAT CANTON DIAZ

Candidate for the degree of Doctor of Science with Orientation in Materials Chemistry

Thesis: Preparation of new tin materials derivatives from ligands multidentate for potential fabrication of optoelectronic devices.

Field of study: Materials Chemistry.
Biography: Born in Mérida, Yucatán, México, on December 1th of 1989.

Education:

Chemistry Engineer Degree Technological Institute of Mérida.
Master of Science of Science with Orientation in Materials Chemistry
Faculty of Chemistry. Autonomous University of Nuevo Leon.

Professional experience:

Sub-production manager: Mayan Fertilizer. Technological Institute of Mérida. 2012 –2013.
Academic professor of chemistry and biology: Ameyali High School. 2013 –2014.
Academic professor of the organic chemistry laboratories of the chemical and environmental engineering degrees. Autonomous University of Nuevo León.

Fulfilled projects:
1.- Elaboration of compost with different substrates. Technological Institute of Mérida.
2.- Elaboration of Humus by Californian earthworm. Technological Institute of Mérida.
3.- Fluorescent Sn (IV) compounds derived from Schiff bases: synthesis, characterization and fabrication of an electroluminescent device. Faculty of Chemistry. Autonomous University of Nuevo León.